Spring 2008

Comparison of Landslides and their Related Outburst Flood Deposits, Owyhee River, Southeastern Oregon

Shannon Marian Othus
Central Washington University

COMPARISON OF LANDSLIDES AND THEIR RELATED OUTBURST FLOOD DEPOSITS, OWYHEE RIVER, SOUTHEASTERN OREGON

A Thesis

Presented to

The Graduate Faculty

Central Washington University

In Partial Fulfillment

of Requirements for the Degree

Master of Science

Geology

---

by

Shannon Marian Othus

May 2008

CENTRAL WASHINGTON UNIVERSITY

Graduate Studies

We hereby approve the thesis of

Shannon Marian Othus

Candidate for the degree of Master of Science

APPROVED FOR THE GRADUATE FACULTY

_____ _____
Dr. Lisa L. Ely, Committee Chair

_____ _____
Dr. Beth Pratt-Sitaula

_____ _____
Dr. Karl Lillquist

_____ _____
Dr. Wendy Bohrson, Geology Department Chair

_____ _____
Dean of Graduate Studies

ABSTRACT

COMPARISON OF LANDSLIDES AND THEIR RELATED OUTBURST FLOOD DEPOSITS, OWYHEE RIVER, SOUTHEASTERN OREGON

by

Shannon Marian Othus

May 2008

Numerous landslides have entered the Owyhee River canyon north of Rome, Oregon. As the river flows through different lithologic units, the style of mass wasting changes from large slump events and small rock falls to large earthflows. The change in mechanism of mass wasting from upstream to downstream seems to depend on several factors: (1) the ratio of the basalt cap to the exposed underlying sediments, (2) the composition of underlying sediments, (3) the canyon geometry, and (4) the extent and frequency of mass wasting. All three mechanisms of mass wasting have the ability to block the river channel and display associated flood deposits downstream. Only earthflows show aggradation deposits upstream, suggesting greater longevity than other types of mass wasting. Also, based on the frequency and size of related outburst flood deposits, smaller rock falls could possibly have the greatest cumulative effect on river channel evolution.

ACKNOWLEDGMENTS

Assistance was provided by many people and organizations during this project. Funding was generously provided by the National Science Foundation grant EAR-0617234, the CWU Department of Graduate Studies, and the Geological Society of America. Special thanks go to my field assistants, Tabitha Trosper and Leslie Hickey, for endless help in the field carrying appliances and tools back and forth across the river and hiking up giant hills in 100°F heat. Thanks also go to P. Kyle House, Liz Safran, Jim E. O'Connor, Gordon Grant, and Rose Wallick for providing hours of fun in the field and meaningful and diverse interpretations of geomorphic deposits and landforms. Thanks also go to Megan Mills-Navoa and Scott Anderson for providing terrace profiles for the Artillery reach, singing in the field, and the butt-rock. Thank you to Cassandra Fenton for providing the cosmogenic dates presented in this paper. Thanks also go to my committee and other faculty and staff of the Department of Geological Sciences, especially Craig Scrivner for putting some much needed computer programs on my laptop. Immense gratitude goes to Vicki Potts for Friday afternoon conversation involving my many students in White Swan, for always being on top of my paperwork, and knowing all of the ins-and-outs related to the bureaucracy of CWU. I would also like to thank the WATERS program for increasing my standard of living exponentially. To my fellow students of 2008, thanks for the many venting sessions regarding the many frustrations as a result of TA-ing and pagination. And my final thanks go to my advisor, Dr. Lisa Ely, whose help in writing and supporting data is immeasurable.

TABLE OF CONTENTS

TABLE OF CONTENTS (continued)

LIST OF TABLES

LIST OF FIGURES

LIST OF FIGURES (continued)

LIST OF FIGURES (continued)

CHAPTER I

INTRODUCTION

This study aims to describe several different types of mass wasting events, including what factors initiate different types of mass wasting and how these events affect a river channel. The three different types of mass wasting styles that were studied, which include rock falls, large slump events, and earthflows, all show the ability to completely block the Owyhee River channel by forming landslide dams that can greatly affect the long-term evolution of the river valley. The data gathered from field observations in this study were used to understand the relationships between various landforms, focusing in large part on the landslides and their related aggradation and/or flood deposits. Results of the study help establish a better understanding of how large, channel encroaching landslides affect long-term channel evolution and incision. Also, because of the hazards associated with mass wasting, it is important to understand the various geologic parameters that promote and initiate large mass wasting events as well as how the persistence and the breach of a landslide dam can affect areas both upstream and downstream of the dam.

The main objective of the project is to investigate and compare large mass wasting events that differ in size, mass wasting mechanism, and material, that appear to have dammed the Owyhee River in southeastern Oregon. This information from the characterization of several mass wasting events in both study reaches will be used to better understand why differing mass wasting mechanisms occur in separate reaches of the Owyhee River and also to compare the effects of these mass wasting events on the

river both upstream and downstream of where the landslide entered the channel. There are two working hypothesis for this project: (1) the type of mass wasting is directly related to ratio of the thickness of the basalt cap to the underlying sediment package, canyon geometry, frequency of mass wasting in the area, and composition of the underlying sediment package and (2) the characteristics of outburst flood deposits depend on the type of mass wasting event creating a landslide dam. The data obtained from this study will then be used in a greater context to help answer the question of whether mass wasting events that impinge on a river channel locally inhibit or promote channel incision and lateral migration, effectively impacting processes related to channel evolution. Though many studies have been done regarding the effects of landslides and landslide dams on rivers (e.g., Adams, 1987; Beebee, 2007; Costa and Schuster, 1988; Ermini and Casagli, 2002; Korup, 2006; Reneau and Dethier, 1996), little attention has been given to quantitative effects of landslide dams on the evolution of river channels (Korup, 2006; Reneau, 2000).

Location

The study area is located on the Owyhee River, in southeastern Oregon, near the western border of Idaho and the northwestern border of Nevada. The Owyhee River, which flows from south to north, has its head waters in northern Nevada and its confluence with the Snake River in Nampa, Idaho (Figure 1). There is one dam located on the Owyhee River that creates Lake Owyhee, just downstream of the river reach

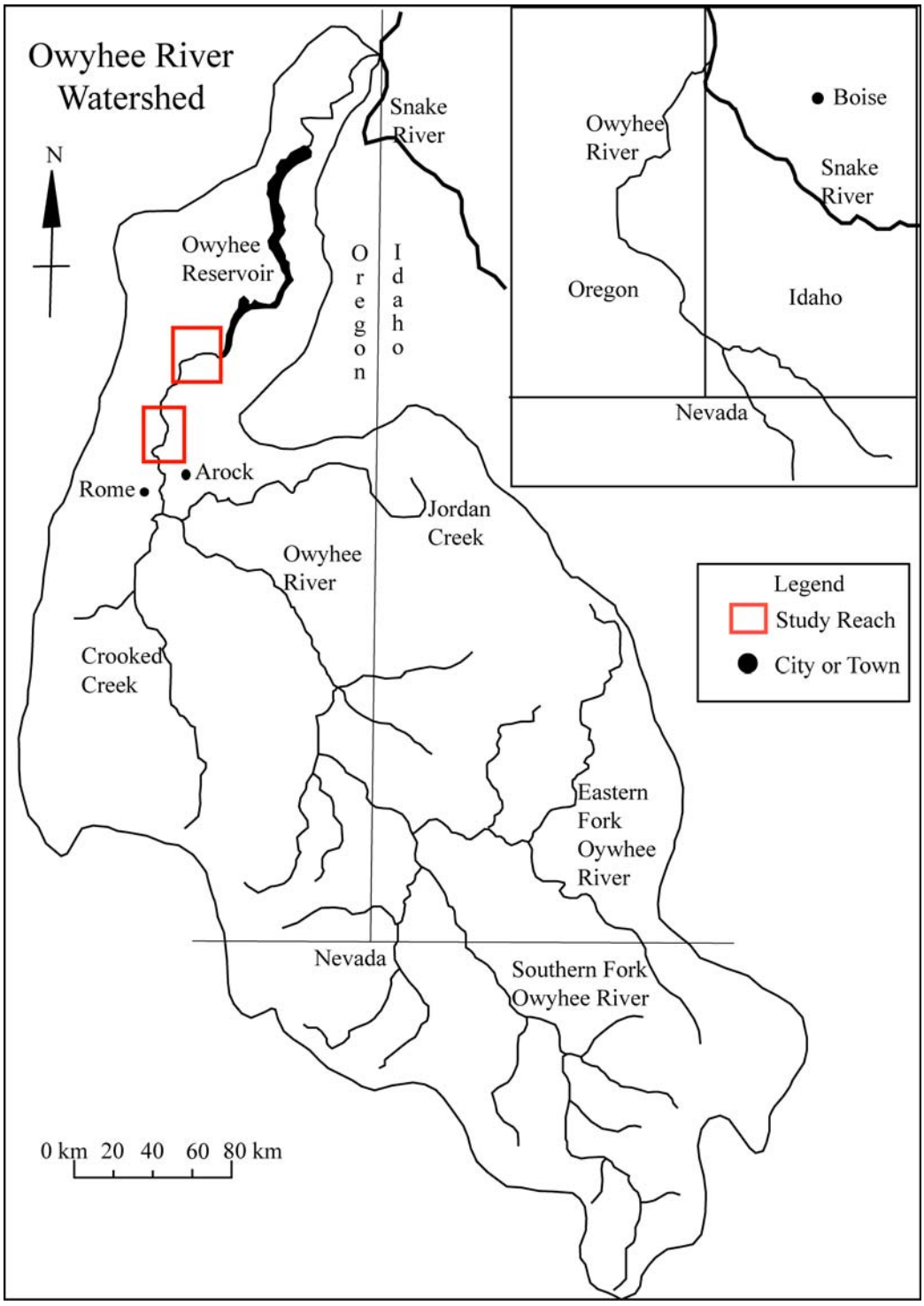

Figure 1. Location map. Shows entire Owyhee River, including the head waters of the southern fork and the eastern fork, both located in Nevada. Also included in the map is the confluence of the Owyhee River with the Snake River in Nampa, Idaho. The towns of Rome and Arock, Oregon and Boise, Idaho are included for reference.

studied in this paper. The stretch of the river being studied begins in the town of Rome, Oregon and ends near the confluence of Birch Creek with the Owyhee River (Figure 2).

Along this stretch of river there are several distinct types of mass wasting: smaller rock falls, rock topples, small slump events composed mainly of basalt, and much larger slump events in the upstream portion of the study area, and large earthflows in the downstream portion of the study area (categorization of events based on Varnes, 1978). The three different types of landslides that were chosen for further study exemplify the common types of mass wasting events in the upstream and the downstream reaches of the Owyhee River canyon study area. Similar mass wasting processes that relate spatially with the mass wasting events chosen for detailed study were also analyzed and mapped. The specific landslides of focus in this paper were chosen based on their relation to outburst flood deposits and their well-developed morphology. The large slump event, called Artillery Landslide, is at river kilometer 35 downstream from Rome, Oregon. It is the largest in a series of five large slump events along river right that increase in age downstream from Artillery Landslide. The rock fall, known as Hell's Gate Rock Fall, that obscures the toe of Artillery Landslide was also chosen for study as it later blocked the channel in the same location as Artillery Landslide. The other mass wasting events of interest are known as the West Spring Earthflow complex and East Spring Earthflow. These two earthflows are located between river kilometers 67 and 71 from Rome, Oregon. These earthflows are the largest and most morphologically intact earthflows in the study area, referred to as the Hole in the Ground. East Spring Earthflow, specifically, is the only event in that study reach whose boundaries were fully delineated.

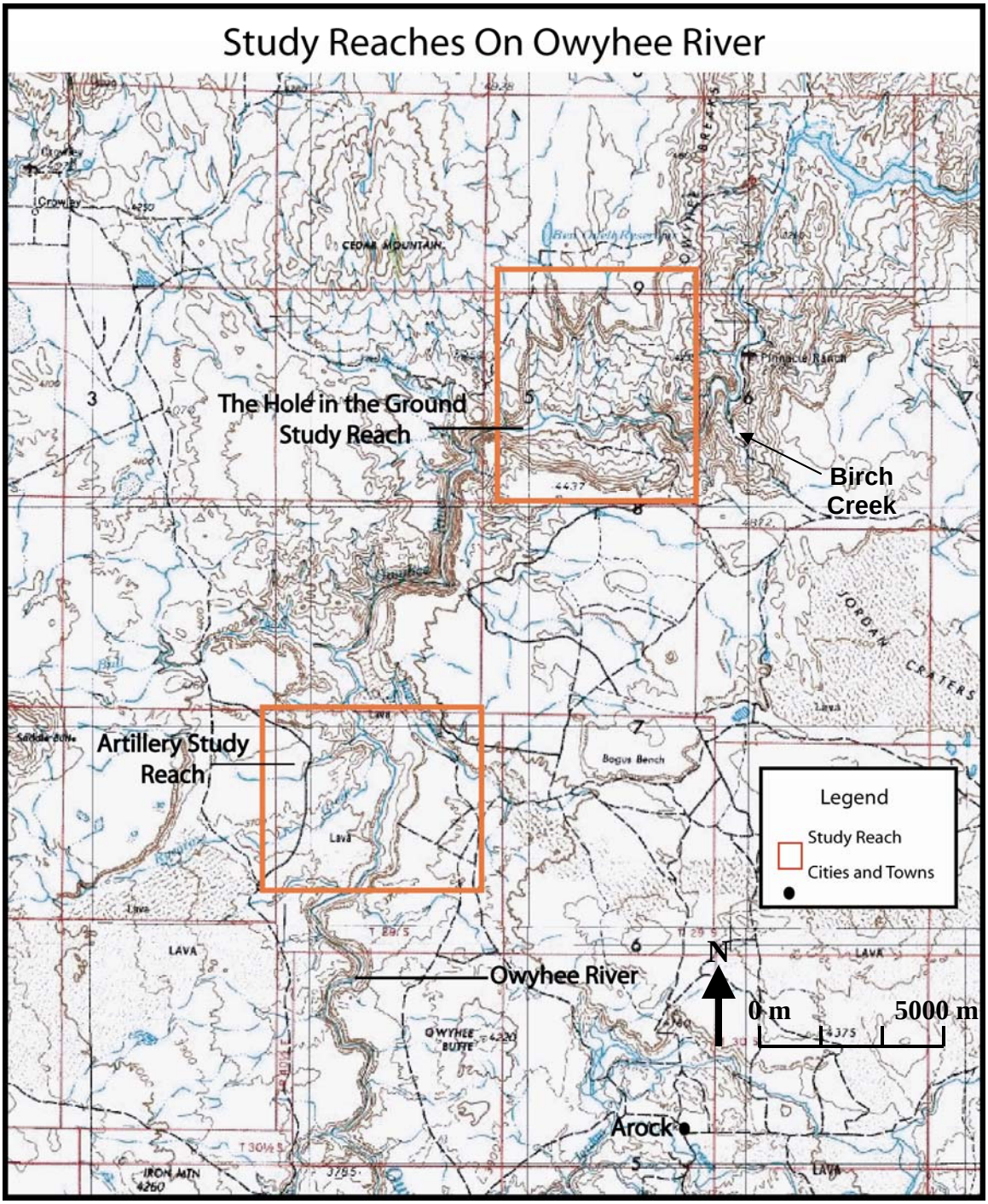

Figure 2. Larger scale map of the study area. Included in red boxes are the study reaches that were mapped for this study. Also included for reference is the town of Arock, Oregon and Jordan Craters Lava Flow.

To fulfill the main objective of this study, field mapping of both landslides and their surrounding areas was used to identify important geomorphic features on the landslides as well as related upstream aggradation and downstream outburst flood deposits. The data gathered from field observations were also used to understand relative age relationships of various landforms in the study reaches to create relative geochronologies of both study reaches, focusing, in large part, on the landslides chosen specifically for study. Results of the study will help establish a better understanding of how large, channel encroaching landslides affect long-term channel evolution and incision.

CHAPTER II

BACKGROUND

Geologic Setting

Geology, specifically composition and structural properties, exerts a first order control on the valley floor and the channel of a fluvial system by two related mechanisms (Grant et al., 2003). The first mechanism is that local geology directly determines the hill-slope processes and landforms impinging on a river valley. These can include mass-wasting events, resistant bedrock outcrops, or easily eroded bedrock outcrops. The second mechanism is the history of geologically mediated disturbances to the river bottom. This can include mass wasting events as well, but also channel-encroaching lava flows. These disturbances are recorded in the local stratigraphy and in valley bottom features, such as flood plains, terraces, and flood bars. Depositional features, such as terraces and flood bars, define the channel morphology and constrain lateral and vertical channel migration (Grant et al., 2003). Thus, it is essential to understand local geology when describing the evolution of a fluvial system.

The study area is part of a regional geologic structure consisting of the Oregon-Idaho Graben (OIG), the Snake River Plain, and the Yellowstone Plateau. These regional geologic structures form a linear, late-Cenozoic volcanic province that is characterized by thick deposits of rhyolite tuffs and interbedded alluvial and lacustrine sedimentary rocks, which are overlain by basalt flows (Rodgers et al., 1990).The OIG is a north-trending, low-elevation synvolcanic graben that is 50-60 km wide and 100 km long (Cummings et al., 2000). The graben is located adjacent to the inferred western margin of the North

American craton (Cummings et al., 2000). The dimensions of the graben have been approximated because of post graben volcanic deposition and sedimentation. The northeastern region of the graben has been truncated by faults that can be identified by abrupt stratigraphic changes (Cummings et al., 2000). The southeastern margin of the graben is defined by a series of north-striking faults located immediately east of the Oregon-Idaho state line (Cumming et al., 2000). The north- to northeast-trending western margin of the graben is well defined by a middle Miocene fault zones that juxtapose resistant flood basalt and other well-lithified volcanic rocks (Cumming et al., 2000). On the southern margin of the OIG, a Pliocene to Holocene basalt field buries the graben (Cumming et al., 2000).

Associated with the formation of the OIG are large-volume eruptions of rhyolite lavas and pyroclastic deposits. These rhyolite flows and ashflows are associated with the Lake Owyhee volcanic field (LOVF), which ranges in age between 15.5 and 15.0 Ma (Cummings et al., 2000). The ash-flow tuffs found in the study area were derived from caldera-forming eruptions and differ from the rhyolite lavas by having a relatively higher silica content (Cummings et al., 2000). The eruptions associated with these rhyolite lavas and ash flow tuffs are temporally and spatially associated with the waning phases of tholeiitic magmatism of the Columbia River Basalt Group and/or Yellowstone plume (Cummings et al., 2000).

Lithologies found within the study site are Tertiary sedimentary and pyroclastic rocks, Tertiary welded tuffs, Tertiary to Quaternary basalts, and Tertiary to Quaternary conglomerate that is associated with an Owyhee River paleochannel (Evans, 1991;

Bondre, 2006; Brossy, 2007). The Tertiary sediments and pyroclastic rocks were deposited in a lacustrine setting, indicated by the presence of chert, limestone, oolites, shell fragments, and thin cross-beds (Evans, 1991). This sedimentary/pyroclastic unit consists mostly of a white to grey, poorly to moderately consolidated bentonitic clays, siltstone, sandstone, and conglomerate with sporadic lenses of tuff, welded tuff, chert, and limestone (Evans, 1991). The Tertiary sedimentary deposits are overlain in many places by the Tertiary and Quaternary basalt flows, which, in turn, are capped in some places by Tertiary and Quaternary fluvial conglomerate and lacustrine deposits. The Tertiary conglomerate is mostly found on the plateau rims on both sides of the river canyon along the Artillery study reach. It is mainly composed of rounded clasts of basalt and welded tuff and also contains some pre-Cenozoic chert and quartzite cobbles (Evans 1991). The Tertiary conglomerate has been found to be as much as 30 m thick in some places.

The OIG is said to have evolved in three different stages. The first stage included constructional volcanogenic features as local topographic highs and the deposition of fluvial arkosic sandstone in local basins (15.4-14.3 Ma) (Cummings, 2000). The second phase of the graben evolution was the breakup of the graben floor into intragraben sub-basins during the eruption of calc-alkaline magmas (14.3-12.6 Ma) (Cummings et al., 2000). Finally, the last phase of OIG evolution was the return of basin sedimentation occurring contemporaneously with a decrease in the rate of subsidence, and waning volcanic and geothermal activity (12.6-10.5 Ma) (Cummings et al., 2000). The later Miocene and younger volcanism, subsidence, and hydrothermal activity have been

connected with the reorientation of regional stresses of the northwest-trending Snake River Plane and east-west-trending Antelope Valley graben (Cummings et al., 2000).

The Owyhee River has incised through the aforementioned dense basalt flows and into the lower, poorly to moderately consolidate fluvial, lacustrine, and pyroclastic layers. This stratigraphic sequence is seen in the hillslopes above the Owyhee River and is prone to large mass wasting events, such as rock falls, slump events, and earthflows. These events create natural dams that have the ability to completely block the river channel because of the narrowness of the valley and the volume of hillslope debris being introduced to the channel.

Landslides and Landslide Dams in Fluvial Systems

Landslide dams have been extensively studied and characterized in the past (Adams, 1987; Beebee, 2007; Bovis and Jakabo, 2000; Costa and Schuster, 1988; Dunning et al., 2005; Ermini and Casagli, 2002; Hermanns et al., 2005; Hewitt, 1998; Korup, 2002, 2005; Reneau and Dethier, 1996). The types of mass wasting that are the focus of this study were described by Varnes (1978) and include rock falls, rotational slump events, and earthflows. Rock falls are characterized by masses of geologic material that detach from a steep slope, commonly from parent material that is well jointed (Varnes, 1978). These types of mass wasting usually occur when the jointing becomes enlarged and the force of gravity overcomes the internal resistance of the rock body (Ritter et al., 2002). Rotational slump events are characterized by failure along a distinct zone of weakness that separates the sliding material from the stable underlying material (Ritter et al., 2002). Slump events result in a failure surface that is upwardly convex and

the movement of the slump occurs along a stationary axis that is parallel to the ground surface (Varnes, 1978). The final mass wasting style of interest is an earthflow. Earthflows are characterized as liquefaction of slope material flowing down slope, and generally creates a deposit with an hourglass shape showing a depression at the head of the event and a lobate toe at the base (Ritter et al., 2002). The majority of the volume of an earthflow is composed of clay- to silt-sized particles and many times the source of an earthflow is part of another, separate earthflow or a landslide of another type (Keefer and Johnson, 1983).

Landslides have been noted to greatly impact the fluvial systems that they impinge on for tens to thousands of years because of their ability to act as natural dams. Natural dams affect a river's two main components: water and sediment (Grant et al., 2003). Costa and Schuster (1988) characterized types of landslide dams by looking at 184 different dams around the world and placing these landslide dams into six different categories. This study uses the characterizations provided by Costa and Schuster (1988) to describe the dams of focus, which are common types of landslide dams. One type of landslide dam analyzed in this study is created by a large slump event. These events are the most common type of landslide dam characterized by Costa and Schuster (1988). They span the entire river valley floor and in some cases can deposit debris on the opposite valley wall. Large slump and sliding events are considered hazardous because of because of their size and ability to block a river channel and form an impounded lake and can possibly lead to a related outburst flood (Korup, 2002).

Another type of landslide dam to be addressed in this study is a landslide dam created by a flow- or an avalanche-type mass wasting event. The dams created by these mechanisms of mass wasting are the second most common type of landslide dam. The flow-type of landslide dam is characterized by debris moving a considerable way both up and downstream from where the flow or avalanche enters the river channel (Costa and Schuster, 1988). These types of dams are also considered hazardous because of their potential to create impounded lakes that can lead to outburst flooding as well as their ability to block tributaries entering the main valley, which causes additional hazardous impounded lakes (Korup, 2002).

The effects of a landslide dam on a fluvial system greatly depend on whether the dam impounds water and sediment, the longevity of the landslide dam, and how quickly breaching occurs (Hewitt, 1998). Conditions that promote the stability and resistance of a landslide dam to erosion are the size and shape of the barrier, the composition and induration of the debris in the dam, and the rate of emplacement (Hewitt, 1998). Though stable geometry and large size are usually imperative for the stability of a landslide dam, the compaction and composition of a dam is more crucial to the dam's longevity. The instability of many landslides dams can be attributed to heterogeneous composition and poor consolidation (Hewitt, 1998).

Effects of Landslide Dams on River Profiles

Landslide dams can alter landscapes in profound ways depending on their size and stability; i.e., landslide dams remaining stable for long periods of time can act as effective sediment traps, whereas some fail rapidly and generate catastrophic downstream

flooding (Reneau and Dethier, 1996; Korup, 2002). The presence of a dam for any amount of time can have effects both upstream and downstream, and these effects are different depending on the size of the impounded lake and the amount of sediment collected behind the dam. The effects of landslide dams can be placed into two different categories, onsite and offsite effects (i.e., upstream and downstream effects) (Korup, 2002). Onsite hazards are bed aggradation of the channel upstream of the dam and secondary landslides into an impounded lake behind the initial landslide dam (Korup, 2002, 2005). Offsite effects include large outburst floods and related Earthflows during the breach of a landslide dam (Korup, 2002).

The typical response of a river to dam emplacement is a sediment surplus above the dam and a sediment deficiency below the dam. When there is a sediment surplus in a river, the channel accumulates sediment leading to channel aggradation, which is a typical upstream response of a river to dam emplacement (Grant et al., 2003; Korup, 2005). When a sediment deficiency exists in a river system, sediment is excavated from its bed and banks. Thus, the typical downstream reaction of a fluvial system to dam emplacement is channel incision and lateral adjustments (Grant et al., 2003). Incision occurs as a response to the interaction between individual floods and the channel bed, which are, in turn, influenced by flood hydrology, sediment transport, channel gradient, and substrate resistance (Reneau, 2000). The variability of channel responses upstream of a dam reflects the relationship between the extent of modification to the natural flow and the rate at which new sediment is supplied to the channel in relation to the amount of sediment trapped behind the dam (Fassenacht et al., 2003).

Another important and lasting effect of landslides entering a river channel is the armoring of the channel by large boulders. Landslides that enter the channel do not have to dam the river to leave remnants that armor the channel. One lasting effect associated with armoring of the channel is a significant inhibition of vertical erosion (Beebee, 2003). Vertical erosion is decreased because the clasts that armor the channel are generally too large to entrain during normal flows and, many times, too large to entrain during meteorological floods. Large clasts deposited where mass wasting events have entered a river channel not only inhibit incision of the channel locally but can also inhibit incision downstream if the channel was completely blocked and the breach of the landslide dam resulted in an outburst flood.

Outburst Flooding

Outburst floods are simply flooding that results when a dam's integrity is compromised, leading to the rapid expulsion of the impounded lake behind the dam. Most landslide dams fail within one year of their formation. Ermini and Casagli (2002) reviewed 500 cases of landslide dams from around the world. In 205 of the cases reviewed failure was documented during the dam's existence; in the cumulative distribution, 40% of the landslide dams failed one day after their formation and 80% failed one year after formation, only 20% persist for longer periods of time. The magnitude of outburst floods, therefore, depend on the stability and longevity of a landslide dam creating an impounded lake, which affects the capacity of the lake behind the dam and the rate of sediment and water flowing into the impounded lake as well as dam composition and dimensions (Adams, 1981; Coast and Schuster, 1988; Ermini and

Casagli, 2002). The capacity of the lake that can form behind a landslide dam affects the amount of water that is released during an outburst flood (Fenton et al., 2006). In fact, the actual magnitude of a flood reflects both the volume and expulsion rates of the water source and the physiographic characteristics of the landscape that receives the flood waters (O'Connor et al., 2002).

The failure of a dam depends on the cohesive strength of the landslide dam materials. Materials such as silts, sands, and cobbles will fail more readily than more cohesive materials, such as large blocks or cohesive clays (Costa and Schuster, 1988). Silts, sands and cobbles become thoroughly saturated, in comparison to large blocks and clays, and saturation of dam materials can lower the shear strength of the dam (Costa and Schuster, 1988). As a result, the dam may not be able to withstand an increase of hydrostatic pressure from the increasing volume of water collecting in the impounded lake behind a landslide dam. If the dam cannot withstand the increase of hydrostatic pressure, the dam can be rapidly eroded during overtopping creating an outburst flood (Costa and Schuster, 1988).

Another factor considered when discussing the breaching of a dam is the geomorphic impact of the outburst flooding. Because landslide dams act as both a sediment and water trap in a fluvial system, outburst floods not only entrain water from behind the dam but also sediment deposited behind the dam. As a result, outburst floods have a greater geomorphic potential than other types of flooding events, such as meteorological floods, which do not entrain as much sediment. Because of the concentration of sediment in the floodwaters, an outburst flood can act more like a

hyperconcentrated flow, which has a greater ability to incise a channel downstream from a landslide dam (Korup, 2002). Another important factor of the geomorphic impact of a landslide dam breach is that the peak discharge of an outburst flood usually depends on the outlet geometry of the breach rather than the lake volume or breach formation rate (Manville et al., 1999).

CHAPTER III

METHODS

Geologic Mapping

A geomorphic map for both study reaches was created as a tool to compare the differences in geology and geomorphic processes in the two reaches. The mapping of this study was based on initial mapping by Plumely (1986), Evans (1991), and Brossy (2007). Specifically, close attention was paid to the various morphological attributes associated with the different exemplary mass wasting events that were the focus of this study. The maps were used to better understand the surface topography and deposits of both study reaches. Mapping was based on both aerial photographs and overland field work for ground truthing. ArcMap 9.2 software was used to create two maps, one of each study reach. Particular attention was given to mapping distinctive characteristics of the landslides chosen for comparison: Hell's Gate Rock Fall, Artillery Landslide, West Spring Earthflow complex, and East Spring Earthflow (Figure 2). Though much of the area mapped within the two study reaches was explored overland, the rim geology of Artillery reach and the larger mass wasting complexes of the Hole in the Ground reach were mapped using color stereo aerial photos and 1:24,000-scale topographic maps. The names of some of the mapped units in Artillery reach and the Hole in the Ground reach were based on maps by Evans (1988) and Plumely (1986) and many of the basalt flow units delineated on both reach maps were based on work by Brossy (2007).

The boundaries of landslides in the Artillery reach were distinguished in the field and on aerial photos based on the orientation of landslide blocks and the shape of the

landslide scarps. In many cases, such as in Artillery Landslide and Landslide 4, the orientation of the uppermost blocks near the shared boundary of both landslides were slanted at opposite angles mimicking the structure of each landslide scarp.

The margins of mass wasting events mapped in the Hole in the Ground reach were much harder to delineate as a result of the reinitiating of landslides as well as younger landslides covering older landslides. Because of these factors, the boundaries of separate landslides are not completely visible. As a result, landslides in the Hole in the Ground study reach were placed into landslide complexes based on topography and contacts with in-situ Tertiary sediments that were emphasized during incision by ephemeral streams. Only one mass wasting event in the Hole in the Ground study reach was fully delineated as a single event, the East Spring Earthflow. The mapped boundaries of the East Spring Earthflow were based on fieldwork. However, the source of the flow was observed from a distance and confirmed by aerial photos.

Characterizing Landslide Events and Composition of Geology Beneath Local Basalt Cap

The four major landslides described in this study were described in detail by measuring various parameters to better compare the different mechanisms of mass wasting and to determine the extent the landslides have affected the river channel. Measurements from the field and topographic maps were used to obtain rough estimates of the following characteristics: the thickness of the local basalt cap, the thickness of exposed underlying sediments, the distance of the main scarp from the river channel, the proposed dam height and length, the width of the channel where the river has incised

through the landslide dams, the size of the clasts composing the dam, the volume eroded from the landslide dams resulting in the current channel morphology, the estimated volume of the reservoir behind the proposed dams, the volume of flood bars downstream of the dams, and the average diameter of the clasts on the downstream flood bars. The estimates of these parameters relating to Artillery Landslide, Hell's Gate Rock Fall, West Spring Earthflow complex, and East Spring Earthflow were placed into a table for comparison.

The volume eroded from dam breaches and the volume of downstream flood bars and impounded lake reservoirs were all calculated by treating each mass as a cube. The length and width of the eroded portions of the landslide dams were estimated using a topographic map and the assumed heights of the landslide dams of focus were estimated based on the height of the preserved landslide and earthflow toes for Artillery Landslide, West Spring Earthflow complex, and East Spring Earthflow and the height of the remnants of Hell's Gate Rock Fall. The calculations for the volume of the flood bars downstream from the mass wasting events of interest was performed by measuring the approximate length and width from a topographic map and using estimates of average height based on longitudinal profiles recorded in the field (discussed in full below). Finally, estimates of reservoir depths were based on the assumed height of each landslide dam above the current river channel. The length of the impounded reservoirs were estimated by finding where the topographic contour associated with the height of each landslide dam crosses the river channel, suggesting the farthest upstream location that could have been affected by the blockage of the river by each landslide of focus. Finally,

15 to 20 measurements of canyon width related to the highest elevation of each landslide dam were taken along the entire estimated length of each impounded reservoir and averaged to calculate an average width of the reservoirs. The estimated heights, widths, and lengths of each reservoir were then used to estimate the maximum volume of the reservoirs.

The geology presumably composing both Artillery Landslide and East Spring Earthflow was determined using both hand sample and thin sections taken from an in-situ outcrop within Artillery Landslide and from an outcrop that has been exposed by stream incision underneath the East Spring Earthflow (Figure 3, A and B). Individual units of the outcrops were sampled for both hand sample and thin section. Individual units of each sampled outcrop in both study reaches were determined based on lithology changes such as differences in visual appearance, texture, grain size, and lithologic composition. A stratigraphic section was described for each of the sample sites (Figure 3, A and B). Hand samples were described in the field by determining rock type through grain size and visible mineral components. Samples composed of predominately clay and silt were differentiated in the field by gauging the gritty texture when the sample was tasted to discern between silt and clay-sized particles. Hand samples were later sent to Wagner Petrographic in Utah to create thin sections.

All hand samples were placed in clear epoxy before being cut to 30 micron sections because of the lack of induration. Samples were then mounted on glass slides and covered with cover slips. The thin sections were described using a petrographic microscope for better characterization of texture, grain size, and mineralogy. The results

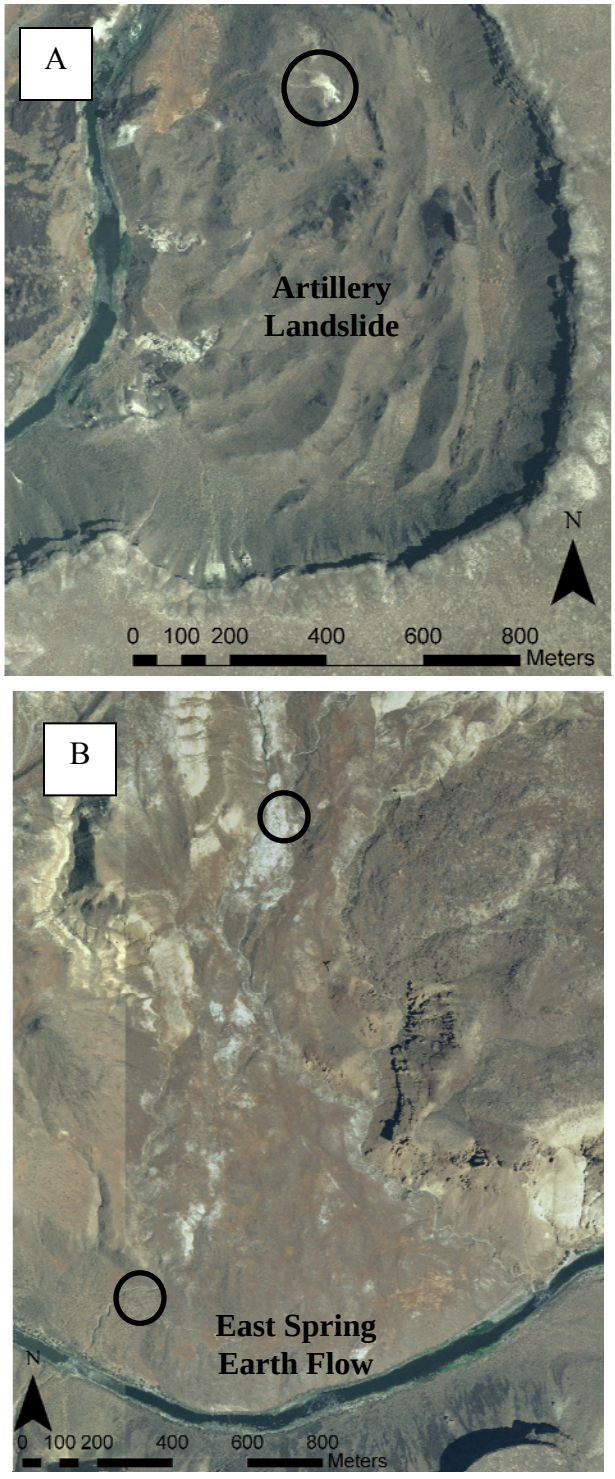

Figure 3. Hand sample and thin section sample locations. (A) Artillery Landslide. (B) East Spring Earthflow. Circles show where samples for sediment analysis were taken to describe the geology underlying the basalt cap for both mass wasting events.

of the hand sample and thin section descriptions were used to compare the geology associated with Artillery Landslide and East Spring Earthflow. The geology described from both reaches was used to determine whether there were any noticeable differences between both reaches regarding the units underlying the basalt caps in the two study reaches that could account for the different mass wasting mechanisms.

Relative and Absolute Dating

The relative ages of landslides in the Artillery reach were based mainly on the freshness of the main scarp, weathering of the topography over the entire landslide, revegetation of the landslide blocks, the pattern of drainages along the edges and within the mass wasting event, the relationship of the toe to the modern river channel, and the relative superposition of the mass wasting event to other mass wasting events as well as to flood bars and terraces near the river channel (McCalpin, 1984; Keaton and DeGraff, 1996). The freshness of landslide blocks was determined based on how coherent the basalt cap was after the landslide block detached from the canyon wall, i.e., if there were still coherent basalt columns in the landslide block as opposed to disaggregated basalt cap. Fewer exposed fresh basalt blocks and a flatter topography over the entire landform was assumed to indicate a greater landslide age and large, fresh basalt blocks lacking vegetation were assumed to be younger. In the Hole in the Ground region, the landslide complexes are too complicated to delineate the relative ages of many of the mass wasting events. However, the dissection of the larger landslide complexes by ephemeral streams and well-established vegetation similar to surrounding areas that lack mass wasting suggests an older age of mass wasting (McCalpin, 1984).

Cosmogenic dating conducted by Dr. C. Fenton (GeoForschungs Zentrum Potsdam) was used in this study to date the young geomorphic features in both study areas. Cosmogenic dating is one type of dating used on young, Quaternary-aged geologic deposits. The dateable age range for cosmogenic dating is between less than 1 ka and several Ma (Lang et al., 1999). Cosmogenic dating is done by measuring the concentration of cosmogenic radionuclides in a given sample. The rates of accumulation of the measured nuclides are proportional to the cosmic ray flux and to the concentration of target nuclides in the surface of the sample material. It is the concentrations of these nuclides that are used to measure the amount of time a sample material has spent at the surface of the earth (Lang et al., 1999).

Cosmogenic isotopes are created by the process of spallation reactions (i.e., shattering of a nucleus) induced by high energy nucleons, secondary thermal neutron capture reactions, and by muon-induced reactions (Cerling and Craig, 1994). Spallation reactions produce daughter isotopes that have a smaller sum of protons and neutrons than the target isotope (Cerling and Craig, 1994). The production of cosmogenic isotopes is a function of cosmogenic ray flux (which changes over time), latitude, altitude, and the length of time the sample has been exposed to cosmic rays (Lang et al., 1999). Three conditions must be satisfied for cosmogenic concentration of isotopes to accurately indicate exposure age: (1) the surface was formed by the excavation of a sufficient amount of rock to prevent any prior exposure to penetrating cosmic rays, (2) the surface has not been reburied or shielded for enough time to alter the amount of cosmogenic isotopes being created, and (3) the sample has not been eroded and lost any significant

amount of material that would affect the concentration of the radiogenic isotopes being measured (Ballantyne et al., 1998). Because the production of nuclides decreases with depth, it is imperative to sample the upper 4 cm of the rock (Cerling and Craig, 1994). Thus, the history of the sample must be well known to accurately interpret the calculated age. Any previous exposure will result in an overestimation of true age and any burial, shielding, or shading will underestimate true age.

The cosmogenic dates reported in this paper are based on ^{3}He from olivine analysis. Cosmogenic ^{3}He ($^{3}He_{c}$) is ideal for use in cosmogenic dating of young basalt and lava flows and basalt-rich geomorphic surfaces because ^{3}He is produced and preserved in olivine and pyroxene phenocrysts (Cerling and Craig, 1994; Fenton et al., 2002; Gosse and Phillips, 2001). Another important reason for the use of ^{3}He in cosmogenic dating is because it is a stable isotope with the highest and most well-established production rate of all in-situ cosmogenic nuclides (Cerling and Craig, 1994; Gosse and Phillips, 2001). Some sources of error in using cosmogenic dating of radiogenic ^{3}He are that it can be inherited and can also be produced by muons other than those created during spallation (Cerling et al., 1999). Also, the datable age range when using ^{3}He is narrower than 1ka to several Ma, because the in situ ^{3}He in material that is older than several Ma overwhelms the concentration of cosmogenically derived ^{3}He nuclides yielding an older apparent age (Lang et al., 1999). Furthermore, atmospheric scaling models for nuclide production are still being refined (e.g., Balco et al., 2008; Amidon et al., 2008).

Although cosmogenic dating has been used to date landslides in the past (Ballantyne et al., 1998; Cerling and Craig, 1994; Lang et al., 1999), the landslides in both reaches have reinitiated movement over their lifetime and have prior exposure dating issues (which will be addressed below). As a result, cosmogenic samples were taken from assumed associated, rounded boulders on flood bars and terraces downstream of the landslide events and also from what is believed to be a spillway located on Artillery Landslide. These samples will be used to obtain minimum ages of Artillery Landslide/Hell's Gate Rock Fall complex and East Spring Earthflow. Since these two mass wasting events are of the greatest importance to this study, the majority of samples were taken from basaltic flood boulders immediately downstream of both landslides, which are assumed to be boulders associated with outburst flooding. Other cosmogenic dates used in this paper are from Fenton (2002) and Brossy (2007) and are associated with spatially related lava flows and terraces.

The cosmogenic samples used for dating in this study were taken in accordance with the collecting protocol described by Goss and Phillips (2001) and Fenton et al. (2002, 2004) and analyzed by Dr. C. Fenton. The olivine was separated from the samples by using magnetic and density separation techniques. The olivine crystals that were separated were then analyzed by a noble gas mass spectrometer at the University of Rochester or at the United States Geological Survey (USGS) in Denver, CO (Brossy, 2007). The samples were melted under vacuum conditions at 1400° C and the helium isotopes were measured (Brossy, 2007).

Flood Boulder Analysis

The exemplary landslides of focus in this study have flood boulder deposits immediately downstream from the assumed blockage where the landslides entered the river channel. In Artillery reach these flood bars are referred to as Terrace 2 and in the Hole in the Ground reach the main flood bars of focus was Greeley Bar (Figure 4, Figure 5). The boulders measured for analyses were very likely deposited by an outburst flood related to the breach of the dams created by the landslides of focus based on the proximity of the flood boulders on related flood bar surfaces to the landslides of interest. Measurements of these flood boulders were used to calculate the shear stress needed to entrain and deposit these boulders as well as the velocity at which these boulders were dropped from suspension. Three different measurements, height, diameter, and

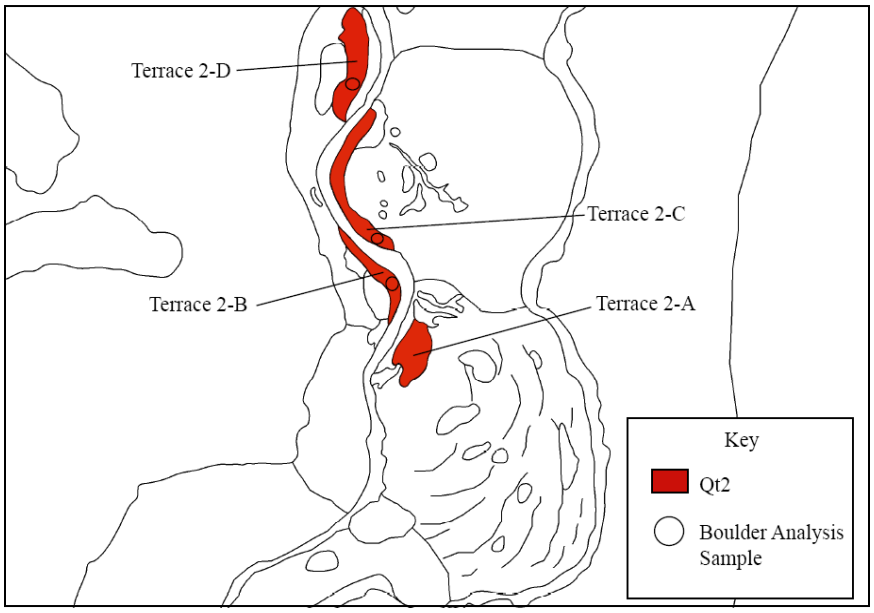

Figure 4. Terrace 2 surfaces. Terrace 2 of Artillery reach is shaded. The small circles indicate the area where flood boulder samples and measurements were taken. Measurements were only taken from Terraces Qt2-B, Qt2-C, and Qt2-D.

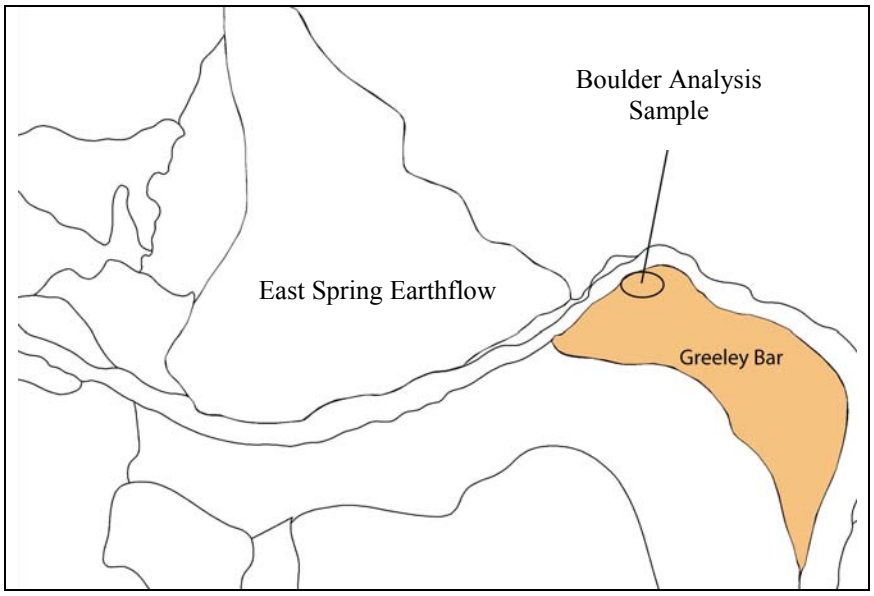

Figure 5. Greeley Bar in relation to East Spring Earthflow. Circle shows location of flood boulders sampled and measured for analysis. Greeley Bar was also the sample site for boulders used in the cosmogenic dating.

circumference, as well as global positioning systems (GPS) locations and hand samples to identify the basalt source for each flood boulder were taken for each flood boulder chosen for analysis. Measurements, locations, and samples were obtained for the five largest boulders on Terraces 2-B, 2-C, and 2-D in Artillery reach and Greeley Bar in the Hole in the Ground reach. The diameter of each boulder was placed into the Shields equation to calculate the boulder's shear stress of entrainment ($N*m^2$). The shear stress of deposition ($N*m^2$) was calculated by placing the boulder diameters into the power functions derived by Costa (1983) and O'Connor (1993). The velocity of deposition for each measured boulder was also calculated using the power function derived by O'Connor (1993). Velocity of deposition was also estimated by placing the diameters of the measured boulder on the velocity of deposition curve produced by Costa (1983). The

following equations were used to obtain shear stress of entrainment, shear stress of deposition, and velocity of deposition:

$$\tau = 26.6D^{1.21} \text{ (Costa, 1983)}$$

$$\tau = 0.33D_1^{1.12} \text{ (O'Connor, 1993)}$$

$$\tau = \tau_{ci}(\rho_s - \rho_l)gD_1 \text{ (Shields, 1936)}$$

$$v = 0.29D_1^{0.60} \text{ (O'Connor, 1993)}$$

where v equals velocity (m/s), D is the diameter of flood boulder (m), τ is shear stress ($N*m^2$), τ_{ci} equals the dimensionless shear stress factor (which is generally 0.06), ρ_s is the density of the sediment (basalt is 3.011 g/cm^3), ρ_l is the density of liquid (water, 1 g/cm^3), and g is the acceleration of gravity (9.8 m/s^2) (Shields, 1936; Costa, 1983; O'Connor, 1993). Values obtained from these equations and values estimated from the velocity of deposition curve from Costa (1983) were placed into tables for comparison. The velocity of deposition was also graphed using the average velocity of deposition calculated for boulders measured in Artillery reach and plotted versus distance from the assumed blockage of the Artillery Landslide/Hell's Gate Rock Fall complex to see how velocity changes with distance from the landslide dam.

Boulders found on the toe of East Spring Earthflow were also measured for comparison with boulders measured on Greeley Bar. Once again, the height, diameter, and circumference were measured on boulders located in the upper and lower portions of the East Spring Earthflow. Boulders that remained on the toe of the earthflow were clearly not entrained during an outburst flood from East Spring Earthflow and as a result

could indicate whether the availability of large boulders was a limiting factor in the size of the boulders deposited immediately downstream of the earthflow.

Terrace Characteristics and Longitudinal Profiles

Initial observation of the terraces in both study reaches showed some relation to the mass wasting events of focus. Thus, characterization of the composition of terraces and flood bars, terrace and flood bar profiles, and the slope of the terraces and flood bars relative to the local river profile was studied to determine the process that created the terraces as well as the possible relation to the landslides of focus. The composition of each terrace was observed and recorded in the field. Terrace long profiles were recorded differently for Artillery reach and the Hole in the Ground reach (Figure 6 and Figure 7, respectively). The Artillery reach terrace profiles were all recorded on Terrace 2 surfaces on Artillery Landslide and also immediately downstream of the Artillery Landslide/Hell's Gate Rock Fall complex (Figure 6). The Artillery reach terrace profiles were recorded by E. Safran (personal communication, 2007) using a Trimble GeoXT GPS unit in the field with 10 readings per vertex that were collected approximately every 10 paces. The accuracy setting was at a minimum of five satellites for data collection. The data were differentially corrected out of field using TerraSync. The coordinates and elevations were then recorded in Microsoft Excel and plotted in a distance vs. elevation graph. The elevations vs. distance graphs were then used to determine how the terraces in Artillery reach and the landslide dams of focus were related to each other based on their respective elevations.

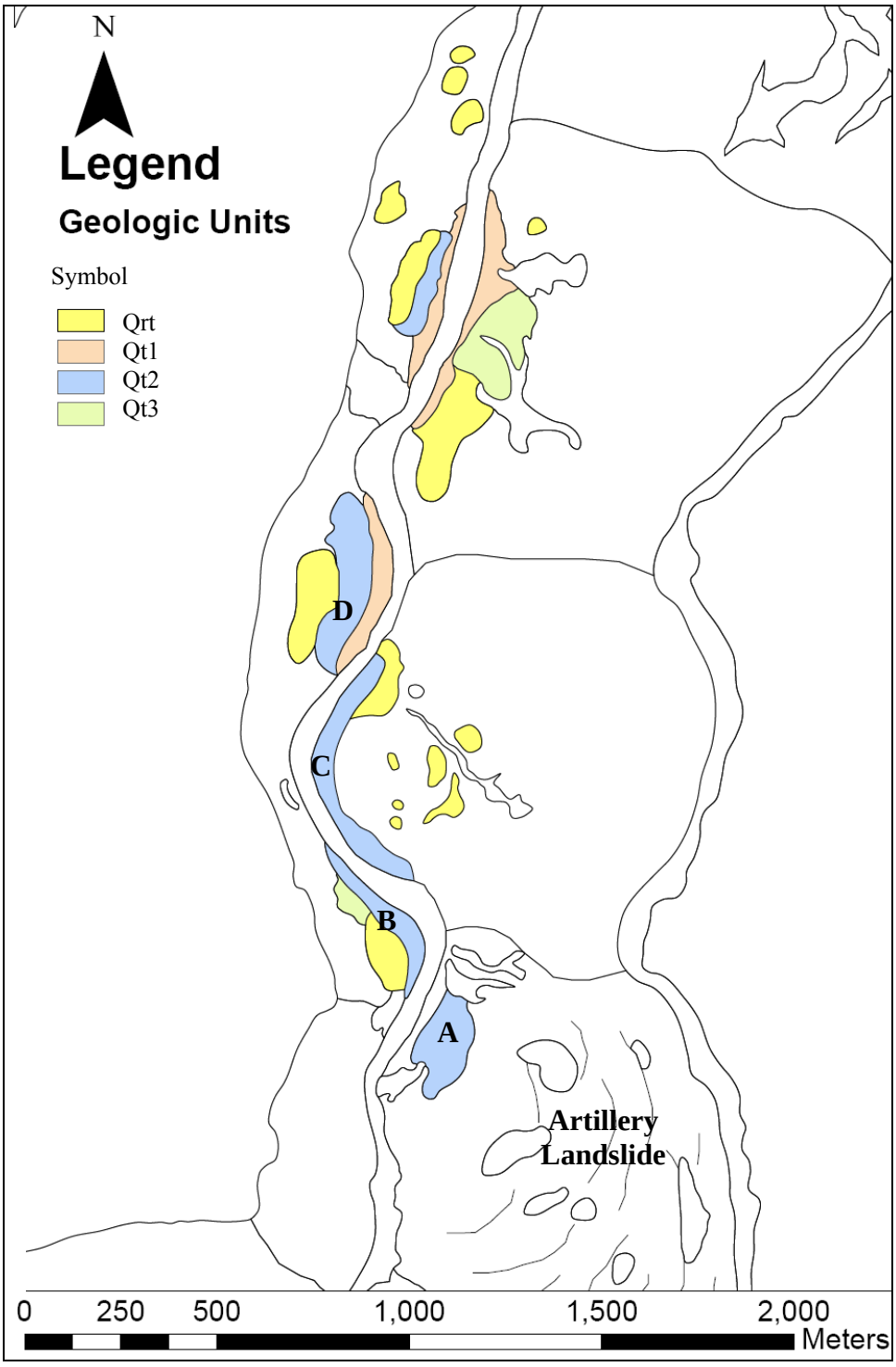

Figure 6. Artillery reach surveyed terraces. The terraces shown in this figure are labeled with the letter that corresponds to the set of terraces. The Terrace 2 surface is shown in blue and is the primary terrace surface that was surveyed. Terrace set D is also shown and has profiles related to all of the terrace surfaces, Qt1 through Qt3.

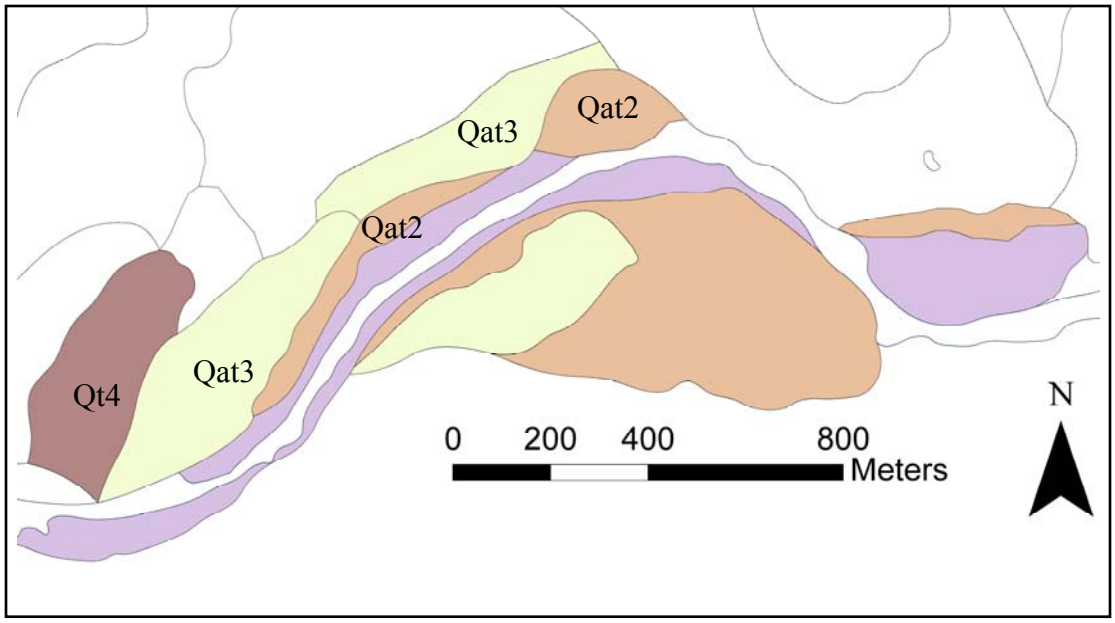

Figure 7. Hole in the Ground surveyed terraces. Terraces that were surveyed for this study are labeled with the appropriate terrace level. Qt1 is the active gravel bar just above the channel.

The profile of terraces found in the Hole in the Ground reach was recorded using a laser range finder in the field. The terraces surveyed in the Hole in the Ground reach were limited to terrace surfaces upstream of the West Spring Earthflow complex and the East Spring Earthflow (Figure 7). The laser range finder was set in a stationary position and a separate person walked the length of the terraces, stopping every 20 paces to take a GPS location and elevation. When the person walking the length of the terrace stopped, the stationary laser range finder was used to find the distance and the difference in height between the person walking the terrace from the stationary laser range finder. All points along the transect were recorded and used in Excel to create a terrace profile.

The terrace profiles described above were then plotted against river profile data obtained from Brossy (2007). The average terrace elevation of each terrace was plotted

against river kilometers to show the elevation of the terraces surveyed above the current river profile along with other elevations of terraces taken in the field with a GPS unit and elevations of terraces estimated from 1:24,000-scale topographic maps. Measurements of height, width, and volume for terraces whose profiles were not recorded in the field were measured using a 1:24,000 topographic map. A terrace–river profile was created for both Artillery reach and the Hole in the Ground reach.

The slope of the terraces of focus, including Terrace 2 in Artillery reach and aggradational Terrace 2 and Terrace 3 in the Hole in the Ground reach, were calculated using the elevations and lengths recorded in the field from longitudinal profiles and from topographic map measurements (Figure 6, Figure 7). These slopes were then compared to the river profile reported in Brossy (2007) to see how the slope of the terraces related to the slope of the river channel and also to compare the slopes of different types of terraces, i.e., flood bars versus aggradational terraces. Terrace longitudinal profiles plotted against the river profile are important for the comparison of different elevations of terraces and also to determine if any trends develop when the terrace elevations are plotted against the modern river profile. Characterizing terraces in these different ways can also potentially show the source of flood terraces and the blockage that created aggradational terraces.

CHAPTER IV

RESULTS AND INITIAL INTERPRETATIONS

Mapping

The mapping of each study reach was done to determine which major rock units were involved in the majority of the mass wasting events of the region as well as to determine the geomorphic features that are related to mass wasting, such as fluvial terraces and the mass wasting events themselves (Plate 1 and Plate 2, appended). The maps created for both study reaches were built upon previous work, giving greater detail to the landslides of focus and related geomorphic features found near the river channel. Evans (1991) mapped the majority of the Artillery reach, but some of the units were mislabeled. Generally, the unit most frequently mislabeled throughout Artillery reach was the Tsv sediments, which are mapped on top of many of the large slump events on river right. The sediments that have been labeled Tsv in Evans (1991) in many cases are Quaternary sand and gravel deposits (Qrt) proposed to be deposited as aggradation behind the lava dam created from the West Crater lava flow encroaching on the Owyhee River channel (Brossy, 2007). Newly mapped geomorphic features include the Quaternary lacustrine deposits (Qfli), Quaternary cobble deposits (Qrt), and all levels of terraces in the Artillery reach (Qt1, Qt2, and Qt3). The units are shown on Plate 1.

The geology of the Hole in the Ground reach was previously described and mapped by Plumely (1986). However, many of the surficial deposits and geomorphic landforms have been further differentiated for this paper in order to better describe channel and hillslope evolution in the reach. The greatest detail of the Hole in the Ground

reach map was given to the geomorphic fluvial features close to the river channel and to East Spring Earthflow. However, many of the hillslope landforms and rock units were also mapped up to the basalt cap at the canyon rim. The newly mapped and described geomorphic features include East Spring Earthflow and other earthflow complexes, at least four levels of flood bar terraces and aggradational terraces, and largely intact alluvial fans capping in-situ rock that has not been affected by mass wasting.

Basalt flows in both study reaches were described first by Plumely (1986) and Evans (1991). The basalt flows delineated by these authors are the Quaternary basalt (Qb) and the Tertiary basalt (Tb) in the Artillery reach (Plate 1) and solely the Tertiary basalt (Tb) in the Hole in the Ground reach (Plate 2). The youngest lava flows of both study reaches have been subsequently further divided into individual units by Brossy (2007), including the Saddle Butte basalt (Qbs), Clarks Butte basalt (Qbc), and West Crater basalt (Qbw) in Artillery reach and Greeley basalt (QTbg) and Upper AMPM basalt (QTbc) in the Hole in the Ground reach and the Bogus Rim basalt (QTbb) in both study reaches (Plates 1 and 2, respectively).

Both maps are a first draft that will contribute to a larger mapping project currently in progress (Kyle House, Nevada Bureau of Mines and Geology, personal communication, 2007). Though the maps provided in this paper are necessary to understand the evolution of the river, further mapping will show more of the geologic context and stratigraphy in both study reaches.

Unit Descriptions (Plate 1)

Artillery reach

Tertiary Interbedded Volcanic and Volcaniclastic Rocks (Tsv)

This sedimentary/pyroclastic unit consists mostly of a white, grey, and brown, poorly to moderately consolidated sandstone, siltstone, conglomerate, and bentonitic clay with sporadic lenses of tuff, welded tuff, chert, and limestone (Evans, 1991). The Tertiary volcanic and volcaniclastic rocks were deposited in a lacustrine setting, indicated by the presence of chert, limestone, oolites, shell fragments, and thin cross-beds (Evans, 1991).

Tertiary Undifferentiated Basalt Flows (Tbu)

The canyon rim basalts are the extensive basalt cap deposited along river right in Artillery reach. These basalt flows were originally mapped by Evans (1991) and were referred to as simply Tertiary basalt. This basalt is lighter in color compared to younger basalt flows in the region, such as the Saddle Butte basalt flows and West Crater basalt flow (Brossy, 2007). The Canyon rim basalts caps the exposed portion of the Tsv sediments that are found on river right along the entire mapped region of the Artillery reach. The Tertiary-aged canyon rim basalt flows are the oldest flows involved in the mass wasting in Artillery reach.

Tertiary Rim Gravel (Trg)

The Trg deposit is not well indurated and is composed primarily of cherty and meta-sedimentary cobbles in a silt to fine-sand matrix. The Tertiary rim gravels cap the canyon rim Tertiary basalt and range in thickness from a thin veneer of a few centimeters to 4 m thick in Artillery reach. However, the Tertiary rim gravels has been found to be as

thick as 30 m in some places. These gravels can be differentiated from the gravels found lower in the Owyhee River canyon because they lack fresh basalt clasts. Evans (1991) reported this deposit as a paleo-Owyhee River cobble deposit.

Quaternary Basalts

The Quaternary basalts present in the Artillery study reach are the Saddle Butte basalt (Qbs), Clarks Butte basalt (Qbc), and the West Crater basalt (Qbw). These flows are fully described in Brossy (2007).

Quaternary Fluvial and Lacustrine Deposits (Qfli)

Another newly described deposit differing from previously published mapping projects is the Quaternary lacustrine deposit (Qfli) (Plate 1). Qfli deposits are only found in the downstream portion of Artillery reach, immediately behind the remnants of the West Crater lava dam. Deposits are found on both sides of the river, overlying the West Crater basalt and the Saddle Butte basalt, and are also located in mounds immediately downstream of Landslide 2 (Figure 8). The Quaternary lacustrine deposits can be differentiated from the Tsv sediments because of their very light, white color and their lack of interbedded basalt flows and fluvial gravels, which are found within the Tsv deposits. Another characteristic of the Quaternary lacustrine sediments that distinguishes them from the Tsv sediments is the competency of the deposit. The Qfli deposits are fairly soft and easily erodable. The Tsv deposits are much more indurated than the Qfli deposits. The relative ages of the two lacustrine deposits were differentiated based on their stratigraphic position in the field. In some places near the West Crater lava dam, Qfli cap preexisting Tsv sediments.

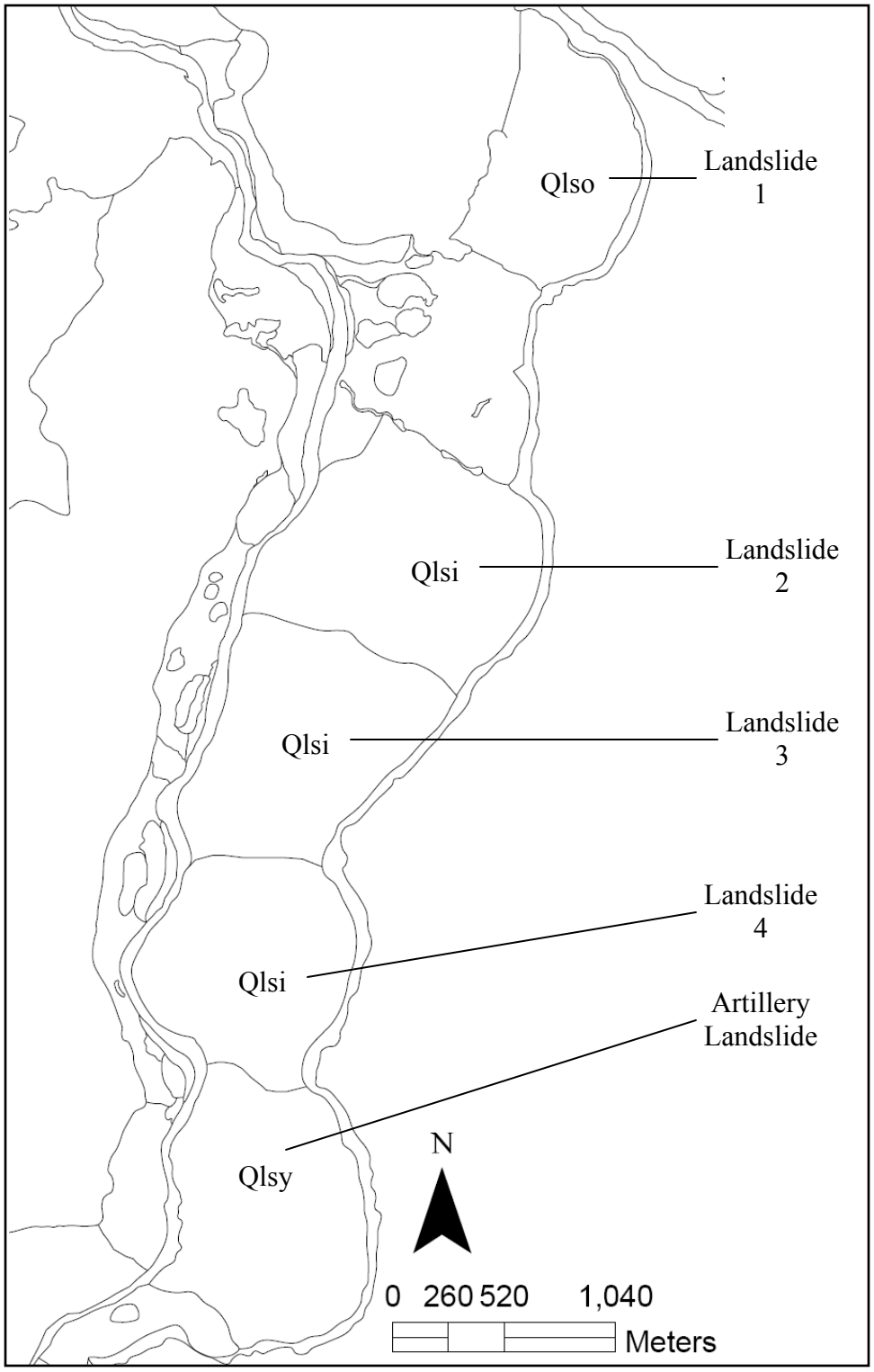

Figure 8. Sequence of landslides in Artillery reach. Unit labels and landslide name is reported.

Undifferentiated Landslides of Unknown Relative Age (Qls)

The undifferentiated landslides in Artillery reach are the events found on river left that occur directly from the Saddle Butte basalt. These mass wasting events include large rock topples, rock falls, and slump events that are much smaller than the slump events found on river right. The compositions of these undifferentiated landslides are mainly clasts of disaggregated Saddle Butte basalt and rarely contain much exposure of the underlying Tsv sediments, unlike the larger slump events found on river right.

Older Quaternary Landslide (Qlso)

Landslide 1 is one of the large slump events that line river right and is the farthest downstream landslide in the sequence (Figure 8). The West Crater basalt covers the toe of the landslide leaving only one landslide block exposed. The basalt cap portion of the landslide block has been completely disaggregated as a result of erosion, leaving a rounded overall morphology to the landslide block. The block has also been somewhat revegetated. Landslide 1 is the oldest of the five large slump events in Artillery reach. This age relationship was determined by the only preserved landslide block showing smoother topography than seen in the landslide blocks of other slump events upstream and almost complete vegetation cover over the landslide surface as well as the contact of the landslide with the West Crater basalt (McCalpin, 1984).

Intermediate Quaternary Landslide (Qlsi)

The intermediate landslides are located between Landslide 1 and Artillery Landslide. These landslides include Landslide 2 through Landslide 4 (Figure 8). The intermediate landslides are not covered by the West Crater basalt, like Landslide 1.

However, the intermediate landslides show some excavation by fluvial action and deposits of Quaternary terrace and aggradation gravel deposits (Qrt) are found on the toes of all the intermediate landslides. Also, the landslide blocks on many Qlsi landslides show well-rounded blocks near the toes and younger, well-preserved landslide blocks near the main scarp. The lower blocks have also been thoroughly revegetated, where as the upper blocks have not been revegetated and still contain cohesive basalt cap as part of their composition.

Younger Quaternary Landslide (Qlsy)

Artillery Landslide (i.e., Qlsy) is located approximately 35 river kilometers north of Rome, OR. Artillery Landslide is the only landslide in the Artillery reach that is referred to as a younger Quaternary landslide (Figure 8). Directly below the scarp are fresh landslide blocks that moved more recently than the toe of the landslide leaving them little time to become weathered or vegetated. The landslide blocks creating the toe of Artillery Landslide show visible, well-defined morphology suggesting a lesser amount of weathering in comparison to the toes of other large slump events. Near the toe of the landslide, landslide blocks differ in orientation from the younger landslide blocks that are found near the scarp. The difference in orientation and greater weathering of the landslide blocks near the toe of the landslide in comparison to landslide blocks near the scarp suggests that movement on Artillery Landslide has reinitiated over its history. The overall preservation of the morphology of Artillery Landslides makes it the only large slump event where reinitiation of the slump can be clearly observed. Artillery Landslide has been determined to be the youngest in the series of landslides on river right based on the

preservation of the landslide blocks near the toe of the landslide and also because of the lack of revegetation found on the upper, near-vertical blocks. Artillery Landslide also lacks the thick deposits of river gravels that are seen deposited on the toes of Landslide 2 through Landslide 4 (Plate 1). Further discussion of Artillery Landslide will occur in Chapter V.

Young Closed Depressions on Landslide Surfaces (Qdy)

Closed depressions are found on the six large slump events that line river right, although the majority of the mapped closed depressions can be found on Artillery Landslide (Qlsy). These closed depressions are generally found behind the backward-rotating blocks that have rafted away from the main landslide scarp. The closed depression found on Artillery landslide are filled with eolian and alluvial silt and those that are closer to the main scarp have thin veneers of rim gravel (Trg) on the surface of the depression.

Terrace and Aggradational Gravel Deposits (Qrt)

Another newly described and extensive deposit in this paper is referred to as the Quaternary terrace and aggradational gravels (Qrt). These gravels have been differentiated from the Tertiary rim gravels (Trg) based on composition and deposition elevation. The Quaternary gravel deposits contain fresh basalt clasts in their composition, unlike Trg, along with the characteristic chert and quartzite gravels that define all Owyhee River fluvial gravel deposits. Deposits of the Quaternary gravels are found much closer to the river channel than the Trg, which are deposited on the canyon rim. The Quaternary gravels compose some of the terraces surfaces and are also deposited on

landslide surfaces, mainly Landslide 2 though Landslide 4. These deposits of Owyhee River gravels were mapped along the river valley upstream from the West Crater lava dam and range in thickness from a few centimeters thick to 26 m of gravels.

Quaternary Aeolian Deposits (Qe)

The eolian deposits in Artillery reach are composed of light-colored clays to fine-grained sands that create dunes on both sides of the river canyon. The eolian dune deposits on river left are deposited on top of the Saddle Butte basalt and on river right eolian dunes are deposited between the base of Landslide 1 and the edge of the West Crater basalt. The eolian deposits are composed mostly of disaggregated lacustrine and fluvial deposits from the sediments initially deposited behind the West Crater lava dam (Qfli).

Colluvium (Qc)

The colluvium deposits generally include both talus slopes of angular rock fragments from the erosion of the basalt flows forming the canyon walls as well as other canyon wall detritus. These generally well-sorted talus slopes can grade into finer-grained deposits down slope that are composed of poorly sorted silts to boulders (Evans, 1991).

Young Spring (Qsy)

These deposits are young, active springs with associated fine-grained deposits that are heavily vegetated and found inside the river canyon. They represent ground water seeps that most likely flow along unit contacts or formation boundaries (Plumely, 1986).

Quaternary Terraces (Qt1, Qt2, and Qt3)

Another newly described group of geomorphic features near the river channel in Artillery reach are the various terraces levels (Plate 1). On the appended map, the terraces have been distinguished by color and represent three different levels of terraces. Several terrace levels, specifically Terrace 2 and Terrace 3, can be found on some of the landslide surfaces in Artillery reach, including Artillery Landslide. The terraces in Artillery reach are flat-topped terraces that change composition from upstream to downstream. Upstream terraces are composed of large basalt boulders in a matrix of both fine sediments and gravels and downstream terraces change in composition to river gravels in a sand/silt matrix and also no longer contain basalt-boulder flood deposits. These downstream sandy terraces are assumed to contain both fluvial and eolian sand deposits.

The upstream terraces, namely Terrace 2, contain two populations of basalt boulders: a subangular population in the gravel/sand and silt matrix and a rounded boulder population resting directly on top of the terrace surface. The exposed portions of the subrounded population of boulders appear to be much smaller than the flood boulders that rest on the upstream surfaces of the terraces. This subrounded boulder population was only moderately shaped by fluvial processes before becoming partially buried by fluvial sediments. The other population of boulders present on many of the terraces, specifically Terrace 2, are large, well-rounded flood boulders resting on top of the terrace surface and, at times, show imbrication, indicating fluvial emplacement by high velocity flood waters.

Alluvium of the Active Fluvial System (Qra)

This unit contains poorly sorted silts to basalt boulders. However, the majority of the unit is Owyhee River cobbles and organic materials that can be found in and along the river channel. The active channel in Artillery reach also shows obvious bedrock exposures, which are expressed as very straight and continuous riffles that span the entire channel. These bedrock exposures can only be seen in very low flows, generally during the summer months.

Unit Descriptions (Plate 2)

The Hole in the Ground Reach

Tertiary Interbedded Volcanic and Volcaniclastic Rocks (Tsv)

This deposit was first described by Plumely (1986) as weakly to moderately indurated volcaniclastic sediments. These sediments are mainly composed of an orange-brown, fine-grained sandstone and siltstone. Bedded deposits of coarser sandstone and conglomerate with thin, interbedded basalt flows are present near the top of the section and exposed in the conduit walls of the East Spring Earthflow. The deposits found in the East Spring Earthflow conduit walls are very similar to the Tsv sediments described in Artillery reach, specifically those sampled within Artillery Landslide.

The Tsv sediment package in the Hole in the Ground reach has a unique lacustrine deposit topping the section that is not found in Artillery reach. The material comprising East Spring Earthflow and many other earthflow deposits is composed of this light colored, thinly bedded, clay-rich lacustrine deposit. This lacustrine deposit caps the other

regionally extensive, brown-colored Tsv sediments described above, which is found in both study reaches.

Tertiary Undifferentiated Basalt Flows (Tbu)

The Tertiary basalt cap, described by Plumely (1986), which defines the landslide scarp on river left of the Hole in the Ground reach has retreated to such degree that it has little input in the stream channel.

Quaternary-Tertiary Basalts

These basalts include the Greeley Bar basalt, Bogus Rim basalt, and the Clarks Butte basalt. These basalt flows are described in Brossy (2007).

Ancient Alluvial Fan Deposit (QTf)

The older fan deposits are mostly found on river right between the basalt cap and the large portion of the canyon wall that is marked by undifferentiated landslides. These alluvial fans are composed of fine-grained canyon wall detritus that began covering the stratigraphically older landslides, which these ancient alluvial fans rest on top of. They are most likely a result of the canyon wall returning to stability after mass wasting had occurred.

Alluvial Fan Deposits (Qfo, Qfi, Qfy)

The Quaternary alluvial fan deposits in the Hole in the Ground study reach include old alluvial fan deposits (Qfo), intermediate-age alluvial fan deposits (Qfi), and young alluvial fan deposits (Qfy), which range from Pleistocene to Holocene in age. These large alluvial fan deposits are only found in the Hole in the Ground reach. The alluvial fans in the Hole in the Ground reach are characterized by their smooth, slightly

dipping surface, and usually form the boundaries between landslide complexes (Plate 2). The alluvial fans that are now relict in the area are both Qfo and Qfi. The relict fans can be differentiated from active alluvial fans based on the presence of ephemeral streams that have incised the alluvial fans and have exposed the bedding of the underlying Tsv sediments.

Undifferentiated Landslide Complexes and Deposits (Qls)

Many mass wasting events mapped in the study reach were placed into earthflow complexes because of their intricate boundary relationships. These earthflow complexes are found only in the Hole in the Ground reach and were created where unconsolidated materials have flowed toward the river channel and, in some cases, have reinitiated flow multiple times. As the sediments mobilize in mass wasting events, they cover other earthflow events creating complexes where clear boundaries between events cannot be determined. The effect of this mass wasting process is a large area with clear landslide morphology, such as large hummocks and closed depressions, but no clear boundaries between different mass wasting events.

These large landslide complexes occur on both sides of the river valley in the Hole in the Ground reach. However, the large landslide complexes are more prevalent on river left. The presence of the steep landslide scarps of Tertiary sediments capped by dense basalt on river left results in continued mass wasting, in the form of slump events, directly from the main landslide scarp, which, further down the canyon become earthflows. The slump events creating the main landslide scarp are not as morphologically well defined as the large slump events found in Artillery reach. The

slump events of the main landslide scarp in the Hole in the Ground reach have less-consolidated, backward-rotating, slump blocks in comparison to the slump events in Artillery reach.

Young Landslide Deposit (Qlsy)

The young landslide deposit (Qlsy), referred to as East Spring Earthflow, is the only earthflow in the reach whose boundaries could be clearly outlined. The source of East Spring Earthflow is fairly close to the basalt cap where the predominant type of mass wasting is slumping. The source material of East Spring Earthflow is composed of light-colored, fine-grained lacustrine sediments. Though the source area of the earthflow has been located, the extent of the source is difficult to fully delineate because of erosion into the soft sediments that fed East Spring Earthflow. The toe of the earthflow is well defined and preserved in comparison to the upper reaches of the earthflow. East Spring Earthflow is hypothesized to be the youngest earthflow event in the reach based on its well preserved morphology displaying characteristic hummocky topography, closed depressions, and a well defined levee, which is the upstream boundary of the earthflow.

Colluvium (Qc)

Generally includes both talus slopes of angular rock fragments from the erosion of basalt flows of the canyon walls as well as other canyon wall detritus, such as Tsv sediments. These generally well sorted talus slopes at times grade into finer-grained deposits down slope that are composed of poorly sorted silts to boulders (Plumely, 1986).

Young Spring (Qsy)

These deposits are young, active springs found along the canyon that have related fine-grained sediments and are heavily vegetated. They represent ground water seeps that most likely flow along unit contacts or formation boundaries (Plumely, 1986).

Quaternary Terraces (Qt1, Qt2, Qt3 and Qt4)

There are four clear levels of depositional terraces in this reach. Qt1 is the active flood plain and contains mainly fluvially rounded, polished basalt boulders. The single Qt4 surface is the first terrace surface to appear in the Hole in the Ground reach, and is deposited immediately upstream and above the fill terrace deposits of the reach (Qat2 and Qat3). Qt4 has rounded basalt flood boulders in its composition that are located at the upstream end of the terraces surface (Figure 7). The terraces of specific focus in this paper are Qt3, which are flood bars found immediately downstream of the West Spring Earthflow complex. These three terrace surfaces are mainly composed of clast-supported, fluvially rounded to subangular basalt boulders in a finer-grained matrix of sands to silts. This elevation of terraces terminates immediately upstream from the East Spring Earthflow (Figure 7).

Aggradational Terraces (Qat2 and Qat3)

The aggradational terrace deposits are found in the upstream portion of the Hole in the Ground study reach and do not extend past the West Spring Earthflow complex. Terrace deposits Qat2 and Qat3 are composed of Owyhee River gravels, with lithologies including chert, quartzite, and basalt in a matrix of fine sands and silt and the clasts are less than 15 cm in size. The fill terraces are fairly rounded because of their easily erodible

composition. The composition, lack of induration, and size of the clasts composing Qat2 and Qat3 suggest that the units are fill terrace deposits created behind a damming of the river upstream.

Greeley Bar

Greeley Bar is immediately downstream of East Spring Earthflow and includes rounded boulders as part of its composition. The composition of Greeley Bar is mainly Owyhee River cobbles in a sand/silt matrix with some small basalt boulders, up to 15 cm in diameter, along the entire stretch of the bar. It thought to have been created by an outburst flood originating from the dam created by the East Spring Earthflow.

Alluvium of the Active Fluvial System (Qra)

This unit contains poorly sorted silts to basalt boulders. However, the majority of the unit is Owyhee River cobbles and organic materials that can be found in and along the river channel.

Characterizing Landslide Events and Composition of Geology Beneath Local Basalt Cap

The characteristics of each landslide discussed in this study are summarized in Table 1. The most important things to note in this table are the differing thicknesses of the local basalt caps in comparison to the exposure of Tsv sediments related to each type of landslide, and the distance of the landslide dams from the main landslide scarp (Table 1). Hell's Gate Rock Fall shows the thinnest basalt cap in both study areas but also has the least exposed Tertiary sediments beneath its related basalt cap. Artillery Landslide shows a somewhat thicker basalt cap and also has a much thicker exposure of Tertiary

sediments available for mass wasting. The earthflows of interest in the Hole in the Ground reach have thicker basalt caps than the other mass wasting events just described. However, the exposure of Tertiary sediments related to the earthflows is approximately five times greater than the exposure of Tsv related to Artillery Landslide and is almost 30 times greater than the exposure of Tertiary sediments related to Hell's Gate Rock Fall.

Another important result shown in Table 1 is the estimated volumes of the impounded lakes that possibly formed behind each of the landslide dams of focus. Based on these calculations, an impounded lake forming behind Hell's Gate Rock Fall would have the largest volume of all the landslide dams discussed, at 1.28×10^8 m^3. This number, however, is contingent on the cohesion and, thus, duration of the Hell's Gate Rock Fall dam. The reservoir associated with Artillery Landslide, like Hell's Gate Rock Fall, is also one magnitude larger than the reservoirs associated with the earthflow dams because of the greater assumed height of the dam, with a volume of 1.17×10^8 m^3. The earthflow dams have reservoirs that are one magnitude smaller than those studied in Artillery reach. The smaller impounded lake volume is most likely a result of the calculated estimates of the earthflow dam heights being half the height of the dams studied in Artillery reach. The dam heights were determined as the height of the spillway located on the toe of Artillery Landslide (which indicates that the reservoir behind either Artillery Landslide and/or Hell's Gate Rock Fall filled to at least that minimum elevation), the height of a presumed paleochannel channel across the toe of East Spring Earthflow, and the highest portion of the preserved toe found immediately above the river channel on river left for West Spring Earthflow complex. West Spring Earthflow

complex has the smallest associated reservoir because of the relatively low elevation of its assumed dam height. East Spring Earthflow has a higher dam height and a larger reservoir volume behind the East Spring Earthflow dam. Even though the dams were not as high for the East Spring Earthflow and West Spring Earthflow complex, the presence of aggradational terraces upstream of these dams indicates that they may have persisted longer than those in Artillery reach, which could contribute to their overall impact on the river, impacts that will be discussed later.

The other estimates calculated were the volume of the landslide dam that was possibly eroded away during the breach of each landslide dam and the volume of the related flood bars found downstream of the four landslides. These calculations were preformed to compare volumes of flood bars downstream from each landslide dam and the volume eroded from each dam were comparable, suggesting a single event, or if the volume of the flood bars suggests several building events. The collective volume of Terraces 2-B, 2-C, and 2-D is greater than the volume of material eroded from the breach of Hell's Gate Rock Fall. The volume of debris estimated to have been eroded from the breach of Artillery Landslide is also less than the volume of debris comprising Terrace 2, suggesting more than one breaching event must have created Terrace 2. The flood bars downstream of the West Spring Earthflow complex have a greater volume than the volume of debris proposed to have been removed from the toe of the West Spring Earthflow during the breach of the dam, also suggesting multiple building events of Terrace 3 in the Hole in the Ground reach. Lastly, the volume of Greeley Bar is less than the volume of debris potentially eroded from the dam of East Spring Earthflow.

However, terraces downstream of the study reach were not taken into account, and thus there is a source of error in the calculation of the volume of terraces downstream of the East Spring Earthflow. This also could possibly suggest that Greeley Bar was created by more than one breaching event.

Also, to help better understand the landslides of interest, hand sample analysis was less conclusive than thin section analysis because of limitations in correctly measuring grain size in many samples and identifying mineral fragments (Appendix A). Hand sample characterization of the two reaches showed that the geology underlying the basalt cap of Artillery Landslide contains units with larger grain sizes than clays and silts, including coarse sands interbedded with fluvial gravels. Texture in hand samples collected from underneath East Spring Earthflow was much more homogeneous, showing only very fine-grained units of clay- to silt-sized grains.

Thin sections allowed for a more thorough analysis of the mineral constituents and overall composition of the hand samples (Appendix B). In both study regions, sediments from the geology underlying the basalt caps were volcanically derived. Thin sections from both study reaches showed a main crystal component of quartz with a lesser degree of plagioclase. There was a larger mineral population in thin sections from Artillery reach, including minor amounts of biotite, pyroxene, and olivine.

Other noticeable differences between study reaches are the differences in texture. The texture of thin section samples from beneath East Spring Earthflow are mainly clays with sparse, angular crystal fragments. Weathered, bentonitic clays were differentiated from

ash based on increased birefringence of altered ash and the rounding of ash fragments from sharp spicules to unidentifiable grains.

Textures and composition of the geology underlying the basalt cap within Artillery Landslide are much more diverse, showing fine sands to conglomerate. Constituents include not only clays as a matrix component in many samples, but there is a much greater presence of rounded mineral fragments, glass shards, perlite, and rounded lithics. Samples generally coarsen upwards through the exposed section of Tsv in Artillery Landslide until reaching the interbedded coarse sand and volcanic conglomerate at the top of the section. This coarse sand and conglomerate unit is capped by a basalt flow.

Absolute Dating

Dating of the landslides in both reaches has proved to be extremely difficult because of unreliable dating techniques. The majority of the relative ages of geomorphic features were based on their stratigraphic relationship to known ages of spatially and temporally related lava flows. The only other dates available for this study are from ^{3}He cosmogenic nuclides collected from boulders on terraces in both reaches, specifically Terrace 2-C in Artillery reach and Greeley Bar in the Hole in the Ground reach, and a tephra sampled from within a closed depression on Artillery Landslide (Figures 3 and 4, respectively). The cosmogenic dates of these boulder samples are reported in Table 2 (Fenton, personal communication, 2007). Both sample sites of dated flood boulders are immediately downstream from where Artillery Landslide and Hell's Gate Rock Fall and where East Spring Earthflow entered the river channel. The flood boulders on the terraces

TABLE 2. AGE DATA COLLECTED FOR BOTH STUDY REACHES

Dating Methods	Data Location	Materials Sampled	Age
Ar/Ar dating[†]	Bogus Creek area, river right	West Crater basalt	60 to 80 ka
Ar/Ar dating[†]	Bogus Bench, Artillery reach river right	Bogus Rim basalt	1.9 Ma
Tephrochronology	In upper most closed depression Artillery Landslide	Mazama ash bed	7.0 ka
Cosmogenic 3He[‡]	Terrace 2-C, Artillery reach	Basalt flood boulder	10 ± 1 ka
Cosmogenic 3He[‡]	Terrace 2-C, Artillery reach	Basalt flood boulder	42 ± 3 ka
Cosmogenic 3He[‡]	Lower Greeley Bar, Hole in the Ground reach	Basalt flood boulder	24 ± 2 ka
Cosmogenic 3He[‡]	Upper Greeley Bar, Hole in the Ground reach	Basalt flood boulder	682 ± 48 ka

[†] Brossy, 2007.
[‡] Fenton, personal communication, 2007.
Note: The dates reported for Terrace 2-C in Artillery reach was provided using two different flood boulders. The dates reported for Greeley Bar are also from samples taken from two different boulders; however, the boulders sampled were located on two different locations on the flood bar. Tephrochronology was conducted by F. Foit at Washington State University.

were identified based on rounding and imbrications, which suggested entrainment by a high velocity flow, with the most likely local source of the flow being the breach of a local landslide dam. Although there were a number of flood boulders, those sampled for the dating were chosen based on the rounding and surface texture of the boulders as specified by Fenton (2002). The dates received from the boulders were used to obtain a minimum age of the outburst flood that deposited them.

Based on the data provided in Table 2, minimum ages can be assigned to Landslide 1, Artillery Landslide, Terrace 2, and Greeley Bar. The Ar/Ar ages of the West Crater basalt suggests that Landslide 1 is older than 60 to 80 ka because the West Crater basalt overlies Landslide 1. Artillery Landslide has a minimum age of 7.7 ka based on the presence of Mount Mazama tephra that was deposited in the uppermost closed depression found within the landslide depression. This gives a minimum date for the youngest phase of mass wasting creating Artillery Landslide and does not suggest the age

of the initial movement that is suspected to have created the landslide dam associated with Artillery Landslide. The presence of Mazama ash in a closed depression nearest the main landslide scarp does suggest that the last phase of mass wasting associated with Artillery Landslide occurred before the eruption of Mount Mazama.

The cosmogenic dating of flood boulders located on flood bars immediately downstream of the landslides of focus in this study returned a large range of ages for both Terrace 2 and Greeley Bar. Terrace 2 shows an age ranging from 10 to 42 ka. Because prior exposure can greatly affect the ages produced when using cosmogenic dating, the younger date reported is more likely to be closer to the date in which the boulders on Terrace 2 were deposited. Thus, the last outburst flood event to have aided in building Terrace 2 would have occurred at a minimum age of 10 ka. Another possibility for the ages of the two boulders is that they were deposited during two separate events at two different times, meaning the terraces would have to have formed in more than two events. The formation of the Terrace 2 surface also most likely post-dates the West Crater lava flow based on the lower position of the terraces in comparison to the elevation of Qrt terrace gravels deposited upstream of the West Crater lava dam. The lower elevation of the Terrace 2 surface suggests that, after the deposition of Qrt, the river had to incise further into the channel to later create the Terrace 2 surface. Thus, the Terrace 2 surface has a maximum age of 60 to 80 ka and a minimum age of 10 ka.

Boulders sampled from Greeley Bar show older dates in comparison to those sampled on Terrace 2-C in Artillery reach. The boulder sampled on the lower portion of Greeley Bar, which is closer to the modern river channel, shows an age of 24 ka, while

the boulder sampled on the upper bar yielded an age of 682 ka. The much greater age obtained from the boulder sampled on upper Greeley Bar could suggest that Greeley Bar was created during multiple outburst flood events. It is, however, quite likely that the flood boulder sampled on the upper bar had previous exposure, which has yielded an apparent age that is much older than the age of the boulder sampled on the lower bar. As a result, it is once again more useful to use the younger age obtained from the boulder sampled on the lower Greeley Bar, 24 ka. This suggests that the last major event to construct Greeley Bar occurred at a minimum age of 24 ka. .

The sources of error relating to cosmogenic dating are most often a result of the exposure history of the surface sampled being poorly known, the surface sampled undergoing significant erosion or shielding during the exposure that is being dated, and making unsupported assumptions based on isotope production rates (Lang et al., 1999). These sources of error are generally compensated by choosing sample surfaces where the general history of the surface is known coupled with recording a profile of possible shielding that could have taken place while the surface was exposed to cosmogenic rays. Although these precautions were taken, the dates reported from both terraces show a large discrepancy between dates of different boulders. Further cosmogenic dating of more boulders on these terrace surfaces and other geomorphic surfaces in conjunction with other dating techniques, such as more tephrochronology and/or optically-stimulated luminescence (OSL) dating of samples of local sediments that have accumulated on or behind the landslide dams or on the flood terraces, will help to better constrain the geochronologic data.

Flood Boulder Analysis

The shear stresses of entrainment and deposition for all measured flood boulders found on Terraces 2-B, 2-C, and 2-D in Artillery reach and Greeley Bar in the Hole in the Ground study reach are reported in Table 3. The velocity of deposition was calculated using the power function derived by O'Connor (1993) and estimated using the velocity of deposition curve from Costa (1983) (Table 4). The results of shear stress analysis show that the shear stress required for entrainment was higher than the shear stress required for deposition of the flood boulders from suspension for both power functions, a result that is to be expected. Another expected result is that the larger the diameter of the flood boulder the more energy needed for entrainment and the higher the shear stress value of deposition for the boulder. Conservation of momentum suggest that it takes less shear stress to keep a boulder in motion or deposit it than accelerate it from rest, and, for this reason, the O'Connor (1993) power function for shear stress of deposition yields lower shear stress values than the Shields equation (Beebee, 2003).

Other noticeable results from the boulder analysis are the discrepancy between the shear stress of deposition for the power function derived by Costa (1983) compared to the values produced by the power function derived by O'Connor (1993). The results obtained from the Costa (1983) power function were one magnitude higher than results received by using the power function derived by O'Connor (1993). O'Connor (1993) also found this to be the case when using the power function derived by Costa's (1983) to find the shear stress of deposition of boulders related to the Bonneville flood. A possible explanation for the large discrepancy is that the two power functions were used initially

TABLE 3. SHEAR STRESS OF MEASURED BOULDERS

Site and boulder	Diameter (cm)	Shear stress ($N*m^2$)		
		Shields equation	$\tau = 0.33D_l^{1.12}$	$\tau = 26.6D^{1.21}$
Artillery reach				
Terrace 2B				
1	315	3706	207	3000
2	290	3412	189	2700
3	210	2471	132	1800
4	250	2941	160	2100
5	250	2941	160	2100
Average	263	3094	170	2340
Terrace 2-C				
1	320	3765	211	3100
2	150	1765	90	1200
3	150	1765	90	1200
4	190	2236	118	1600
5	310	3647	204	2900
Average	224	2636	143	2000
Terrace 2-D				
1	220	2588	139	1900
2	280	3294	182	2500
3	190	2236	118	1600
4	200	2353	125	1700
5	195	2294	121	1650
Average	217	2553	137	1870
Hole in the Ground reach				
Greeley Bar				
1	170	2000	104	1400
2	140	1647	84	1100
3	120	1412	70	850
4	160	1883	97	1300
5	160	1883	97	1300
Average	150	1765	90	1190

Notes: Shear stresses necessary for boulder entrainment using the Shields equation and deposition based on power functions derived by O'Connor (1993) and Costa (1983), respectively, and using flood boulders measured on Terraces 2-B, 2-C, and 2-D in Artillery reach and Greeley Bar in the Hole in the Ground reach.

TABLE 4. VELOCITY OF DEPOSITION

Site and boulder	Diameter (cm)	Velocity (m/s)			Distance from dam
		$v = 0.29D_l^{0.60}$	Costa (1983)	Average	
Artillery reach					
Terrace 2-B					
1	315	9.1	8.1	8.6	392.70
2	290	8.7	7.3	8.0	405.10
3	210	7.2	6.7	6.9	413.60
4	250	8.0	7.2	7.6	420.10
5	250	8.0	7.2	7.6	401.40
Terrace 2-C					
1	320	9.2	8.2	8.7	568.10
2	150	5.9	5.5	5.7	570.80
3	150	5.9	5.5	5.7	566.60
4	190	6.8	5.8	6.3	572.40
5	310	9.1	8.0	8.5	578.20
Terrace 2-D					
1	220	7.4	6.4	6.9	1171.10
2	280	8.5	7.2	7.9	1172.10
3	190	6.8	5.8	6.3	1190.50
4	200	7.0	6.5	6.7	1197.70
5	195	6.9	5.9	6.4	1185.20
The Hole In The Ground					
Greeley Bar					
1	170	4.7	5.7	5.2	344.50
2	140	4.1	5.4	4.8	344.50
3	120	3.7	4.8	4.3	344.50
4	160	4.5	5.6	5.1	344.50
5	160	4.5	5.6	5.1	344.50

Notes: Different velocities needed for measured flood boulder to drop from suspension of an outburst floods occurring downstream of Artillery Landslide and East Spring Earthflow. Power function from O'Conner (1993) and other velocity numbers were estimated using the power function curve from Costa (1983).

to measure boulders dropped from suspension in two different flood situations. O'Connor (1993) used the power function derived in the paper to determine the shear stress values for the deposition of large flood boulders entrained during the catastrophic Bonneville outburst flood and Costa (1983) used the power function derived in his paper to measure

shear stress values for the deposition of smaller clasts during meteorological floods. Because the authors were measuring different clast sizes, it is possible that the power function derived by Costa (1983) is not useful in determining the shear stress threshold for clasts in large outburst floods.

The velocity of deposition power function derived by O'Connor (1993) and the power function curve presented by Costa (1983) shows much closer results for the velocity needed to release boulders from suspension. The results of this analysis are suspect, however, because the velocity of deposition was obtained by two different methods, one calculated by the power function derived by O'Connor (1993) and the other estimated using the power function curve produced by Costa (1983) and presented in O'Connor (1993) (Figure 9). The basic results of both the calculation and estimation are similar between the two results. Results show that the velocity at which clasts are released from suspension increases as the size of the boulder increases.

When the average of the calculations and estimates of velocity of deposition for Artillery reach are plotted versus the distance of the boulder from the dam where the related breach is proposed to have occurred, one can see a general decrease in velocity when moving downstream from the dam (Figure 10). Although there was a large range of boulders measured on Terrace 2-C, the boulders measured still fit the general trend that is presented in Figure 10.

Boulders were also measured on the upper and lower toes of East Spring Earthflow, on both sides of the paleochannel located along the length of the earthflow toe. The boulder measurements are reported in Table 5. These measurements show that

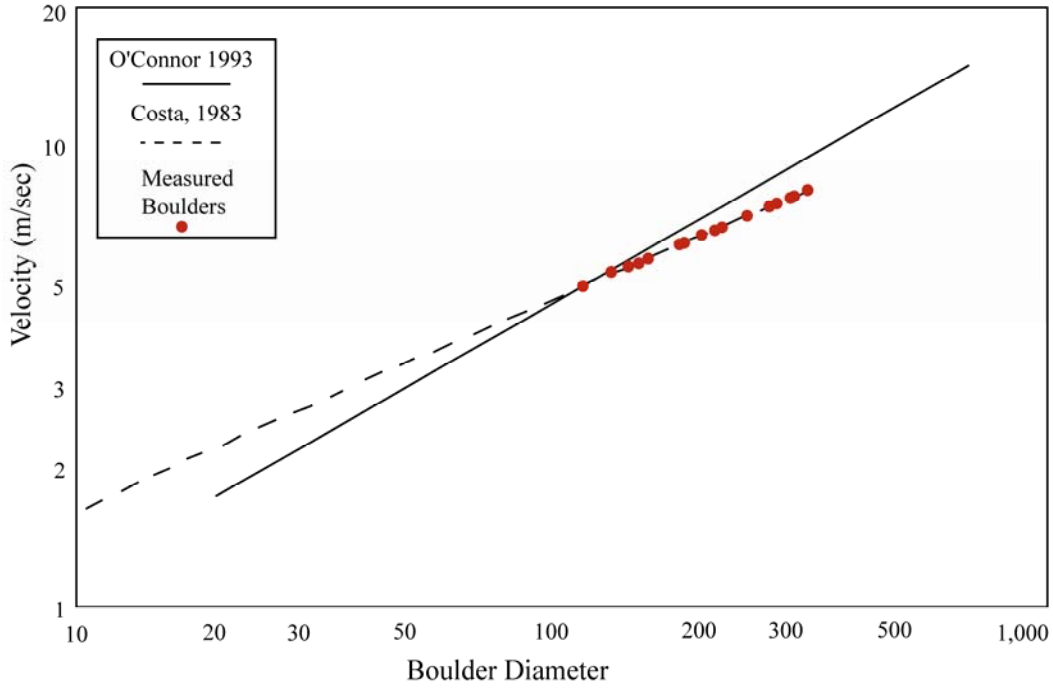

Figure 9. Measured boulder diameter plotted on power function derived by Costa (1983), reported in O'Conner (1993). Measured boulders were placed on the velocity of deposition curve derived by Costa (1983) and then compared to calculated measurements of velocity of deposition from O'Conner (1993).

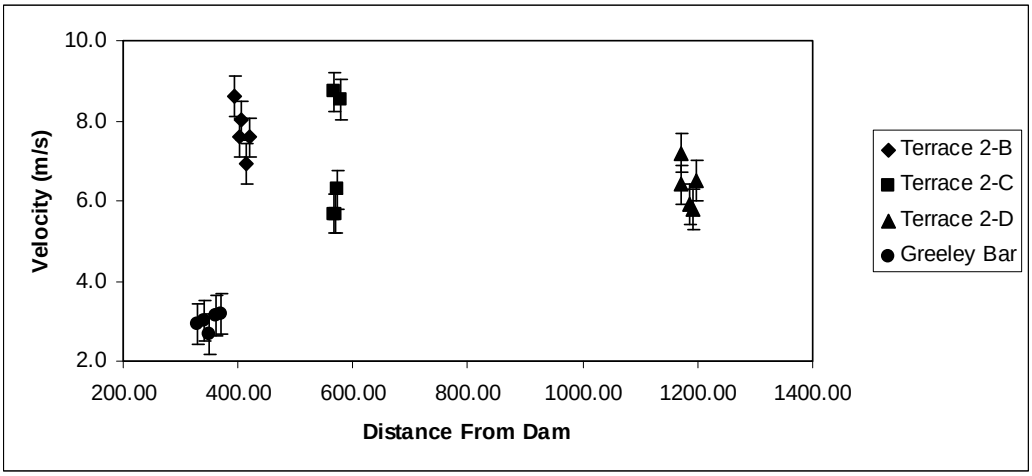

Figure 10. Graphic of velocity change from the dam breach in Artillery reach. There is a general decrease in velocity from the dam site. Velocity calculations from boulders measured on Greeley Bar are added for comparison, showing a much lower velocity of deposition.

TABLE 5. BOULDER MEASUREMENTS OF EAST SPRING EARTHFLOW AND GREELEY BAR

Site and boulder	Height (cm)	Diameter (cm)	Circumference (cm)
Greeley Bar			
1	70	170	370
2	90	140	250
3	120	120	320
4	100	160	410
5	95	160	430
Average	95	150	356
East Spring Earthflow			
Lower toe			
1	90	140	318
2	97	183	441
3	140	181	432
4	102	140	450
5	90	177	465
Average	104	164	421
Upper toe			
1	224	162	556
2	92	182	490
3	130	201	576
4	191	161	490
5	110	330	818
Average	149	207	586

Notes: The upper and lower portions of the toe of East Spring Earthflow are separated by a paleochannel that contains only a few boulders in its composition. This paleochannel is further described in Chapter V.

almost all of the boulders found on the lower toe of East Spring Earthflow are larger than the boulders found on Greeley Bar with the exception of one measured boulder. The boulders measured on the upper toe of East Spring Earthflow are much larger than those found on Greeley Bar. The comparisons of these measurements suggest that there was a threshold of entrainment above which boulders of a certain size were no longer entrained by the outburst flood resulting from the breach of East Spring Earthflow. This observation indicates that the availability of large boulders was not a limiting factor in the

size of boulders deposited downstream on Greeley Bar. The numbers provided in Table 5 help to give a maximum boulder size that could have been entrained during the outburst flood, a boulder size that can be compared with the shear stress of entrainment and deposition and velocity of deposition reported in Table 3 and Table 4.

Terrace Composition and Longitudinal Profiles

The terraces of focus in Artillery reach are mainly Terrace 2. The main terrace surfaces of focus are Terraces 2-A, 2-B, 2-C, and 2-D, which are all flat-surfaced terraces that have flood boulders resting on the top, with the exception of Terrace 2-A. The Terrace 2 surface is thought to have been created by several events, the last of which deposited the rounded flood boulders on the surfaces of Terraces 2-B, 2-C, and 2-D. Longitudinal profiles of Terrace 2 (Terrace 2-A through Terrace 2-D) and the other terrace surfaces related to Terrace 2-D (Terrace 1-D through Terrace 4-D) are reported in Appendix C (Figure 4). When comparing Terrace 2-A through Terrace 2-D, the elevations of the terraces lie within an elevation range between 970 m and 958 m. The terrace surface at the lowest elevation is Terrace 2-C, on river right, with an average elevation of 958 m above sea level. The other terrace surfaces, Terrace 2-A, 2-B, and 2-D, have average heights of 968 m, 962 m, and 964 m above sea level, respectively (Figure 4 and Figure 6).

There are two types of depositional terraces found above the river along the entire 6.3-km Hole in the Ground reach: boulder-rich flood bars and two levels of aggradation deposits found upstream of the two earthflow dams described in this paper (Figure 11).

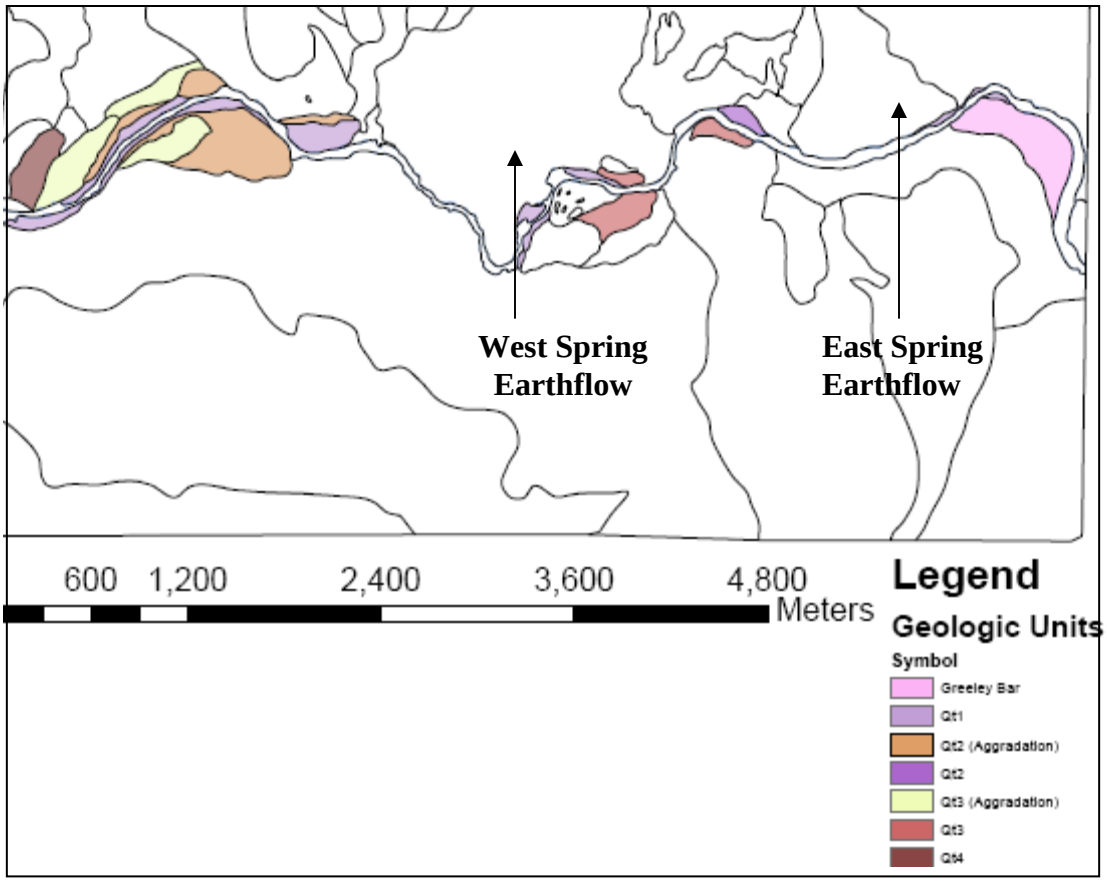

Figure 11. Terraces of the Hole in the Ground reach. All terrace surfaces are labeled by their composition and elevation. Qt4 is the only flood terrace found in the upper reaches of the study reach and is the very first terrace surface seen. All other flood bars are found immediately downstream of large Earthflows that show evidence of damming the river.

The aggradational deposits Qat2 and Qat3 are composed of poorly indurated river gravels and cobbles (Figure 11). The aggradational terraces found on river left were the only terraces surveyed in the reach. (Appendix C, Figure C8) The flood bars in the Hole in the Ground reach are mainly composed of clast supported rounded to subangular boulders in a fine-sediment matrix of sand to silt. With the exception of Terrace 4, found at the very upstream portion of the Hole in the Ground reach on river right, all other flood bars are found directly downstream from Earthflow blockages. The Qt3 surface is found deposited

immediately downstream of the West Spring Earthflow complex and Greeley Bar is found immediately downstream of the East Spring Earthflow (Figure 11).

The terrace profile from the Hole in the Ground reach shows three terrace levels, aggradational Qat2 and Qat3 and flood deposit Qt4, on river left (Figure 7). The only occurrence of Terrace 4 seen in the Hole in the Ground study reach is at the eastern edge of the mapped area, where the valley widens into the Hole in the Ground (Figure 7). The profile shows that the active flood plain, Terrace 1, is at an elevation of 870 m above sea level. The other levels of terraces, Qat2, Qat3, and Qt4, are at elevations of 882 m, 888 m, and 890 m, respectively.

The average terrace elevation of all the Terrace 2 surfaces, 2-A through 2-D, and the elevations of the terrace elevations of Qat2, Qat3, Qt3, and Greeley bar elevations were then plotted on an elevation versus river kilometer graph to get a sense of the height of the terraces above the river channel (Figure 12). The terrace elevations related to the Artillery Landslide/Hell's Gate Rock Fall complex show that there is a decrease in terrace elevation when moving from the blockage site. Also, the elevation of Terrace 2-C is at a lower elevation than the other Terrace 2 surfaces. The terrace elevations over the river profile in the Hole in the Ground reach show two different types of terraces. The elevations of the aggradational terraces taken from both sides of the river show that the longitudinal slope of Qat2 and Qat3 along the river is lower than that of the modern river channel. The nearly flat slope along with the terrace composition suggests that these terraces were not created by outburst floods. Other terrace elevations are related to flood bars that occur immediately downstream from the blockages that most likely created

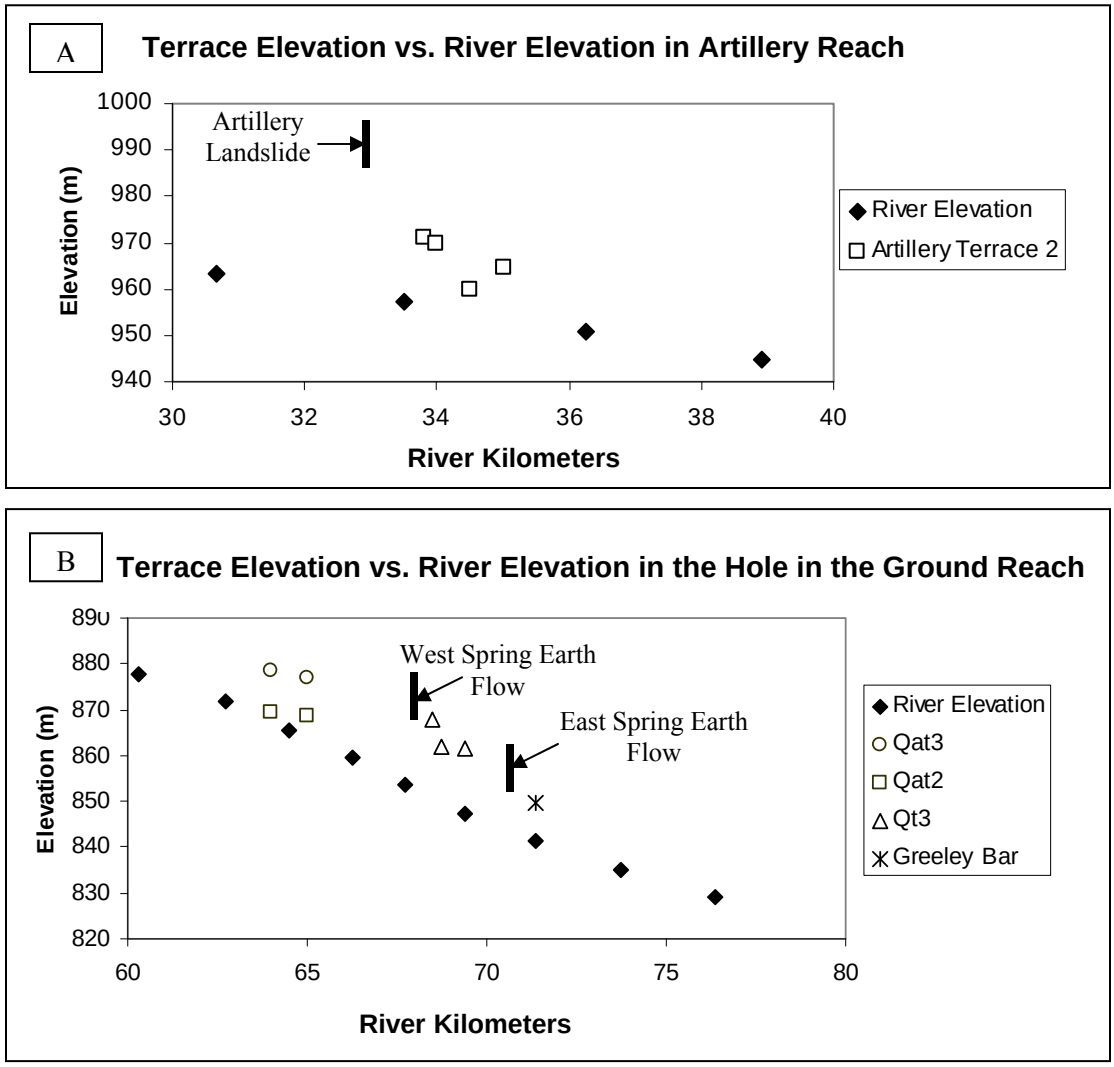

Figure 12. Terrace height above the Owyhee River. (A) The height of Terrace 2 over the river channel. Terrace 2 is the terrace surface thought to be associated with an outburst flood from the Hell's Gate Rock Fall. (B) The height of Qt3 over the river channel. The Qt3 surface is thought to be related to the East Spring Earthflow landslide dam. Also shown on both profiles are the locations of known damming events. The estimated heights of the dams above the river channel are shown.

them. The elevation of the flood bars decreases relatively rapidly downstream. Based on the lack of significant slope, it can be assumed that the aggradational terrace surfaces grade to a significant location, for instance, the blockage downstream that created them. In comparison to the aggradational terraces studied, no real trend can be said about the

flood bars related to the breach of the East Spring Earthflow. All that can be inferred from the river-terrace profiles about Greeley Bar is that it is located immediately downstream of the East Spring Earthflow.

Finally, the slope of the aggradational terraces and flood bars were taken into account to see how the slopes differ. The results are presented in Table 6. What is obvious from the calculations of slope is that the flood bars in both Artillery reach and the Hole in the Ground reach have a greater slope from upstream to downstream than the aggradational terraces found in the Hole in the Ground reach. In fact, the aggradational terraces show almost no decrease in elevation when moving downstream. The flood

TABLE 6. SLOPE OF TERRACE SURFACES AND RIVER CHANNEL

	Slope (m)	Associated river slope (m)
Artillery reach		
Terrace		
Qt2-A	0.028	0.0022
Qt2-B	0.015	0.0022
Qt2-C	0.003	0.0022
Qt2-D	0.010	0.0022
Hole in the Ground		
Terrace		
Qat2	0.004	0.0025
Qat3	0.002	0.0025
Qt3	0.017	0.0025

Note: Slopes of terraces were based on the height of the terrace over the river channel and the length of the terrace. The slope of the river channel was calculated using the river profile created by Brossy (2007).

bars, however, have a slope that is one magnitude higher than both the aggradational terraces and the river channel slope. These different slopes suggest that the aggradational terraces grade to some blockage in the river and the flood bars lose elevation downstream from a potential breach site.

CHAPTER V

DISCUSSION

Artillery Reach

The most striking landforms in this study reach are the slump events located on river right (Figure 3). There are also other mechanisms of mass wasting in Artillery reach including smaller slumps, rock falls, and large rock topples along the river channel, most of which are on river left. The composition of Tsv on both sides of the canyon and the dip of the bedding is similar, however, there are more springs present on river right, where the large slump events originate, which could help to initiate slump events. However, based on the composition of the rock falls, rock topples and smaller slump events, the difference in mass wasting on the two sides of the river valley is most likely a result of the differing thickness of the basalt cap and the extent of the exposure of Tsv along the canyon walls above the river channel and the proximity of the basalt cap to the river channel.

On river left, there are both the first and second advances of the Saddle Butte lava flow, which can be up to 60 m in thickness (Brossy, 2007). The very base of the Saddle Butte basalt sequence is not fully exposed. Thus, the thickness of the Saddle Butte basalt package was estimated based on exposures of the underlying Tsv sediments (Tsv) along the river channel (Plate 1). The height of the canyon wall on river left along Artillery reach ranges between approximately 75 m and 100 m, meaning the majority of the canyon wall is composed of the Saddle Butte basalt flows. The resulting mass wasting events are rock falls, large blocks of basalt cantilevering away from the canyon wall, and

smaller slump events composed mainly of basalt blocks sliding on the underlying Tsv unit. The larger slump events on river right are a result of a thicker package of exposed underlying Tsv sediments between the valley bottom and the basalt cap and a greater horizontal and vertical space to accommodate the larger slump events. The composition of the right valley wall, including approximately 80 m thickness of basalt cap and 75 m of exposed Tsv, has approximately an equal amount of exposed sediments and basalt cap. The basalt cap is approximately 750 m from the river channel, precluding large rock falls and rock topples from entering the river channel from river right.

Based on the overall morphology of the large slump events and their contacts with other map units, the large slump events seem to become consecutively younger upstream from Landslide 1, with Artillery Landslide being the youngest landslide in the series (Figure 5, Figure 7). There are several lines of evidence that suggest that Landslide 1 is the oldest landslide of the sequence. Foremost, Landslide 1 is buried by the West Crater lava flow, making the landslide older than 60-80 ka, which is the age of the West Crater lava flow (Bondre, 2006; Brossy, 2007; Figure 13). Also, the overall morphology of Landslide 1 suggests it is the oldest of the large slump events lining river right in Artillery reach (Figure 8). As stated in Chapter III, the relative ages of slump events were inferred based on the amount of weathering over the entire surface of the landslide and the amount of vegetation reestablished on the landslide blocks of each landslide.

Landslide 1 has only one exposed landslide block that lies immediately to the east of the West Crater basalt. The landslide block has been thoroughly weathered and the remnants of the block are very rounded with no cohesive basalt cap in the constituents of

Figure 13. Morphology and contacts of Landslide 1. West Crater lava flow obscures the base of Landslide 1. One landslide block is preserved and has been weathered to such an extent as to disaggregate the remnants of the basalt cap and begin weathering the underlying sediments, creating the rounded landslide block.

the block. This differs from the landslide blocks of the other, younger slump events that have retained cohesive remnants of the basalt cap as part of their composition. Other landslides in the area display slices of the canyon wall that retain the exact composition of the canyon wall from which they separated and these younger landslide blocks have not been revegetated.

The intermediate-aged landslides, Landslide 2 through Landslide 4, have a less eroded appearance and more exposed landslide blocks than Landslide 1. The landslide blocks of the intermediate landslides are somewhat weathered, especially near the toes of the landslides, but still generally retain the composition of the canyon wall. The youngest

landslide blocks of the intermediate landslides show an intact basalt cap and a backward-rotated orientation near the main scarp. Much of the overall surface of all intermediate landslides has been somewhat rounded and eroded and all intermediate landslides show fluvial alteration on their toes by the blanketing of Qrt gravels on surfaces below 1036 m.

The most well-defined landslide morphology of the intermediate-aged landslides is associated with Landslide 4. It has well preserved landslide blocks near the landslide scarp, where the landslide blocks have rotated back very little from their initial vertical position. The composition of these landslide blocks mirrors the composition of the main landslide scarp. The toe of Landslide 4 has been scoured into a bowl shape and contains both rounded boulders up to approximately 0.3 m in diameter and deposits of Qrt. The presence of rounded boulders and gravels suggests fluvial alteration of the toe of Landslide 4. In fact, the scoured toe of Landslide 4 has been modified to such a degree that the landslide blocks are no longer recognizable.

The large slump events found on river right in Artillery reach began initiating movement sometime before the deposition of the West Crater lava flow and its corresponding lava dam based on the presence of Qrt on the intermediate landslides, a sedimentary unit thought to have aggraded behind the West Crater lava dam. The Qrt deposits are found only at elevations below 1036 m, which is the proposed height of the West Crater lava dam. These gravel deposits range in thickness from thin veneers of only a few centimeters thick up to more than 26 m thick in the Artillery reach. The thickest deposits of Qrt can be found immediately behind the remnants of the West Crater lava dam. Where Qrt deposits are thicker they form rounded, hill-like deposits on both sides of

the river (Figure 14). The Qrt deposits are found all the way upstream to Artillery Landslide. It has been interpreted that Qrt is associated with the West Crater lava dam and was deposited at some point during the dam's existence because the initial presence and thickest deposits of Qrt are immediately upstream of the West Crater lava dam remnants (Figure 11). However, the exact age of Qrt is unknown.

There is a question regarding whether movement of Artillery Landslide initiated before or after the emplacement of the West Crater lava dam because Artillery Landslide lacks the thick Qrt deposits below 1036 m elevation that are present on Landslide 2 through Landslide 4. There is a deposit of river gravels, a few centimeters thick, found on top of the spillway located at the downstream end of the Artillery Landslide above Terrace 2-A (Figure 15). These river gravels are also deposited in other spatially related

Figure 14. Qrt deposit capping Terrace 2-E. Photograph, taken from river right, of a Qrt deposit on river left. This gravel deposit shows a rounded top which is characteristic of the Quaternary gravel deposits in Artillery reach. This gravel deposit can be differentiated from nearby terrace surfaces based on its weathering into a curved surface as opposed to flatter terrace surfaces.

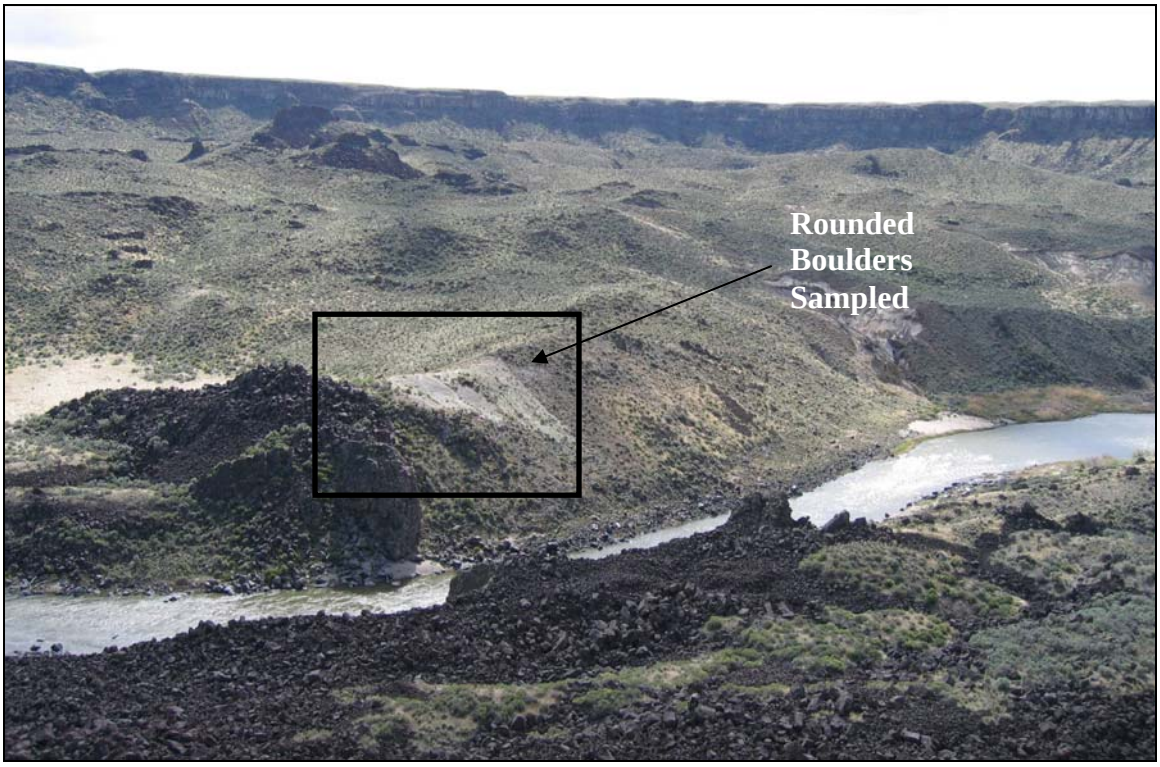

Figure 15. Artillery spillway. The box encompasses the entire area of the spillway on Artillery Landslide immediately behind the Saddle Butte Rock fall, referred to as Hell's Gate. The spillway has associated river gravels draping both sides, suggesting that water once flowed over the area. Rounded boulders near the spillway (shown with an arrow) have been sampled for cosmogenic dating. It is unknown whether this spillway was used during the breach of Artillery Landslide, Hell's Gate, or both.

ephemeral stream channels that incise the toe of Artillery Landslide. These gravels, however, are thinner than the gravel deposits found on the intermediate-aged, downstream landslides, including Landslide 4, which is immediately adjacent to Artillery Landslide. Also, these thin deposits of Owyhee river gravels were deposited well below the 1036 m elevation, which is the elevation consistent with the height of the West Crater lava dam. The thinner gravel deposits on Artillery Landslide could possibly be related the breach of a later mass wasting blockage in the river, possibly even Hell's Gate, or the gravel deposits on Artillery Landslide are Qrt but simply differ in depositional character

from other Qrt deposits on the older, downstream landslides. However, the thin gravel deposits and the well-defined morphology of Artillery Landslide suggest that it was never inundated with water like the intermediate landslides downstream. This evidence supports the interpretation that Artillery Landslide was initiated after the West Crater lava dam was breached.

If Artillery Landslide was created after the breach of West Crater lava dam, it is possible that the presence of a long-lived impounded lake behind the West Crater lava dam allowed the exposed Tsv sediments underlying the canyon rim basalt cap to become saturated by river water. Once the incision of the West Crater lava dam began, the lake behind the dam would drain, resulting in a loss of lateral support of the Tsv sediments. After the impounded lake was fully drained, the weight of the overlying basalt cap could have overcome the strength of the Tertiary sediments allowing for the Artillery slump event to initiate.

Other possible factors in initiating large landslides, such as those found in Artillery reach, is a wetter climate leading to increased infiltration of water into the Tsv unit or a local seismic event that triggered mass wasting. These two possibilities have been noted in other literature to be the most common landslide triggering mechanisms (Reneau and Dethier, 1996; Korup 2002). Both triggering mechanisms mentioned are possible triggering mechanisms based on the presence of numerous springs located within the large slump events as well as the presence of faults just downstream of Artillery reach.

Artillery Landslide

Artillery Landslide was the main slump event of focus in this reach because of its well-preserved morphology and the presence of outburst flood deposits immediately downstream of the landslide. The landslide can be differentiated into two different phases of slumping. The first phase of slumping moved in a north-northwesterly direction and would have most likely blocked the river (Figure 16). The second phase of slumping occurred in a westerly direction, directly from the current landslide scarp (Figure 16). The second phase of slumping has been dated using tephrochrnology and has a minimum age of approximately 7.7 ka BP based on the presence of Mazama tephra. The tephra was

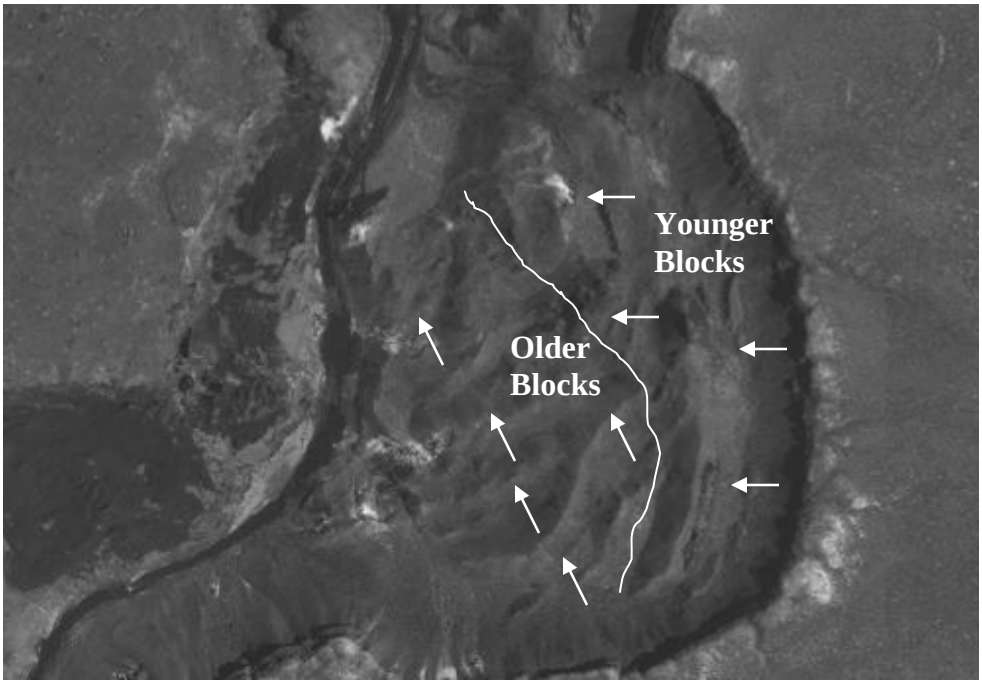

Figure 16. Surface morphology of Artillery Landslide. The landslide blocks near the scarp move in a westerly direction and are much less rounded than the blocks near the toe of the landslide. The older landslide blocks moved in a northwesterly direction and are much more rounded at the surface.

found in a closed depression located immediately below the main landslide scarp. The sample was taken from a depth of approximately 2 m, is white in color and composed of silt-sized grains. The sample was geochemically identified as Mazama tephra by F. Foit at Washington State University (personal communication, 2007).

The landslide blocks of the second phase of slumping are much fresher than the blocks associated with the first phase of slumping. The slump blocks of the second phase of slumping are still mostly vertical, having slid only a short distance. These blocks also show intact basalt cap that has not undergone much erosion or revegetation, unlike the blocks of the initial Artillery Landslide slump event, which are nearer to the river channel. The hummocky topography and closed depressions of the second phase of slumping are also better-defined than those associated with the older slumping phase. The differences in morphology of these two sets of landslide blocks suggest reinitiation of large slump events after the initial slumping.

The remnants of Artillery Landslide are not found across the river on river left. Thus, it cannot be definitively proven that Artillery Landslide dammed the river when it entered the channel. The river channel itself, though, seems to have been forced to river left where it currently flows around the remnants of the toe of Artillery Landslide. Though the forcing of the channel to river left does not prove that Artillery Landslide blocked the river channel, it does suggest that the encroachment of Artillery Landslide into the river channel has affected the course of the river, forcing the river to go around the landslide's toe. If Artillery Landslide did not completely block the channel when it entered the river, the restriction of the river channel to the left side of the canyon could

have initiated undercutting of the canyon wall, which could possibly have resulted in the mass wasting seen on river left.

Sedimentology of Tsv Sediments at Artillery Landslide

Samples of Tsv sediments were collected from an outcrop located on the downstream portion of Artillery Landslide and were used to better understand the composition of the Tertiary sediments involved in the large slump events (Figure 17). A 3.6-m-thick outcrop of in-situ Tsv was found near the boundary of Artillery Landslide with Landslide 4 (Figure 17). Four samples were taken from different units within the outcrop to describe each unit in hand sample and thin section. The samples taken from

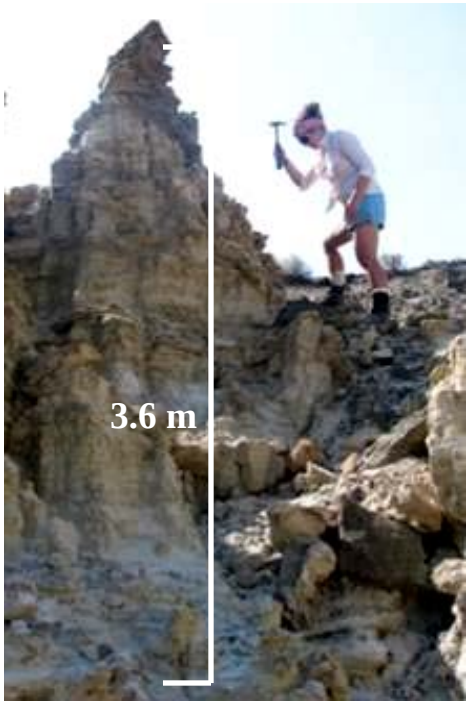

Figure 17. In-situ exposure of Tsv sediments on Artillery Landslide. The sediments are found in the upstream portion of the Artillery Landslide depression. Samples of this exposure were taken and described in both hand sample and thin section to better understand the slip-surface of Artillery Landslide.

this exposure of in-situ Tsv showed an initial lacustrine deposit at the base of the exposed section that grades into interbedded coarse sands and a volcanic conglomerate (Appendix A).

The environment of deposition for this particular exposure of in-situ Tsv sediments is an initial, low-energy, lacustrine environment leading to a low-energy fluvial system that increased in energy through time. The majority of the sampled units of the outcrop are fluvially derived, though the energy of this system seems to fluctuate though time, as shown by the medium sands of Unit 1.2 to the fine sands of Unit 1.3 and finally with the highest energy unit, Unit 1.4, composed of both coarse sands and conglomerate (Figure 18). The changing in the energy of deposition in this manner could suggest that the fluvial channel depositing these units is migrating laterally in its valley, and the size of the particles in any given unit suggest the proximity of the unit (adjacent or distant) to the active fluvial channel. These fluvial and lacustrine sediments are characteristic of the Tsv sediments that outcrop above the river channel along this entire stretch of the study area.

An important aspect to the slip-surface of Artillery Landslide is the grain size of the fluvial sand and conglomerate units. Because the sands and conglomerate have a larger grain size than silts or clays, there is a greater possibility for water to infiltrate these units, leading to saturation. As the underlying sediments become saturated, the weight of the thick, dense basalt cap is able to overcome the strength of the underlying sediment, initiating mass wasting.

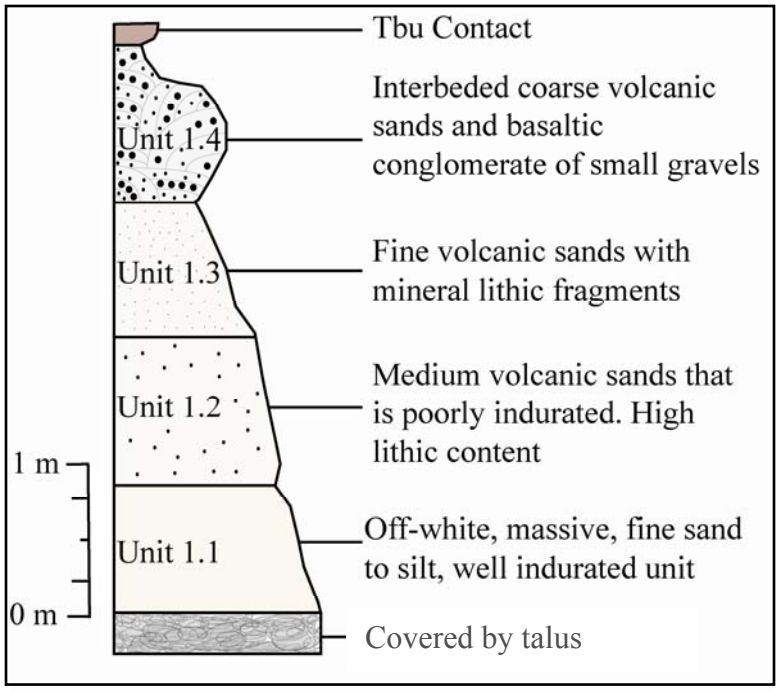

Figure 18. Schematic stratigraphic section of geology underlying the basalt cap in Artillery Landslide. The basal unit, 1.1, is the finest grained unit, directly on top of this unit is a medium sand capped by a fine sand, and finally, Unit 1.4, that shows interbedded coarse sands and conglomerate. Unit 1.4 has an upper contact with a basalt flow.

Hell's Gate Rock Fall

At the downstream end of Artillery Landslide, a rock fall obscures the landslide toe. The rock fall, referred to in this paper as Hell's Gate Rock Fall, originated from river left and was deposited directly on top of the remnants of the toe of Artillery Landslide (Figure 19, A and B). The rock fall is completely composed of Saddle Butte basalt rubble, and several of the remnant basalt blocks of the rock fall near the channel are extremely large basalt boulders. On river left, resting half way in the channel, is a boulder that is 4 m in height and 3 m in diameter, and on river right there is a much larger boulder that is 15 m in height and 10 m in diameter (Figure 19A). These boulders are the largest remnants of the Hell's Gate rock fall. The size of these boulders that persist on either side

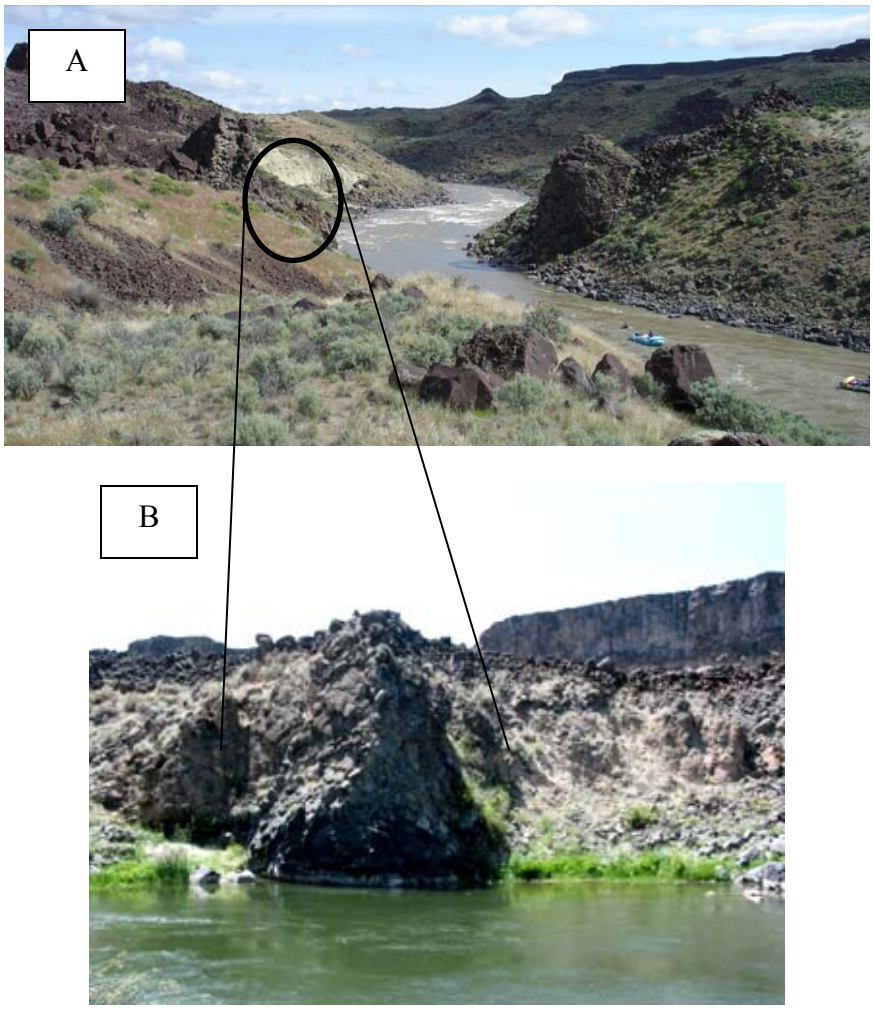

Figure 19. Hell's Gate Rock Fall. (A) a view of Hell's Gate from upstream, with obvious remnants on river right, including large basalt boulder and basalt rubble. (B) Large boulder on river left associated with Hell's Gate Rock Fall. The remnants on both sides of the river, especially the larger boulders, suggest that this rock fall blocked the channel at some point.

of the channel suggest that there were other boulders, perhaps just as large, deposited in the channel when the rock fall was emplaced. Based on the rock fall remnants on both sides of the river and the large boulders that constitute the rock fall, it is assumed that the Hell's Gate Rock Fall blocked the Owyhee River at one point.

Approximately 2 m immediately upstream of the rock fall remnants on the toe of Artillery Landslide, is an outcrop of Tsv sediments that is no longer in-situ on river right. The outcrop is expressed as a thin finger of sediment just upstream of Terrace 2 and is assumed to be a portion of the preserved toe of Artillery Landslide (Figure 15). It is this thin, finger-like remnant of the toe of Artillery Landslide that the Hell's Gate Rock Fall was deposited on. The outcrop has been thoroughly weathered and no original bedding remains in the exposure. The outcrop has been thinly draped with Owyhee River gravels only a few centimeters thick and there are rounded boulders present on both the upstream and downstream sides of two shallow swales on the top of the exposure (i.e., above Terrace 2-A and above the river channel). Approximately 4 m upstream of the spillway are rounded boulders approximately 1 m to 2 m in diameter (Figure 15, arrow points to the location of rounded boulders). These rounded boulders are composed of the canyon rim basalt (Tbu) and were sampled for cosmogenic analysis.

The presence of this weathered saddle-like exposure of Tsv that is no longer in-situ behind the rock fall, coupled with the Owyhee River gravels deposits and rounded boulders on top of the toe of Artillery Landslide in this location, suggests that this thin portion of the toe of Artillery Landslide was once a spillway for a river blockage. Because of the proximity of the spillway to the Hell's Gate Rock Fall, it is very likely that the spillway was used while Hell's Gate Rock Fall blocked the channel. Though the blockage of the river caused by Hell's Gate Rock Fall is the most likely source for the water that spilled over the spillway, it is possible that the spillway was utilized by an impounded lake that formed behind the blockage of Artillery Landslide as well.

Artillery Reach Outburst Flood Deposits

As described above, either Hell's Gate Rock Fall, Artillery Landslide, or both mass wasting events dammed the river in approximately the same location. Flood bars deposited immediately downstream from Artillery Landslide are referred to as Terrace 2 (Figure 4, Plate 1). Both blockage sites of Artillery Landslide and Hell's Gate Rock Fall are at the correct elevation (1006 m) to produce the flood deposits seen on Terrace 2 (elevation 962 m). At least one of these landslide dams appears to have failed catastrophically.

Terrace 2 is distinguished from other terraces in the region by its particularly flat surface and the two distinct populations of basalt boulders that compose the terrace. The first population of boulders is subrounded and partially buried and is deposited along the entire length of the terrace surface. The second population of boulders found on Terraces 2-B, 2-C, and 2-D consists of well-rounded basalt boulders that rest directly on top of the terrace surface (Figure 3). The rounded boulder population is only found on the upstream end of the Terraces 2-B, 2-C, and 2-D, unlike the buried boulder population, which is found along the entire lengths of the terrace surfaces. These boulders were clearly fluvially deposited after the subrounded boulder population was deposited. The fluvial deposition of the rounded boulder population is based not only on the rounding of the boulders but also imbrication of the boulders found on Terrace 2-B. The size of this population of boulders, with maximum diameters ranging between 3.2 m on Terrace 2-C and 1.2 m on Terrace 2-D, suggests deposition by a high velocity flow, i.e., an outburst flood from upstream of the boulder deposit.

Other evidence suggesting that this rounded boulder population was deposited by an outburst flood is the character of the outburst flood deposits. The largest boulders measured on Terrace 2-B, Terrace 2-C, and Terrace 2-D, are all composed of the Saddle Butte basalt, even the boulders measured on Terrace 2-C on river right. A single event most likely deposited the population of large rounded flood boulders on top of the Terrace 2 surface. This conclusion is based on the flood boulders being completely composed of Saddle Butte basalt, which also composes the Hell's Gate Rock Fall. No measured flood boulders were composed of the Tertiary basalt, which forms the canyon rims on river right and comprises the basalt portion of the blocks of Artillery Landslide. Another characteristic of outburst flood deposits is that boulders deposited during an outburst flood decrease in size from upstream to downstream as a result of the outburst flood water losing velocity as it flows downstream from the source (Scott and Gravlee, 1968; Table 2, Figure 5). This general trend was seen in the boulders measured for analysis on Terraces 2-B, 2-C and 2-D (Figure 10).

The composition and morphology of Terrace 2 suggests that there have been at least two stages of formation by high energy fluvial events, if not more. The earlier event would have buried and perhaps started the fluvial rounding of the population of subrounded, partially buried boulders. This event could have also created the very flat surface that the second population of large, rounded boulders was deposited on. The later event would be the outburst flood that deposited the second population of large, rounded boulders on top of the smoothed terrace surface. This population of boulders shows an

age range of 10 to 42 ka from cosmogenic dates of flood boulders sampled on Terrace 2-C (Table 2; Fenton, personal communication, 2007).

These ages are consistent with the minimum age of 7.7 ka BP for the second phase of slumping forming Artillery Landslide. It is this second population of boulders that was most likely deposited by an outburst flood originating from the breach of Hell's Gate Rock Fall. This assumption is based on the proximity of the boulders to the rock fall and composition of the rounded boulders on top of Terrace 2, which are composed of Saddle Butte basalt. Landslide Dams as large as Artillery Landslide that fill hundreds of meters of the river channel are more likely to be overtopped and eroded by headward erosion before the dam is completely compromised, which can still result in an outburst flood (O'Connor et al., 2002). Because the basalt component of Artillery Landslide would have been Tertiary basalt (Tbu), an outburst flood from Artillery Landslide would most likely deposit boulders composed of Tbu downstream, not Saddle Butte basalt. Based on this evidence, it is likely that the flood boulders on Terrace 2 were deposited by a breach of the Hell's Gate Rock Fall. It is also possible, although unlikely, that neither Artillery Landslide nor Hell's Gate Rock Fall created the flooding events that deposited the flood boulders on Terrace 2-B, 2-C, and 2-D. More cosmogenic dating of boulders on Terrace 2-B and 2-C as well as the boulders sampled on the spillway of the toe of Artillery Landslide will help to better constrain the sequence of events that occurred at the Artillery Landslide/Hell's Gate Complex and which events created Terrace 2.

Terrace 2-A is the only terrace of the Terrace 2 surfaces that does not have the characteristic composition of the two basalt boulder populations composing the terrace.

Terrace 2-A does show a sub-rounded boulder population that is fully buried by fine-grained sediments and only crops out along the edge of the terrace surface. However, Terrace 2-A has only two large, rounded boulders resting on its surface and these boulders are on the downstream portion of the terrace surface. One possibility for the formation of Terrace 2-A is that it is an abandoned paleochannel that was blocked and preserved when Artillery Landslide entered the river channel. Another possibility for the formation of Terrace 2-A is that is a backwater deposit emplaced after the breach of Artillery Landslide and/or Hell's Gate Rock Fall. This explanation could explain the lack of large basalt boulders on the terrace surface. However, more work, such as augering, needs to be done on Terrace 2-A to characterize the composition of the terrace. If the terrace is composed mainly of fine-grained sediments then it is most likely a backwater deposit that was most likely emplaced during the breach of a dam created by Artillery Landslide or Hell's Gate Rock Fall. If the terrace surface is composed of river gravels and/or larger clasts instead of fines, than the terrace surface would have more likely been a paleochannel that was last utilized before Artillery Landslide entered the river channel.

The Hole in the Ground

The mass wasting in the Hole in the Ground area shows slump events near the top of the canyon, directly from the main landslide scarp, where the Tertiary basalt cap is still intact. At the base of these slump events, flow-type mass wasting events have occurred (Figure 20). The Hole in the Ground reach has had a greater frequency of mass wasting than the Artillery study reach. In fact, the majority of the area mapped on both sides of the river in the Hole in the Ground study reach has been affected by multiple generations

of mass wasting events. Unlike Artillery reach, there has been little recent interference by intra-canyon basalt flows in this study reach that are relevant to the focus of this paper. The only basalt to play a key role in the mass wasting of the Hole in the Ground reach is the Tertiary basalt cap (Tbu) that overlies the undifferentiated Tertiary volcanic and volcaniclastic sediments (Tsv) in the reach. Though both the Bogus Rim lava flow (1.9 Ma; Bondre, 2006) and the older Greeley Bar lava flow could have blocked the channel at one point, they have had little input on the current river channel morphology. When

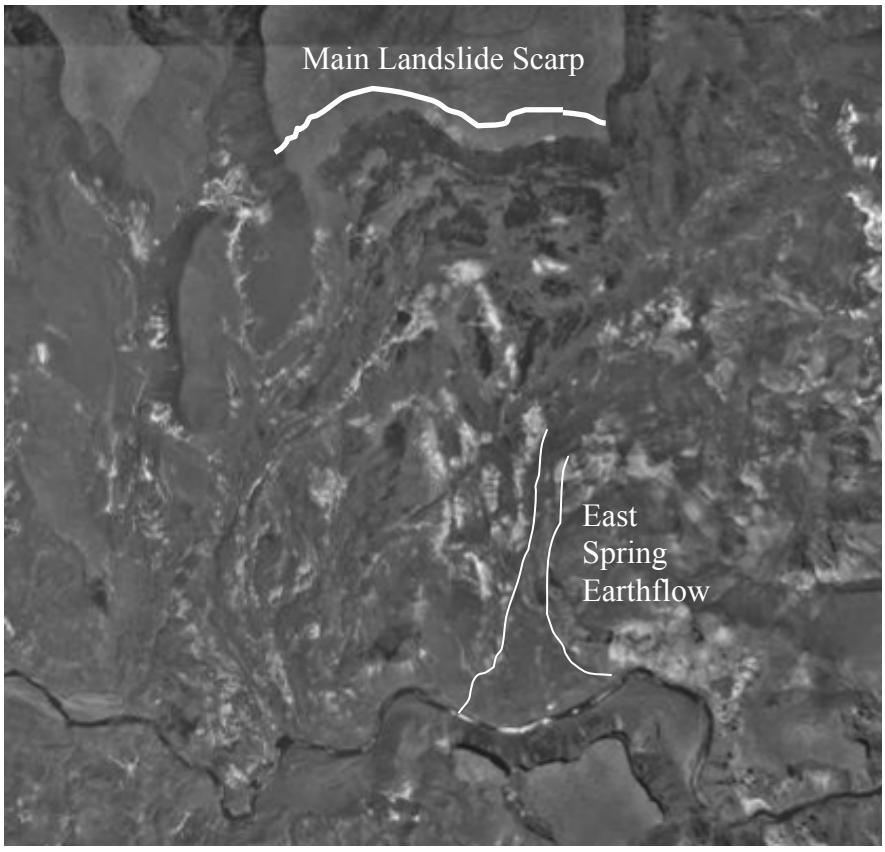

Figure 20. East Spring Earthflow and associated landslide complex scarp. Figure shows both slump events near the main scarp with characteristic landslide blocks as well as large earthflows (such as East Spring Earthflow) originating from the slump-affected areas. In this study reach, earthflows originate from areas where the basalt cap has retreated because of initial slump events.

these two lava flows were emplaced the river channel was at a much higher elevation, thus these lava flows did not enter the modern Owyhee River channel. The Tertiary basalt cap, which defines the landslide scarp on river left in the Hole in the Ground reach, has little input into the stream channel because it has retreated up to 4983 m from the current river channel (Figure 20).

Once incision of the canyon by the Owyhee River took place, the Tsv sediments below the basalt cap became exposed and the canyon was subjected to a large amount of mass wasting. The Tsv sediments that underlie Tbu in the Hole in the Ground contain a localized lacustrine unit that is found stratigraphically immediately below the Tertiary basalt and is not found in Artillery reach. This deposit of light-colored lacustrine sediments is approximately 176 m thick from the top of the first in-situ exposure of the lacustrine sediment to the in-situ lacustrine sediments found directly below East Spring Earthflow (Appendices A and B, Plate 1). However, the thickness of the deposit probably varies horizontally because it was deposited in a lacustrine environment. The spatially localized character of these lacustrine sediments, which have only been recognized in the eastern portion of the Hole in the Ground reach, possibly explains the presence of the Hole in the Ground. The Hole in the Ground reach is the widest part of the canyon within the entire study area from Rome, Oregon to Lake Owyhee and is the area most affected by mass wasting. The presence of this localized lake deposit possibly aids in the retreat of the basalt cap and also provides the material for subsequent large earthflows.

There are two types of mass wasting deposits mapped within the Hole in the Ground reach: (1) the single, morphologically well-defined East Spring Earthflow and (2)

other undifferentiated earthflows and slump events referred as landslide complexes (Plate 2). Because of the complex boundary relationships, very few of the boundaries of the earthflows in the study reach can be completely defined, thus, the chronology of mass wasting in the area is unknown. However, it seems that initial mass wasting in the area began with slump events. This interpretation is based on the presence of slump events near the modern landslide scarp.

Earthflow Dams

West Spring Earthflow complex

There are two identifiable blockages of the river in the Hole in the Ground reach; East Spring Earthflow and another, more complicated dam, originating from river left, referred to as West Spring Earthflow complex (Plate 2, Figure 21). The age of the West Spring Earthflow complex is inferred to be older than the East Spring Earthflow based on the complex's overall weathered appearance and the incision of its surface by ephemeral streams. Remnants of the West Spring Earthflow complex have been found on river right, across from the main portion of the complex. The remnants of the earthflow complex show characteristic earthflow morphology, such as hummocky topography and poorly sorted material making up the composition of the earthflow. The only possible source of these earthflow remnants is an earthflow originating from river left whose toe has been incised by the river. Based on the presence of these remnants, West Spring Earthflow complex must have completely blocked the channel at least once (Plate 2, Figure 21). Other evidence that supports West Spring Earthflow complex completely blocking the flow of the river is a thin deposit of river gravels on top of the earthflow remnants located

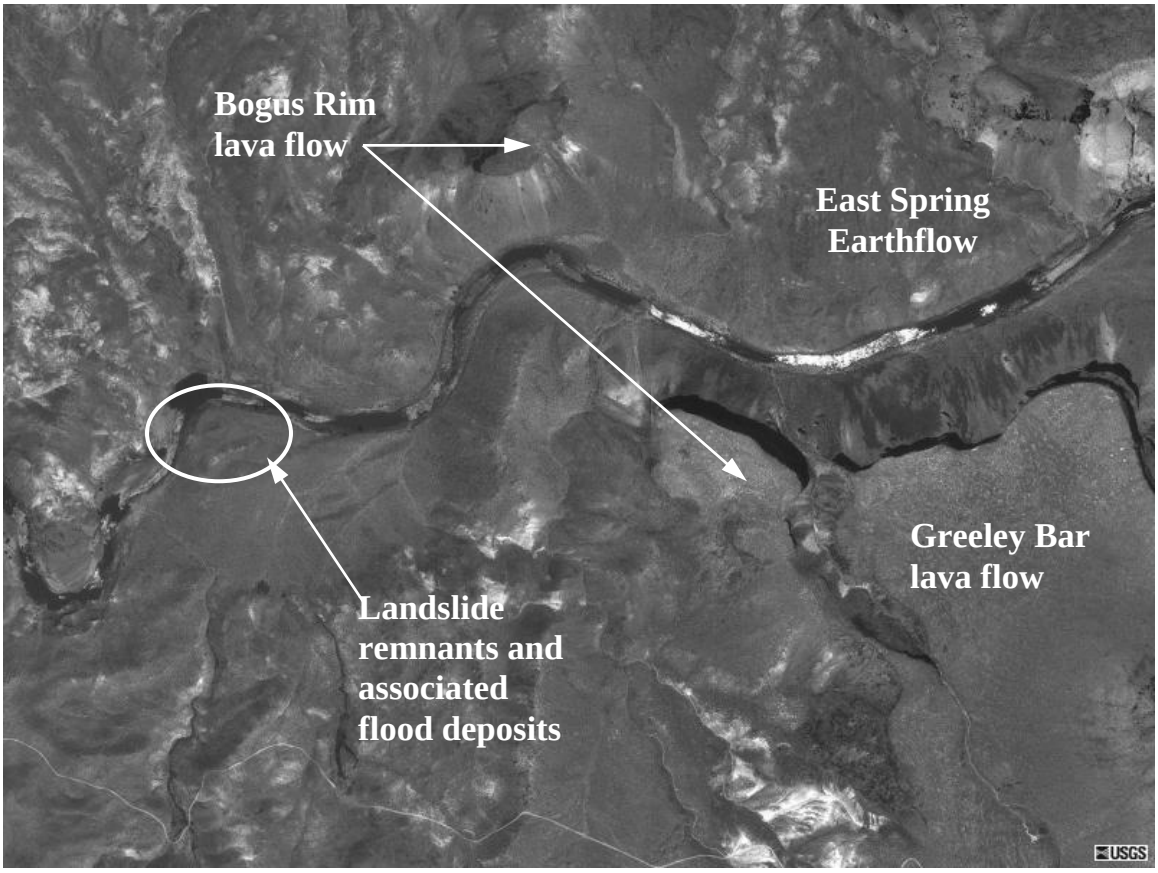

Figure 21. West Spring Earthflow complex. West Spring Earthflow clearly blocked the river channel based on the landslide remnants found on both sides of the river channel (remnants on river right are in the white circle). Flood deposits can be found on the surface on river right, near a deposit of Terrace 3, immediately south of the landslide dam remnants.

on river right and spatially related flood bar deposits downstream of the earthflow remnants on both sides of the channel, referred to as Qt3. Based on the thickness of the gravel deposits compared to upstream aggradation deposits, it is unlikely that the thin gravel deposits on the earthflow remnants are aggradation deposits from a downstream river blockage.

East Spring Earthflow

The other known blockage, East Spring Earthflow, is the youngest large-scale, extrafluvial event to encroach on the river channel in the Hole in the Ground reach. The body of the earthflow is composed of a lower portion that fans out into the river channel and upper reaches that are very constricted (Figure 22). These upper reaches are bound by a conduit of in-situ Tertiary fluvial and lacustrine sediments (Tsv). As a result, all of the material of the event was squeezed through a narrow passage before it fanned out and formed the toe. The conduit, described above, was unaffected by any mass wasting. This observation is supported by the presence of intact bedding surfaces found in the surrounding wall rock forming the upper boundaries. The upstream portion of the earthflow toe fanning out into the river channel is bound by a large levee and the downstream portion of the toe is bound by an exposure of in-situ rhyolite bedrock.

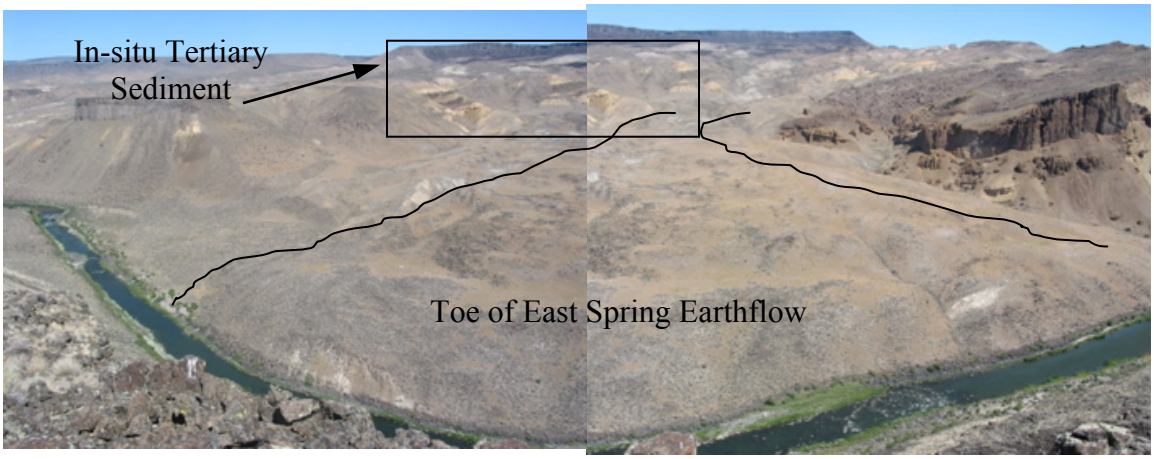

Figure 22. Panorama of East Spring Earthflow from river right. The toe of the landslide is much larger than the neck of the earthflow that fed the toe. The neck of the earthflow can be seen outlined in black immediately to the right of clearly in-situ Tsv sediment in the black box.

All of the boundaries described above separate East Spring Earthflow from other large mass wasting events and allow the event to be easily delineated.

The source of East Spring Earthflow has not been completely delineated (Plate 2). However, it is clear that the source location is composed of the localized Tertiary lacustrine sediments described earlier in Chapter V. This localized Tertiary lacustrine deposit is a layer of semi-indurated bentonitic clay that is stratigraphically on top of the other, darker brow Tsv sediments that form the in-situ boundary walls of the upper reaches of the earthflow (Figure 23, A and B). These lighter Tertiary lacustrine sediments are the source material of the East Spring Earthflow (Figure 23B). The contacts in Figure 23B highlight the compositional differences between the light colored sediments of East Spring Earthflow and the darker ubiquitous Tsv sediments.

Based on the size of East Spring Earthflow and its effect on the current river channel, it is likely the earthflow completely blocked the channel at one point. The toe of East Spring Earthflow fans out into the river and has pinned the current river channel to the other side of the canyon (Figure 24). The current river channel curves around the lobate shape of the toe of East Spring Earthflow, creating a bend in the flow of the river channel. Three lines of evidence that suggests East Spring Earthflow blocked the natural flow of the river is an abandoned paleochannel on top of the toe of the earthflow, the presence of a flood boulder bar, referred to as Greeley Bar, immediately downstream of the earthflow, and its possible association with aggradational terraces upstream. The abandoned paleochannel is characterized by a swale that disrupts the natural angle of the earthflow surface. This swale is composed of very fine-grained, light colored silts to

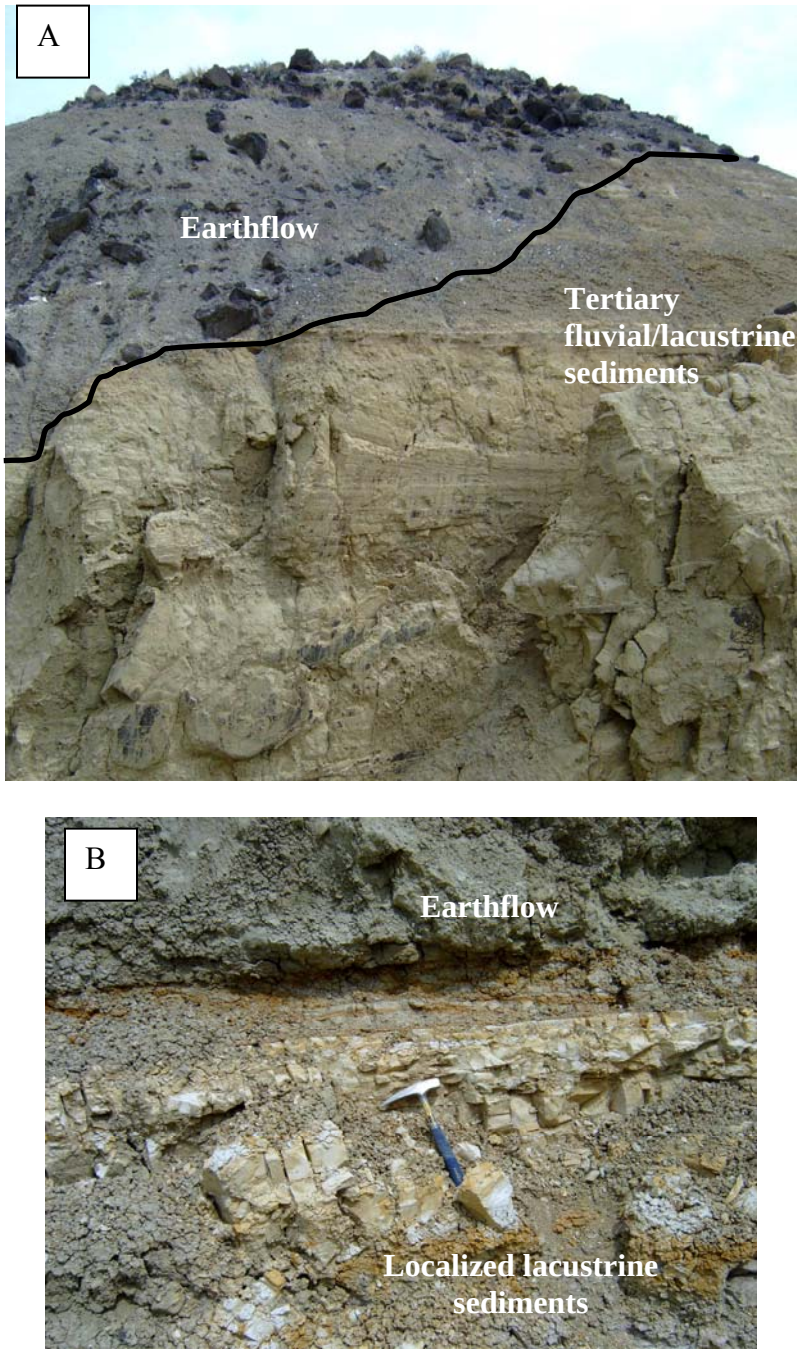

Figure 23. Contacts of East Spring Earthflow. (A) Contact between the Tsv sediments and East Spring Earthflow, approximately 10 m from the where B is located. The Tsv sediments are a light brown in color, which differs from the localized lacustrine deposits, which are light gray in color. (B) Contact of East Spring Earthflow with underlying local Tertiary lacustrine deposit, which is the source material for the earthflow.

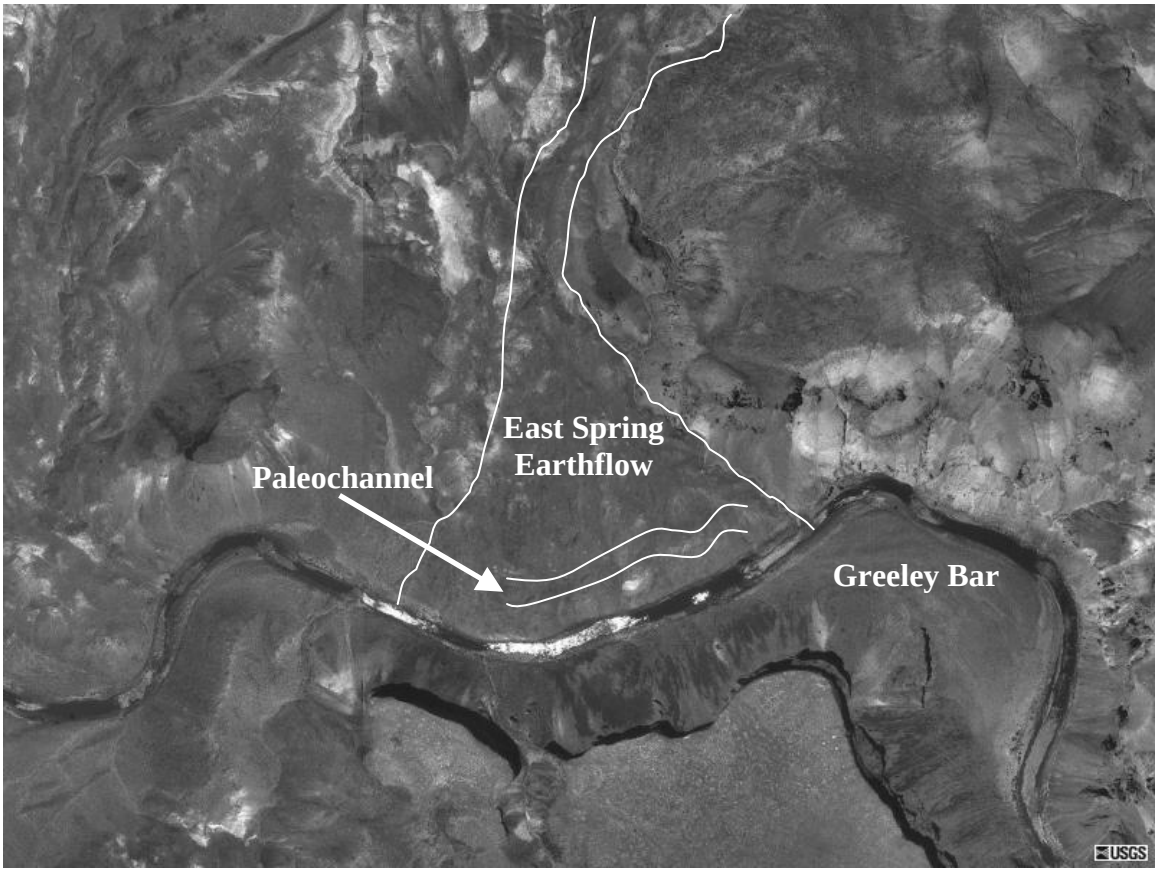

Figure 24. East Spring Earthflow and associated paleochannel. The toe of the earthflow has pinned the channel against the opposite side of the river valley. The paleochannel on the toe of the earthflow has been outlined.

sands and contains only a few rounded basalt boulders, up to 15 cm in diameter, within the swale. The elevation of the toe increases toward the present river channel from the abandoned paleochannel and there is a deposit of large, subangular boulders along the entire toe of the earthflow that continue to the edge of the earthflow, directly above the river channel. This population of subangular boulders shows little, if any, rounding by fluvial action.

The presence of subangular boulders closer to the modern channel and a swale farther up on the earthflow toe, which lacks these subangular boulders, suggests that this

depression was formed in a different way than the very edge of the toe of the landslide. The long, sinuous shape of the depression suggests that it was created as a paleochannel that flowed in a west to east direction, the same orientation of the current flow of the river. The only possible source of water running through this paleochannel would be the Owyhee River if it was once at the same elevation as the paleochannel. For the river to be at that elevation, the river would have to have been dammed by East Spring Earthflow, creating an impounded lake of 21 m depth to form behind the dam. This paleochannel was eventually abandoned as the modern channel cut down through the toe of the earthflow closer to the river right canyon wall.

Sedimentology of East Spring Earthflow

The East Spring Earthflow is composed of ash that has been altered to bentonitic clay and large basalt clasts (Figure 17B). There is laminar bedding present in Unit 1.3, but Units 1.2 and 1.1 were more massive in character (Figure 20). The three different units show very little to no reworking, suggesting that these units were deposited in a low-energy environment, such as a lacustrine setting. This conclusion is supported by the composition of Unit 1.1, which contains a large amount of fossilized plant debris (Appendix A). A higher energy environment, such as a river, would preserve neither the laminar bedding nor the large amount of fossilized plant debris found in Unit 1.1 (Figure 25).

The composition of the clay the matrix of the East Spring Earthflow, which caps the units sampled, is the same bentonitic clay and volcaniclastic material from the localized lacustrine deposit that is located on top of the darker colored, coarser-grained

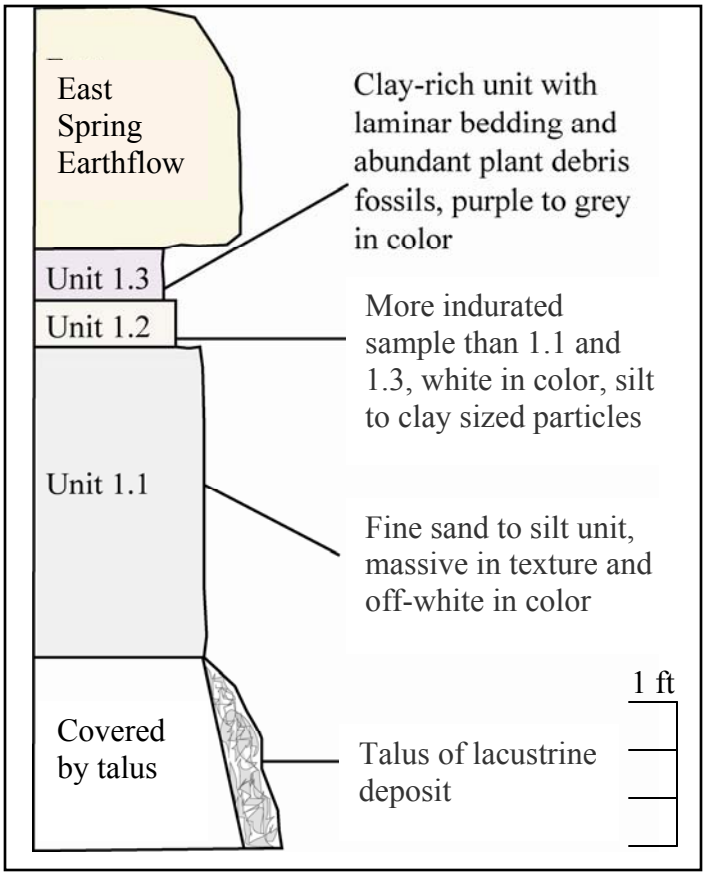

Figure 25. Schematic stratigraphic section of East Spring Earthflow geology underlying the basalt cap. Figure shows the three units that were sampled for thin section and hand sample analysis, Appendices A and B. Also shown is the contact of the in-situ lacustrine sediment with the overlying earthflow.

Tsv deposit in the Hole in the Ground reach (Figure 25). A sample of the darker Tsv unit was taken directly 10 m southeast of the lighter lacustrine outcrop that was sampled as well and another two samples of the darker Tsv deposit were taken from an in-situ out crop found lower along the upstream boundary of the earthflow (Figure 3). These three samples of the Tsv sediments are distinguished by their dark brown color, compared to the units located immediately beneath the earthflow. Both darker Tsv outcrops sampled showed syndeposition alterations in the form of calcite veining. These hydrothermal

alterations, observed both in thin section and seen in the outcrop, are only found in the darker Tsv units. The hydrothermal alterations are another defining characteristic that sets apart the lighter lacustrine sediments composing the earthflow as a completely different geologic unit in comparison to the darker, more ubiquitous Tsv sediments.

Aggradation Deposits and Flood Bars Of The Hole in the Ground Reach

Aggradational Terraces

One geomorphic feature that has been linked to landslide events that have been theorized to have completely blocked the natural flow of the river are aggradation terraces located directly upstream from the two main earthflow dams in the Hole in the Ground Study reach described earlier. These fill terraces, terraces are referred to as Qat2 and Qat3 and most likely represent at least two different occasions where the river channel was completely blocked by a dam (Figure 26). Qat2 and Qat3 are aggradational deposits, which were described in the background and data sections (Figure 26). All of the fill terraces are composed of Owyhee River gravels in a matrix of fine sand and silt. These fill terrace deposits are fairly rounded because of their easily erodible, non-indurated composition. Terrace surfaces Qat2 and Qat3 in the Hole in the Ground reach lack flood boulders in their composition, unlike many of the other terrace surfaces found in both Artillery reach and the Hole in the Ground reach. The absence of large, rounded flood boulders on the surface of the aggradational terraces is the best evidence suggesting the Hole in the Ground fill terraces were formed behind a blockage in the river, such as a landslide dam, and were not created by outburst flooding, like other terrace surfaces.

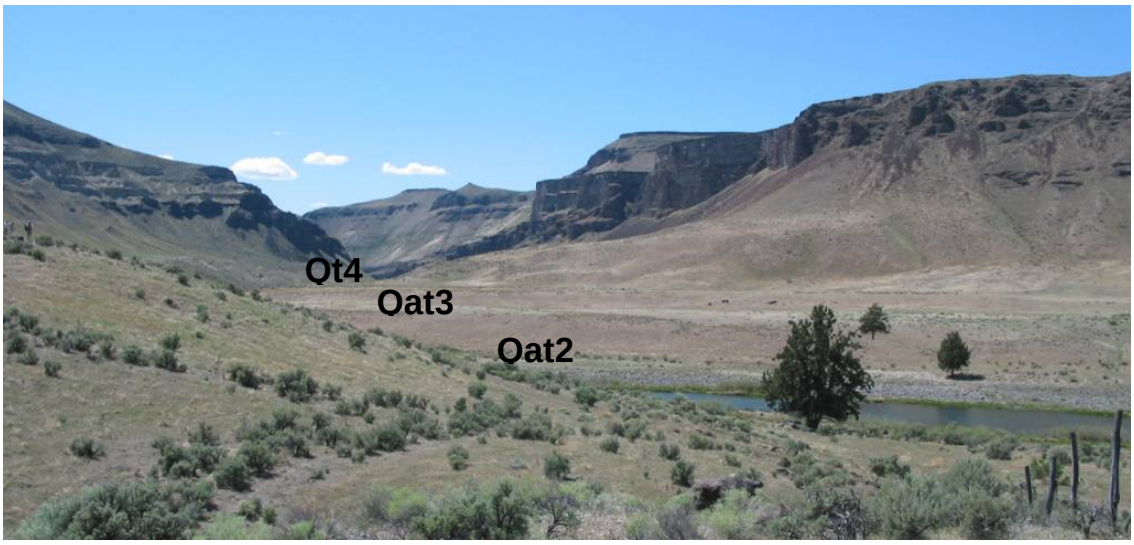

Figure 26. Different fill terrace levels located in the Hole in the Ground reach. Qat2 and Qat3 are composed of Owyhee River gravels in a fine-grained, sandy matrix. These fill terraces are related to blockages found upstream.

The aggradation deposits were most likely created during a damming event of the river somewhere downstream of the deposits. The specific location of the aggradation deposits, located only in the upstream region of the Hole in the Ground reach, suggests they were created by a local event. Thus, it is unlikely that the aggradation deposits were created by climate changes. The location of the two different levels of aggradation terraces immediately upstream of the two known earthflow dams, West Spring Earthflow complex and East Spring Earthflow, suggests that the damming of the river by these two events possibly created the terraces found in this study reach. The presence of the deposits also suggests that these two earthflow dams created long-lived impounded lakes allowing for upstream aggradation.

Assuming the two aggradational terrace levels were created by the two known earthflow dams, it can be inferred that the initial damming of the river channel by the

West Spring Earthflow complex created Qat3 and the later damming of the river by the East Spring Earthflow allowed for the deposit of Qat2. If this conceptual model is supported by chronology data, such as dating by OSL on fine-grained terrace sediments or cosmogenic dating of cobbles from the terrace deposit, it has implications for the breach of the two Earthflow dams. If the aggradational terraces were deposited behind these two damming events, then the West Spring Earthflow complex dammed the river channel and breached before the East Spring Earthflow dam was emplaced.

Flood Bars Downstream of West Spring Earthflow Complex

Terrace surfaces found immediately downstream of the West Spring Earthflow complex, referred to as Qt3, are composed mainly of subrounded to rounded basalt boulders in a sand to silt matrix. These terrace surfaces are much different from aggradation terraces found upstream stream of the East Spring Earthflow and West Spring Earthflow complex, which are composed completely of piles of Owyhee River cobbles (Qat2 and Qat3). The Qt3 surfaces are found immediately downstream of the remnants of the East Spring Earthflow found on river right, on the same surface, and are also found directly across the river on river left from the earthflow remnant surface. One surface is also found directly upstream of East Spring Earthflow on river right (Figure 27; Figure 11). There are three possibilities that could have created these terrace surfaces.

The first possibility is that the West Spring Earthflow complex blocked the river, creating an impounded lake upstream. Once the impounded lake was full, an outburst flood occurred which deposited the wedge of sediment referred to as Qt3 just downstream of the West Spring Earthflow dam (Figure 27). After the breach of the West

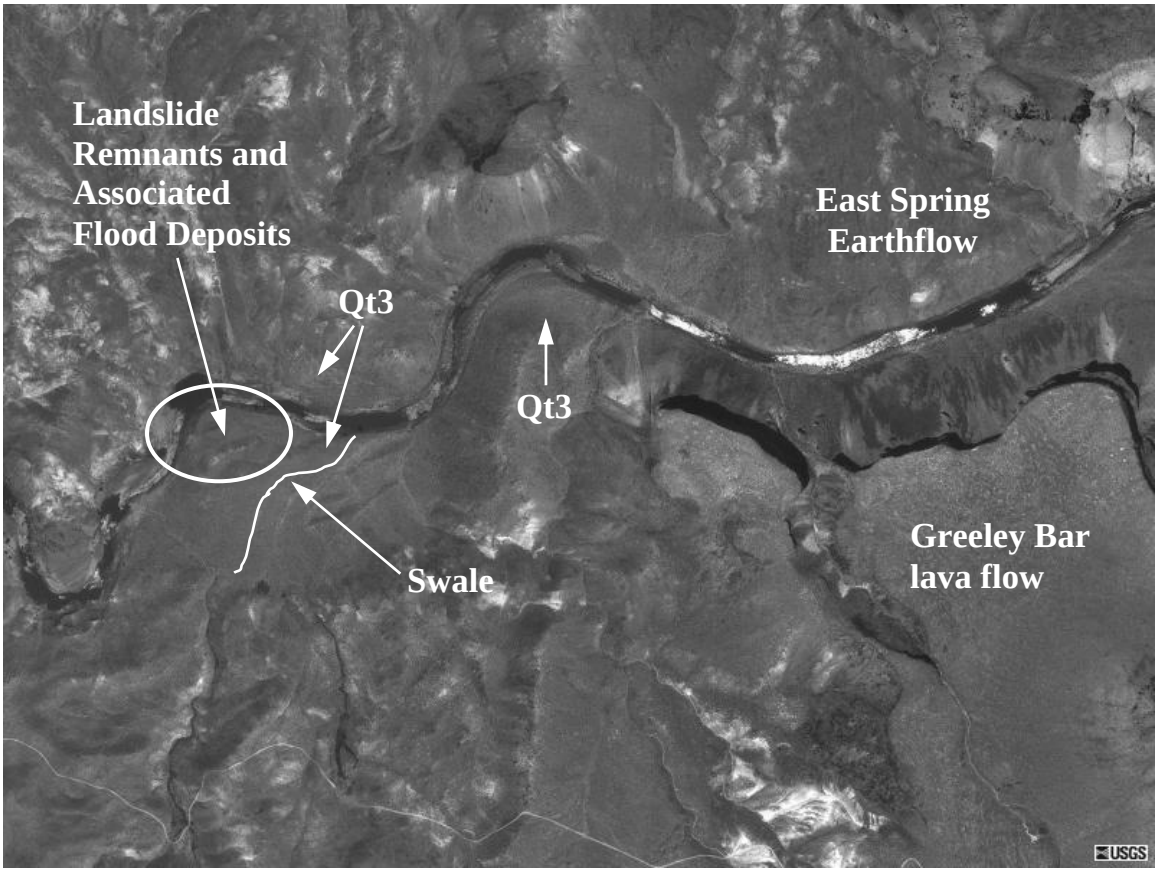

Figure 27. Qt3 surface. The breach of West Spring Earthflow (remnants on river right are in the white circle) is the most likely source of Qt3. These flood deposits can be found immediately downstream of the landslide dam remnants and are labeled on the figure. Also shown is the approximate outline of a swale that is most likely a paleochannel last used during the breach of the West Spring Earthflow complex.

Spring Earthflow complex, the river cut down into its current position, leaving landslide Remnants and Qt3 on both sides of the river channel. This possibility requires that the breach of the East Spring Earthflow dam occurred prior to East Spring Earthflow damming the river channel. This possibility also accounts for the presence of thin veneers of gravels that are found draping the landslide remnants on river right. However, this possibility does not account for the presence of what is most likely a swale immediately

south of the landslide remnants on river right from the West Spring Earthflow complex (Figure 27).

Another possibility that could have created the Qt3 surface found between the West Spring Earthflow complex and the East Spring Earthflow is that after the West Spring Earthflow complex entered the river channel, the river was forced farther to the south. This explains the presence of what is assumed to be a paleochannel at the base of the West Spring Earthflow complex remnants found on river right immediately upstream of Qt3 (Figure 27). The presumed paleochannel can be distinguished as a shelf that rises approximately 1 m above the flat part of this terrace surface and contains subrounded to rounded boulders that define the very edge of the shelf (Figure 27). The river flowed through this paleochannel for some time until the East Spring Earthflow entered the river channel just upstream of the earthflow complex, and completely blocked the river. Once the East Spring Earthflow dam was emplaced, an impounded lake began to form behind the dam, completely filling the paleochannel and totally covering the toe of the West Spring Earthflow complex. Once the impounded lake behind the East Spring Earthflow dam filled with water and/or sediment, the dam eventually breached. It was at this time that the river began to incise into its current position, abandoning its paleochannel and cutting through the toe of the West Spring Earthflow complex. This scenario, however, does not explain the presence of the rounded boulder bar that is found just south of the earthflow complex remnants or the Qt3 surface found just downstream of the proposed dam site of West Spring Earthflow complex.

Of these two scenarios, the second scenario described seems like the most probable scenario to create the surface preserved across the river from the large West Spring Earthflow complex. The second scenario accounts for the presence of the paleochannel found on the intricate surface containing the earthflow remnants, the Qt3 surfaces downstream of the beach, and the paleochannel found on the East Spring Earthflow. Further dating of boulders found on both the intricate surface containing Earthflow remnants on river right, the flood boulders found on Greeley Bar, and perhaps dating of boulders found on the East Spring Earthflow could further constrain the chronology of events that created the various geomorphic surfaces found in the Hole in the Ground reach.

Greeley Bar

A flood deposit most likely related to the dam created by East Spring Earthflow in the Hole in the Ground reach is referred to as Greeley Bar (Figure 28). The bar is located immediately downstream of the toe of East Spring Earthflow. It is a fairly large surface, approximately 183 m in width and approximately 776 m in length along the river channel, with an estimated volume of 2.10×10^6 m^3 (Table 1). The composition of Greeley Bar is mainly Owyhee River cobbles in a sand/silt matrix with some small basalt boulders, up to 15cm in diameter, that are found along the entire length of the flood bar. On the upstream end of the bar are larger, rounded basalt boulders that are approximately ≥1.7 m in diameter, rest on top of the surface of the bar.

Based on the presence of flood boulders on the upstream portion of the bar, Greeley Bar was at least partially formed or modified by an outburst flood. There is a

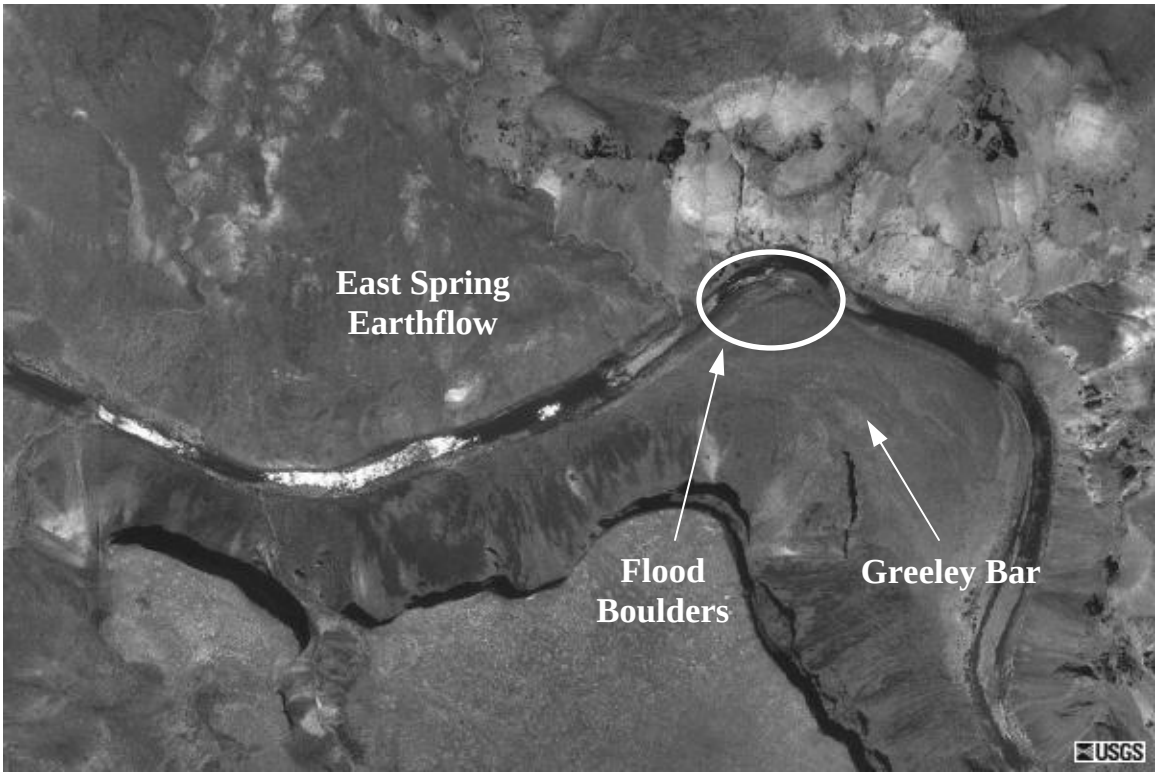

Figure 28. Greeley Bar. Greeley Bar is found immediately downstream of the toe of East Spring Earthflow. Greeley Bar has large, rounded flood boulders located on its surface on the upstream part of the flood bar (in the white circle). These boulders suggest a different mode of deposition in comparison to the aggradational terraces upstream of East Spring Earthflow.

strong possibility that Greeley Bar was created by more than one event. This interpretation is based on the composition of the bar, which includes smaller rounded basalt boulders along the entire surface of the bar, multiple surfaces of boulders wrapping around the bend where the bar is located, and the presence of more than one known earthflow dam upstream of the flood bar. The location of Greeley Bar is also a likely location for gravel bar to form, which is an inside of a meander bend.

Landslide Comparison

Mode of Mass Wasting

There are a few parameters that seem to have the largest control on the style of mass wasting to occur in a given area in the Owyhee River study area: (1) the ratio of Tertiary sediments to thickness of the area's basalt cap, (2) the composition of sediments underlying the local basalt cap, (3) the canyon geometry, and (4) the extent of mass wasting in the area. It is most likely a combination of these factors that create the different style of mass wasting in the two study areas. Initially, it is the ratio between the underlying sediments exposed by river incision to the thickness of the basalt cap that first determines the type of mass wasting present. In areas that show large slump events, like the slump events found in Artillery reach, the canyon is not as deep as the canyon in the Hole in the Ground reach. The exposures of Tsv sediments underlying the basalt cap in Artillery reach are between 75 m and 143 m thick. This exposure is a thinner package of sediments than those exposed in the Hole in the Ground reach, which shows approximately 439 m of exposed Tsv sediments. Hell's Gate Rock Fall is a much smaller mass wasting event and has a basalt cap thickness of approximately 60 m and only 15 m of exposed Tsv sediments in the canyon on river left in Artillery reach. The canyon wall on river left in Artillery reach shows mainly smaller mass wasting events in comparison to Artillery Landslide and the earthflows of the Hole in the Ground reach. The thickness of exposed Tertiary sediments at the location of East Spring Earthflow can be up to almost 30 times greater than river left and approximately in Artillery reach six times greater than river right in Artillery reach. It is clear that the amount of exposed sediments

vulnerable to mass wasting is much greater in the Hole in the Ground reach than in Artillery reach.

The ratio of the basalt cap to the exposed Tsv sediments is one of the key factors determining mechanisms of mass wasting in both study areas. Artillery Landslide has a ratio of almost 1:1 (80 m to 75 m) of basalt cap to exposed underlying sediments. This ratio is lower than the ratio found at the Hole in the Ground reach, which is approximately a 1: 3.6 ratio (122 m to 439 m) of basalt cap to exposed Tsv sediments. Hell's Gate Rock Fall has a 4:1 ratio (60 m to 15 m) of basalt cap to exposed Tsv sediments, which creates smaller mass wasting events mainly composed of disaggregated basalt cap. Because there is an equal exposure of basalt to Tsv sediments in the Artillery reach on river right, the mass wasting events that occur there will be composed of almost equal parts of basalt cap and Tsv sediments. The higher ratio of coherent basalt cap in the mass wasting event composition of river right in Artillery reach most likely inhibits the formation of earthflows because much of the constituents of the mass wasting events are too coarse-grained to create an earthflow. Also, if the basalt cap were to become disaggregated, as seen in the first phase of slumping in Artillery Landslide, there would still not be enough material exposed in Artillery Landslide or enough space in the canyon of Artillery reach to initiate the large earthflows like those found in the Hole in the Ground reach.

The previously described characteristics of the ratio of basalt cap to exposed Tsv in turn, contribute to the frequency of mass wasting and canyon geometry present in a region. As stated before, the greater the depth the river channel has incised into its

channel will expose more sediment available for mass wasting events. There has been much less Tsv sediment exposed in Artillery reach, so the volume of material available for mass wasting events is far less. Thus, fewer large mass wasting events are needed for the slope surrounding the river channel to reach quasi-stability. Based on the incision of the river in the canyon to approximately 439 m depth at the Hole in the Ground reach, more debris would need to be excavated from the hillslope to create stable slope conditions within the canyon, resulting in more or larger-sized mass wasting events.

Another interesting difference between the two study reaches is the difference in the width of the canyon where the exemplary landslides have occurred. The canyon where Artillery Landslide is located is approximately 1323 m in width and the canyon width where East Spring Earthflow occurred is approximately 4719 m. Thus, the canyon where East Spring Earthflow occurred is more than 3.5 times wider than where Artillery Landslide occurred. Also, East Spring Earthflow did not occur directly from the scarp but farther down the canyon where underlying sediments were well exposed. Large slump events are the first mass wasting events initiated in both study reaches and the events are excavated directly from the main landslide scarp near the canyon rims. In the Hole in the Ground study reach, however, the basalt cap has retreated to a much greater extent exposing a larger volume of underlying sediments and also providing space for later generations of earthflows. The secondary earthflows in the Hole in the Ground reach suggest the area has had a greater frequency of mass wasting than the Artillery reach.

Finally, one of the most important factors in the differing style of mass wasting in the study reaches is the presence of a large, localized lacustrine deposit that caps the

spatially extensive Tsv sediments in the Hole in the Ground reach. The lacustrine sediments compose the majority of the East Spring Earthflow, as well as many of the other large Earthflows found nearby, such as West Spring Earthflow complex. This lacustrine deposit was eventually covered by the Tbu basalt flows, creating the local basalt cap. This local lacustrine deposit is the first to be exposed and begin weathering after initial slump events and likely the first unit to begin the mass wasting process by earthflows. In Artillery reach, the Tsv sediments that underlie the local basalt cap on river right are coarser-grained, more indurated sediments. The thick lacustrine deposit capping the Tsv deposits in the Hole in the Ground reach were not found in Artillery reach. Consequently, the mass wasting in Artillery reach is less likely to be events composed of fine-grained sediments because there is not an easily mobilized layer of lacustrine sediments like those found in the Hole in the ground reach.

Dam Breach and Related Geomorphic Surfaces

The height of the dams created by Artillery Landslide as well as Hell's Gate Rock Fall are at approximately 40 m height and the height of the dams created by West Spring Earthflow complex and East Spring Earthflow would have been approximately 20 m in height. In both cases the dam height is a minimum estimate because of the possibility of erosion during dam breach. Based on the presence of outburst flood deposits immediately downstream of Artillery Landslide/ Hell's Gate Rock Fall complex, West Spring Earthflow complex, and East Spring Earthflow, it is likely that the river channel was fully blocked by each landslide because of the emplacement of the debris downstream of each of the mass wasting event. The impounded lakes that accumulated behind the dams could

have eventually led to a catastrophic dam breach, entraining the debris of the landslide dam and depositing this debris downstream of the dam into the flood deposits observed in the field.

The breaching of the Artillery Landslide dam and Hell's Gate Rock Fall dam would have differed based on the geometry and composition of the two dams. The length of the Artillery Landslide dam, which would be composed of disaggregated basalt and Tsv sediments, is estimated to be up to approximately 480 m in length and the estimated length of Hell's Gate Rock Fall dam, which is composed solely of basalt clasts, is approximately 55 m in length (Table 1). Hell's Gate Rock Fall also lacks the fine-grained component that would have been present in the Artillery Landslide. The fine-grained portion of the Artillery Landslide dam would help to prevent seepage through the dam. Based on the composition of Hell's Gate Rock Fall dam in conjunction with its shorter length, it is more likely that Hell's Gate Rock Fall dam would be compromised by leaking than Artillery Landslide dam.

The composition of West Spring Earthflow complex and East Spring Earthflow creates an ideal dam because the basalt boulder component retards erosion and the fine-grained matrix forms a low-permeability barrier (Adams, 1981). There would be a low chance of seepage through both earthflow dams because of the low permeability of a clay-rich dam and the length of both dams. The dam created by Artillery Landslide, on the other hand, had a somewhat greater chance of seepage based on the sandier composition of the matrix and the greater abundance of basalt boulders. Hell's Gate Rock

Fall dam would have the highest chance of seepage because its only components were large basalt boulders, which easily succumb to seepage.

Based on the assumption that the dams formed by East Spring Earthflow and the West Spring Earthflow complex were more cohesive than the dams created by either Artillery Landslide or Hell's Gate Rock Fall, the persistence of both proposed earthflow dams would have been longer than the dams of Artillery Landslide or Hell's Gate Rock Fall. This assumption is further supported by the presence of aggradation deposits upstream of West Spring Earthflow complex and East Spring Earthflow. These aggradation deposits are expressed as extensive fill terraces, of which there are approximately two levels, each level presumably related to a different blockage. There are no aggradational terraces present upstream of Artillery Landslide or Hell's Gate Rock Fall. The lack of aggradational deposits is most easily explained by a quick breach of the blockages created by Artillery Landslide or Hell's Gate Rock Fall before any aggradation could occur.

The impounded lake volumes for all mass wasting events described were in both reaches was determined by estimating the height of the dam blocking the river channel, the average width of the proposed impounded lake, and the estimated length of the impounded lake. The impounded lake volumes calculated the blockage of the river by West Spring Earthflow complex and East Spring Earthflow are 1.17×10^8 m^3 and 1.28×10^8 $m^{3,}$ respectively (Table 1). The impounded lakes created by blockages from Artillery Landslide and Hell's Gate Rock Fall are 3.20×10^7 m^3 and 4.73×10^7 m^3, respectively (Table 1). The impounded lakes in Artillery reach were calculated as one magnitude

larger than the impounded lakes in the Hole in the Ground. This difference in impounded lake volume is mainly a result of the dams in Artillery reach being twice as tall as those in the Hole in the Ground reach. However, it is possible that, because of the composition of Artillery Landslide dam and Hell's Gate Rock Fall dams, their impounded lakes did not fully fill before failing as a result of seepage through the dams. The modeling of outburst floods relating to these blockages will help to better understand the breach dynamics of each damming site described above.

Flood Boulder Analysis

Immediately downstream from all of the landslides compared in this paper are large flood boulder deposits, which provide evidence for outburst floods resulting from the breach of the landslide dams discussed earlier. The diameter measurements from these flood boulders, found on Terraces 2-B, 2-C, and 2-D in Artillery reach and Greeley Bar in the Hole in the Ground reach, were used to find the shear stress of entrainment and deposition as well as the velocity of deposition for each flood boulder measured (Table 3).

Comparing shear stress results of both reaches shows that the flood boulders deposited on Terraces 2-B, 2-C, and 2-D in Artillery reach were much larger than the boulders measured on Greeley Bar downstream of East Spring Earthflow (Figure 10). The difference in size of flood boulders is most likely a result of a lower velocity of an outburst flood originating from East Spring Earthflow. The boulders measured on Greeley bar are smaller than those measured downstream of the Artillery Landslide/Hell's Gate Rock Fall complex. The boulders that were measured on Greeley

Bar, which averaged in 150 cm in diameter, were also smaller than boulders measured on the lower part of the toe of East Spring Earthflow, which average 164 cm in diameter, and are also much smaller than the boulders that were measured on the upper part of the toe of East Spring Earthflow, which average 207 cm in diameter (Table 5). Based on the larger size of the boulders found still deposited on the toe of East Spring Earthflow it can be assumed that the boulders deposited and measured on Greeley bar were the largest boulders that could have been entrained by the outburst flood originating from East Spring Earthflow. This suggests that the outburst floods that originate from the earthflows have a lower velocity and shear stress than the outburst flood that originated from Hell's Gate Rock Fall (Figure 10).

Another important result garnered from the flood boulder analysis regarding the Terrace 2 surface in Artillery reach is the change in velocity of the outburst flood from upstream near the dam breach to flood deposits further downstream (Figure 10). Flood boulders measured on Terraces 2-B, 2-C, and 2-D, downstream from the dam sight of Artillery Landslide/Hell's Gate Rock Fall complex, were used to find the velocity needed for the boulders to be dropped from suspension of an outburst flood. The graph shows a general decrease in the velocity of deposition of the largest flood boulders when moving from the initial dam site (Figure 10). This is a characteristic of deposits created by outburst flooding.

Another characteristic that seems to differ between slump events, rock falls, and earthflows is the longevity of the dam created by the event. As discussed previously, the aggradational terraces found upstream of the earthflows in the Hole in the Ground reach

suggest earthflow dams most likely have greater longevity in comparison to rock falls and slump events that dam the river. The only other aggradation deposits found along the entire study reach, from Rome, Oregon to Owyhee Lake, are associated with lava dams, which are generally very stable dams (Fenton et al., 2004) These aggradation deposits could very likely affect the amount of water available during an outburst flood originating from a breach of an earthflow dam because the impounded lakes could have been partially filled with aggradation deposits that displaced much of the water that would have initially accumulated behind the earthflow dam. The presence of these aggradation deposits would also help to explain why the measured outburst flood velocity and shear stress related to the East Spring Earthflow was lower than calculations for the of outburst floods of Artillery reach.

Thus, though the outburst floods related to the East Spring Earthflow have a lower calculated shear stress of entrainment and deposition and velocity of deposition, earthflow type dams seem to have a much greater impact on the river channel upstream of the earthflow dam as a result of their longevity, which creates aggradation deposits that inhibit channel incision. Also, at least immediately downstream of both proposed earthflow dams, channel incision is inhibited as a result of the deposition of flood deposits. After much of the larger sediment was released from suspension, it is possible that the flood waters could have increased incision farther downstream from the breach; however, downstream channel incision would be extremely hard to quantify.

Artillery Landslide shows only flood bars immediately downstream of where the landslide dam was thought to have blocked the river and does not have any associated

upstream aggradation deposits. This suggests that slump events do not block the channel for as long of a period of time as earthflow events block the river channel. However, it can be assumed, based on landslide dam geometry and composition, that Artillery Landslide dam was more stable than the Hell's Gate Rock Fall dam. Artillery Landslide dam would have filled a greater portion of the river channel and also has a fine-grained component along with a basalt clast component that would have prevented seepage through the dam, and created a more stable dam.

The presumably shortest-lived landslide dam studied was the Hell's Gate Rock Fall dam, which also has no associated aggradation deposits upstream of the dam site but presumably armored the channel immediately downstream of the breach site with large flood boulders, up to 3.2 m in diameter. These boulders, which persist along the river channel today, would have inhibited channel incision immediately downstream of the dam. However, the outburst flood could have eventually promoted incision of the river channel farther from the breach site when much of the larger debris was dropped from suspension as a result of the decrease in shear stress and velocity of deposition of the boulders when moving downstream.

Though more work needs to be done on the flood deposits in both study areas, initial work shows that outburst floods can occur in both regions where landslide events that dam the channel differ in mass wasting mechanism. All mass wasting mechanisms studied, slumps, rock falls, and earthflows, have associated outburst flood deposits located immediately downstream from the dam site. However, the flood deposits differ in character and size. Calculations of shear stress of entrainment and deposition and the

velocity of deposition of flood boulders for both reaches initially show that the outburst floods of Artillery reach, specifically thought to be associated with the breach Hell's Gate Rock Fall, had a higher velocity and shear stress of deposition than the outburst floods associated with the breach of East Spring Earthflow. Initial work on the flood boulders measured in Artillery reach suggests that the energy of the flood waters thought to have originated from Hell's Gate Rock Fall dam quickly dissipated as the water flowed downstream. This observation is important because it indicates that the area near landslide dam breaches is more likely to be affected by armoring of the channel by large flood boulders than other areas. Also, the stability and resistance of earthflow dams in the river channel create aggradation deposits upstream of the dam that can also inhibit channel incision.

Finally, large slump events and earthflows do not occur as frequently as smaller rock falls, which are found along the entire river study area. Also, the breach of Hell's Gate Rock Fall dam likely deposited the largest flood boulders that were measured for this study in comparison to the flood boulders related the breaches of the other, larger landslide dams studied. These larger boulders armored the channel and most likely inhibited incision immediately downstream of the breach and still persist along the river channel. Based on the frequency and spatially widespread nature of rock falls along the river channel, it is likely that the rock falls that block the river channel have a greater cumulative effect on channel evolution than larger slump and earthflow events.

CHAPTER VI

SUMMARY AND CONCLUSIONS

The change in mechanisms of mass wasting from upstream to downstream seems to depend on several factors: (1) ratio of exposed Tertiary sediments to thickness of the local basalt cap, (2) the composition of underlying sediments present, (3) the dimensions of the canyon, and (4) the frequency of mass wasting in the area. The characteristics of valley morphology and composition work in conjunction to determine the style of mass wasting that occurred within the Owyhee River study area. Based on field evidence, smaller events, such as rock falls, are initiated in areas that have a greater ratio of basalt cap to exposed underlying Tsv sediments. Earthflows, which were the largest events studied, occur where there is a smaller ratio of basalt cap to exposed underlying sediments and the presence of fine-grained, less indurated, lacustrine sediments. More cohesive mass wasting events composed of landslide blocks, like the slump events in Artillery reach, have coarser-grained, fluvial sediments underlying the basalt cap that are much more indurated than those found in the Hole in the Ground reach. Finally, a deeper and wider canyon, like the conditions found in the Hole in the Ground reach, expose a greater area of sediments available for mass wasting and can also lead to increased frequency and amount of mass wasting in a given area. Artillery reach does not have enough exposed sediments available or enough space to accommodate large earthflow events like those found in the Hole in the Ground reach.

With regard to how different types of landslides dams affect the river channel, rock falls are the smallest events of focus and have the ability to block the channel

completely. Based on their composition and the smaller dimensions of the dam, specifically width and length, rock fall dams are more likely to fail rapidly. The breach of the Hell's Gate Rock Fall dam apparently resulted in the highest velocity outburst flood in this study. The flood deposits immediately downstream of the Hell's Gate Rock Fall are composed solely of large, Saddle Butte basalt boulders up to 3.2 m in diameter. The velocity of deposition of boulders this size would have been up to approximately 9.2 m/s. The flood boulders form the most recent deposits covering the Terrace 2 surfaces in Artillery reach.

No aggradation deposits were found upstream from Hell's Gate Rock Fall, suggesting that the dam was unstable and did not block the channel for an extended period of time. Because of the lack of aggradational deposits upstream of the rock fall dam remnants, channel incision upstream was likely unaffected after the breach of the dam. Channel incision downstream of a rock fall breach will likely be inhibited because of the armoring of the channel by large flood boulders that cannot be entrained by meteorological floods or the normal flow of the river. Based on the length and the width of the Hell's Gate Rock Fall, it is unlikely that lateral migration of the river was much influenced by the addition of a single rock fall event into the river channel. However, based on the spatial and possibly temporal frequency of these types of mass wasting events into the river channel, it is quite possible that the cumulative effects of both smaller rock falls entering the river channel and inhibiting the lateral migration as a result of the frequent introduction of canyon wall detritus to the channel and can also promote incision because the power of the related outburst floods.

Although older than Hell's Gate Rock Fall, Artillery Landslide was the youngest large slump event of focus in Artillery reach and also most likely blocked the channel completely. The dam was similar in height to the Hell's Gate Rock Fall dam but would have been much longer and wider. The composition of the dam would have also been much more stable than the Hell's Gate Rock Fall because of the presence of a fine-grained component of Tsv sediments. The composition and length of Artillery Landslide dam would have prevented seepage through the dam, unlike the composition and size of Hell's Gate Rock Fall dam. Decreased seepage through Artillery landslide dam would decrease the likelihood of a dam breach and the dam would more likely have been overtopped and experienced considerable headward erosion before breaching completely. Based on the proximity of the landslide to the Terrace 2 surfaces and the calculated volume of Terrace 2 in relation to the amount of sediment eroded from the breach of Hell's Gate Rock Fall, it is likely that a breach from Artillery Landslide dam would have aided in building the Terrace 2 surface.

The encroachment of Artillery Landslide into the river channel would have most likely inhibited channel incision by the deposition of flood bars immediately downstream of the landslide dam. However, because of the lack of aggradation deposits upstream of the large slump events, channel incision upstream was likely unaffected. Also, lateral incision of the river channel was affected by this slump event because it forced the channel to the other side of the canyon to accommodate the toe of the slump. Channel migration is also most likely affected by the presence of the flood bars downstream, which inhibit the migration of the river channel.

The East Spring Earthflow entered the Owyhee River channel and dammed the river in the Hole in the Ground reach. The dimensions and composition of the landslide dam created a very stable dam. The composition of the dam consists of a clay-rich matrix that reduces seepage and basalt boulder clasts that retard erosion. The stability of the dam is recorded in the presence of aggradation deposits immediately upstream of the dam. Aggradation deposits are also seen behind known lava dams, like the West Crater lava dam, which are stable dams that persist in the channel for thousands of years. By proxy, the aggradation deposits upstream of the earthflows of focus suggest that earthflow-type dams are stable for enough time to create aggradational terraces up to 4 m in height immediately upstream. Though stable, East Spring Earthflow was eventually overtopped, shown by the presence of a paleochannel located on the toe of the earthflow.

Overtopping continued and was most likely accompanied by headword erosion of the toe of the earthflow until a breach of East Spring Earthflow occurred creating an outburst flood. This outburst flood is recorded by the presence of flood boulders deposited immediately downstream of the earthflow toe on the upstream end of Greeley bar. The boulders that were deposited on Greeley Bar were smaller than the boulders measured on the toe of the earthflow, supporting the validity of the calculations of velocity and shear stress of the associated outburst flood from the boulders measured on Greeley Bar.

The earthflow type of mass wasting events inhibit river incision both upstream because of aggradation deposits and downstream because of the armoring of channel by flood boulders and the deposition of flood bars. Earthflows also affect lateral migration

by pushing the channel to the opposite side of the canyon and forcing the channel around the toe of the earthflow. Also, lateral migration would have been inhibited by the deposition of the aggradation terraces upstream and the flood bars downstream of the toe of the landslide.

Finally, based on the large size of the flood boulders found downstream of the Hell's Gate Rock Fall dam breach site and the frequency of rock falls along the entire study reach, it can be inferred that smaller rock fall events may have a significant cumulative effect on river channel evolution. The size of the boulders related to the breach of Hell's Gate Rock Fall dam suggests that outburst floods from smaller dams that lack a fine-grained component to reduce seepage and erosion are quickly breached resulting in high velocity outburst floods able to entrain the large clasts that compose the dam. The clasts entrained during the breach are then deposited downstream of the dam, armoring the channel and impeding incision directly downstream of the breach. Because larger landslide dams, like those created by Artillery Landslide, West Spring Earthflow complex, and East Spring Earthflow, have much longer dams, it is less likely that these larger dams are compromised by seepage. As a result, longer dams are most likely overtopped and incised by headward erosion before breaching, which could greatly reduce the size of their impounded lake through partial draining of the impounded lake or filling with aggradional deposits resulting in a reduction in the magnitude of their related outburst flood. These larger mass wasting events also occur less frequently than small rock falls, rock topples, and small, basalt-rich slump events that enter the channel along the entire study area of the river. Based on these observations, it is likely the cumulative

effects of these smaller events on river channel evolution are perhaps as important, if not more important, to river evolution as the much larger mass wasting events.

Future Work

This is a preliminary study to explore the causes and effects of different mechanisms of mass wasting along the Owyhee River valley. The study of the flood deposits is groundwork for a more detailed study of the outburst flood deposits along the entire study reach. The initial finding based on measurements of flood boulders taken in the field were used to demonstrate: (1) that outburst flooding does occur in relation to large mass wasting events encroaching on the river channel and (2) that the different mechanisms of mass wasting found in the entire study reach will have a different net effect on the river channel with respect to upstream aggradation and downstream flooding, if the landslide dams the river channel. The differing size of the flood boulders in both reaches studied initially suggests that the magnitude of the floods differ depending on the mechanism of mass wasting that created the dam in the river channel. Further study needs to be done on the flood deposits studied in this paper as well as other flood deposits found outside the mapped areas to include dating, additional field observations, and modeling of the related outburst floods.

The other key component important to understanding the geologic history of this region is better age constraints of geomorphic landforms and geologic units and formations. Currently, there are few dates that have been acquired through the use of cosmogenic dating. This technique was mainly used to date flood boulders on various river terraces found along the river channel as well as some younger basalt flow surfaces

in the study reach. Though the ages have shed some light on the chronology of events occurring in the study region, many more dates are required to both verify the dates already received and to better understand valley evolution in the region. Samples collected from flood boulders on the terraces and landslides in this study area are currently being processed. These samples and additional samples along the river will aid in better understanding the Owyhee River canyon evolution. It could also be valuable to use other dating techniques on different materials to confirm dates found by using cosmogenic dating. Other useful dating techniques that could be utilized in the study area are OSL and cosmogenic dating of gravels using chlorine or beryllium.

REFERENCES CITED

Adams, J., 1981, Earthquake-dammed lakes in New Zealand: Geology, v. 9, p. 215-219.

Amidon, W.H., Farley, K.A., Burbank, D.W., Pratt-Sitaula, B., 2008, Anomalous cosmogenic ^{3}He production and elevation scaling in the high Himalaya: Earth and Planetary Science Letters, v. 256, p. 287-301.

Baker, V.R., 1983, Late Pleistocene fluvial systems, *in* S.C. Porter and H.E. Wright Jr., eds., Late-Quaternary Environments of the United States Volume 1, The Late Pleistocene. University of Minnesota Press, Minneapolis, Minnesota, p. 115-129.

Balco, G., Stone, J.O., Lifton, N.A., and Dunai, T.J., 2008, A complete and easily accessible means of calculating surface exposure ages or erosion rates from ^{10}Be and ^{26}Al measurements: Quaternary Geochronology, v. 3, p. 174-195.

Ballantyne, C.K., Stone, J.O., and Fifield, L.K., 1998, Cosmogenic Cl-36 dating of postglacial landsliding at The Storr, Isle of Skye, Scotland: The Holocene, v. 8, p. 347-351.

Beebee, R.A., 2003, Snowmelt hydrology, paleohydrology, and landslide dams in the Deschutes River Basin, Oregon. [Ph.D thesis]. Eugene, University of Oregon, 185 pp.

Bovis, M.J. and Jakbo, M., 2000, The July 29, 1998, Earthflow and landslide dam at Capricorn Creek, Mount Meager Volcanic Complex, southern coast Mountains, British Columbia: Canadian Journal of Earth Science, v. 37, p. 1321-1334.

Brossy, C.C., 2007, Fluvial responses to intra-canyon lava flows, Owyhee River, southeastern Oregon [Master's thesis]. Ellensburg, Central Washington University, 104 pp.

Cerling, T.E. and Craig, H., 1994, Geomorphic and in-situ cosmogenic isotopes: Annual Review of Earth and Planetary Science, v. 22, p. 273-317.

Cerling, T.E, Webb, R.H., Poreda, R.J., Rigby, A.D., and Melis, T.S., 1999, Cosmogenic ^{3}He ages and frequency of late Holocene debris flows from Prospect Canyon, Grand Canyon, USA: Geomorphology, v. 27, p. 93-111.

Costa, J.E., 1983, Paleohydraulic reconstruction of flash-flood peaks from boulder deposits in the Colorado Front Range: GSA Bulletin, v. 94, no. 8, p. 986–1004.

Costa, J.E. and Schuster, R.L., 1988, The formation and failure of natural dams: GSA Bulletin, v. 100, p. 1054-1068.

Cumming, M.L., Evans, J.G., Ferns, M.L., and Lees, K.R., 2000, Stratigraphic and structural evolution of the middle Miocene synvolcanic Oregon-Idaho graben: GSA Bulletin, v. 112, p. 668-682.

Dunning, S.A., Rosser, N.J., Petley, D.N., and Massey, C.R., 2005, Formation and failure of the Tsatichhu landslide dam, Bhutan: Landslides, v. 3, p. 107-113.

Ermini, L. and Casagli, N., 2002, Prediction of the behavior of landslides dams using a geomorphological dimensionless index: Earth Surface Processes and Landforms, v. 28, p. 31-47.

Evans, J.G., Turner, R.L., Plouff, D., Sawatzky, D.L., and Linne, J.M., 1988, Mineral resources of the Upper West Little Owyhee Wilderness Study Area, Malheur County, Oregon. United States, Department of the Interior, Reston, VA (US), Pages. 14 p.

Fassenacht, H., McClure, E.M., Grant, G.E., and Klingeman, P.C., 2003, Downstream effects of the Pelton-Round Butte hydroelectric project on bedload transport, channel morphology, and channel-bed texture, Lower Deschutes River: Water Science and Application, v. 7, p. 175-207.

Fenton, C.R., Poreda, .J., Nash, B.P, Webb, R.H., and Cerling, T.E., 2004. Geochemical discrimination of five Pleistocene lava-dam outburst flood deposits, Western Grand Canyon, Arizona: Journal of Geology, v. 112, p. 91-110.

Fenton, C.R., Webb, R.H., and Cerling, T.E., 2006, Peak discharge of a Pleistocene lava-dam outburst flood in Grand Canyon, Arizona, USA: Quaternary Research, v. 65, p. 324-335.

Grant, G.E., Schmidt, J.C., and Lewis, S.L., 2003, A geologic framework for interpreting downstream effects of dams on rivers, *in* O'Connor, J.E. and Grant, G.E., eds., A Peculiar River-Geology, Geomorphology, and Hydrology of the Deschutes River, Oregon: American Geophysical Union, Washington D.C., p. 209-225.

Hermanns, R.L. and Strecker, M.R., 1999, Structural and lithologic controls on large Quaternary rock avalanches (sturzstroms) in arid northwestern Argentina: GSA Bulletin, v. 111, p. 934-048.

Hermanns, R.L., Niedermann, S., Ivy-Ochs, S., and Kubik, P.W., 2004, Rock avalanching into a landslide-dammed lake causing multiple dam failure in Las Conchas valley, (NW Argentina)---evidence from surface exposure dating and stratigraphic analyses: Landslides, v. 2, p. 113-122.

Hewitt, K., 1998, Catastrophic landslides and their effects on the Upper Indus streams, Karakoram Himalaya, northern Pakistan: Geomorphology, v. 26, p. 47-80.

Howard, K.A., Shervais, J.W., and McKee, E.H., 1982, Canyon-filling lavas and lava dams on the Boise River, Idaho, and their significance for evaluating downcutting during the last two million years, *in* Bonnichsen, B., and Breckenridge, R.M., eds., Cenozoic geology of Idaho. Idaho Bureau of Mines and Geology Bulletin 26, p. 629-641.

Keaton, J.R. and DeGraff, J.V., 1996. Surface observation and geologic mapping, *in* Turner, A.K., Schuster, R.L., eds., Landslides investigation and mitigation, Transportation Research Board Special Report 247, National Research Council, Washington D. C., p. 178-225.

Korup, O., 2002, Recent research on landslide dams—a literature review with special attention to New Zealand: Progress in Physical Geography, v. 26, p. 206-235.

Korup, O., 2005, Geomorphic hazards assessment of landslide dams in South Westland, New Zealand: Fundamental problems and approaches: Geomorphology, v. 66, p. 167-188.

Korup, O., 2006, Rock-slope failure and the river long profile: Geological Geology, v. 34, p. 45-48.

Lang, A., Moya, J., Schrott, L., and Dikau, R., 1999, Classis and new dating methods for assessing the temporal occurrence of mass movements: Geomorphology, v. 30, p. 33-52.

McCalpin, J., 1984, Preliminary age classification of landslides for inventory mapping: 21st Annual Symposium on Engineering Geology and Soils Engineering, Proceedings, University of Idaho, Moscow, ID, p. 99-111.

Manville, V., White, J.D.L., Houghton, B.F., and Wilson, C.J.N., 1999, Paleohydrology and sedimentology of a post--1.8 ka breakout flood from intracaldera Lake Tuapo, North island, New Zealand: GSA Bulletin, v. 111., p. 1435-1447.

Manville, V., Hodgson, K.A., and Nairn, I.A., 2007, A review of break-out floods from volcanogenic lakes in New Zealand: New Zealand Journal of Geology and geophysics, v. 50, p. 131-150.

O'Connor, J.E., 1993, Hydrology, hydraulics, and geomorphology of the Bonneville flood, Geological Society of America Special Paper 274, 83 p.

O'Connor, J.E., Grant, G.E, and Costa, J.E., 2002, The geology and geography of floods, *in* House, K.P., Webb, R.H., Baker, V.R. and Levish, D.R., eds., Ancient floods, modern hazards: principles and applications of paleoflood hydrology: Water Science and Application, v. 5, p. 359-385.

Palmer, L., 1977, Large landslides of the Columbia River Gorge, Oregon and Washington, *in* Coates, D.R., ed., Landslides: The Geologic Society of America Reviews in Engineering Geology, v. 3, p. 69-84.

Plumley, P.S., 1986, Volcanic stratigraphy and geochemistry of the Hole in the Ground area, Owyhee Plateau, southeastern Oregon [Master's Thesis]. Moscow, University of Idaho, 161 p.

Reneau, S.L and Dethier, D.P., 1996, Late-Pleistocene landslide –dammed lakes along the Rio Grande, White Rock Canyon, New Mexico: GSA bulletin, v. 108, p. 1492-1507.

Reneau, S.L., 2000, Stream incision and terrace development in Frijoles Canyon, Badalier National Monument, New Mexico, and the influence of lithology and climate: Geomorphology, v. 32, p. 171-193.

Rodgers, D.W., Hackett, W.R., and Ore, H.T., 1990, Extension of the Yellowstone Plateau, eastern Snake River Plain, and Owyhee Plateau: Geology, v. 18, p. 1138-1141.

Scott, K.M. and Gravlee, G.C., 1968, Flood surge on the Rubicon River, California—hydrology, hydraulics, and boulder transport. USGS professional paper 422-M. from physiographic and hydraulic studies of rivers, 1961, professional paper 422.

Trauth, M.H., Alonso, R.A., Haselton, K.R., Hermanns, R.L., and Strecker, M.R., 2000, Climate change and mass movements in NW Argentine Andes: Earth and Planetary Science Letters, v. 179, p. 243-256.

Varnes, J.D., 1978, Landslide movement types and process, *in* Schuster, R.L. and Krizak, R., eds., Landslides, p. 11-33.

Waythomas, C.F., Walder, J.S., McGimsey, R.G., and Neal, C.A., 1996, A catastrophic flood caused by drainage of a caldera lake at Aniakchak Volcano, Alaska, and implications for volcanic hazards assessment: GSA Bulletin, v. 108, p. 861-871.

APPENDICES

Appendix A

Hand Sample Descriptions

Artillery Geology Underlying the Basalt Cap

Artillery landslide sedimentary rocks were taken from the very first outcrop of in-situ sedimentary rocks when walking in from a downstream location. These rocks are found close to the downstream potion of the landslide, near the boundary between Artillery Landslide and Landslide 4 (Figure 3A, Figure 18).

Sample
03082007-1.1
This lowest layer, sampled at 3.4 m, looks like a fine sandstone with fine, well-formed crystals (feldspar or quartz) and some very small lithic fragments in an off-white matrix/cement. It looks fairly altered as well and is very well indurated.

03082007-1.2
This sample was taken at 2.8 m from the top of the outcrop. This sample is very similar to Unit 1.1 but has a coarser grain size of a medium sand. It is composed of the same volcanic sediments as Unit 1.1 not as extensive. Another interesting textural feature is the presence of what look to be vesicles or voids in the rock.

03082007-1.3
The sample was taken at approximately 0.9 m from the top of the outcrop. This unit has very distinct laminar bedding in it and is made of clay up to a small percentage of sand sized particles. Some areas take on a pinkish color but the overall color is an off-white color. Also present are well-formed, small crystals of quartz and another mineral with cleavage, most likely plagioclase.

03082007-1.4
The sample was taken at 0.2 m from the top of the outcrop surface. The very top of the outcrop is capped by a basalt flow and directly under the basalt is a very altered, orange layer of the unit that was clearly altered by contact metamorphism. This particular layer consists of two types of interbedded stratum; a coarse grained sand (lithic aranite) and a pea-gravel, matrix supported conglomerate. The pea-sized gravel clasts are all composed of basalt and the matrix is a medium to coarse grained volcanic sand. There is a lot of quartz in the sandstone and it seems to also be cemented by quartz. This unit is also not nearly as well-indurated as the lower units.

East Spring Earthflow Geology Underlying the Basalt Cap

Samples of the East Spring Earthflow geology underlying the basalt cap were taken from beneath the Earthflow in an ephemeral stream channel that has incised into the Earthflow. This ephemeral stream has exposed both the underlying sediments of the Earthflow as well as the lateral boundaries of the Earthflow with the darker Tertiary fluvial/lacustrine sediments (Figure 3B; lacustrine sediments, Figure 23B; Tertiary fluvial/lacustrine sediments, Figure 23A)

Sample

02082007-1.1

Depth of unit is 1.2 m from the outcrop contact with the overlying Earthflow. The unit a fine sand unit composed of much altered volcanic sediments with some crystals, up to 5 mm in size. Some black grains are present that could be carbon or perlite in a matrix of off-white fine sands to silt. The unit is mostly massive in character; no clear bedding surfaces are visible.

02082007-1.2

The depth of this unit is approximately 0.98 m from the top of the outcrop. The unit is a light cream color that is massive in character and is composed of mainly clay-sized particles. It does not contain any visible crystals or fossils. The unit is the most indurated unit of the outcrop.

02082007-1.3

The unit was sampled 0.27 m from the top of the outcrop and is purple to grey in color with obvious fossils that appear to be mostly woody or leafy debris. The sample has a platy fabric and is mainly composed of clay particles, though some silt particles are present (≥10%).

Tertiary Fluvial/Lacustrine Sediments Adjacent to East Spring Earthflow

02082007-2.1

The sample was taken at 4.6 m from the surface of the outcrop. This sample was the only sample taken from the outcrop. It was mostly massive with some areas of very distinct bedding surfaces. This outcrop had a distinct color from the first outcrop, and is as a dark brownish-orange in color. Upon closer inspection, one can see very small fossils, between 1 and 2 cm, of what appears to be small vegetative debris. Also, there are sporadic, large translucent crystals up to 0.5 cm in size.

02082007-3.1

The unit was sample 1.5 m from the surface of the outcrop. This outcrop was located further down East Spring Earthflow than the samples described above. The outcrop was

dark brown and appears to contain hydrothermal alterations of calcite or quartz veins. This unit was a thinly bedded unit, about 20cm thick. The unit is highly altered with a grain size of silts to clays. The unit contains translucent crystals scattered throughout it, approximately 5 mm in size. The rock seems to be almost completely altered.

02082007-3.2

The sample was taken 1.8 m from the surface of the outcrop. This unit is more cohesive than the upper portion of the outcrop. The component looks almost identical to unit 3.1 but is less altered and is much more indurated. It resembles a crystal rich ash fall tuff. The upper, bedded-looking layer is possible from redeposition of this lower layer or that the top part is a highly altered from contact metamorphism. This could perhaps explain the hydrothermal veins or at least the much altered characteristic of the top layer of rocks.

Appendix B

Thin Section Descriptions

Artillery Geology underlying the Basalt Cap

Sample

080307-1.1

This sample was found at the base of the section and has the finest grain size of all of the samples. The majority of the sample is altered ash with few small, unaltered ash shards still present. There are mineral fragments and small lithics also present in the ashy matrix. The majority of them seem to be quartz and plagioclase. There could be sanidine present as well (suggesting high temperature during eruption of the ash) but no accurate interference figures were obtained from the sample. There are also some larger volcanic glass fragments present in addition to the ash, these glass fragments are rounder and dark in color, possibly perlite. There are very few rounded lithics that are too small to identify. The mineral fragments range in size between >0.1 mm and 0.2 mm. The lithics are up to 0.5 mm but are usually smaller. The remaining, unaltered glass shards are up to 0.5 mm in size on average.

080307-1.2

The sample is a medium, clasts supported sand composed of mineral fragments and lithics. The fine matrix is most likely clay created from altered ash, however there is very little matrix so it is hard to determine the composition. The mineral fragments are composed mostly of quartz and a smaller amount of plagioclase, and there are very minor constituents of pyroxene, biotite, and olivine (this composes approximately >5%, mafic minerals are rare and stand out because of pleochroism). The lithic size is mostly 0.7 mm, but ranges up to 2.5 mm (rare). The mineral fragments size is smaller ranging from >0.1 mm to 0.7 mm, though on average the mineral fragments are around 0.3 mm. The lithics appear to be mostly igneous in nature, based on texture and mineral composition, though some appear to have rounded quartz, suggesting a metamorphic or sedimentary composition. Finally, there are some small fragments of volcanic glass shards in the texture, though not as much as seen in other samples. The lithic clasts and mineral fragments in these samples are all fairly rounded to subrounded, suggesting reworking before deposition.

080307-1.3

The sample is much finer sand than the sands in unit 1.4. The sand, however, is composed of mineral fragments in a matrix of altered ash, shown by the matrix's birefringence. Larger brown fragments that have no birefringence are assumed to be volcanic glass or perlite. The volcanic glass seems to be much more rounded than the other constituents in the sand, suggesting that the glass is most easily altered. The mineral fragments are 0.2 mm to 0.25 mm, making this a very fine sand to silt. The mineral constituents are mostly composed of plagioclase (showing polysynthetic twinning and

zoning features), quartz, and minor amounts of biotite and pyroxene. Though there are quite a few mineral fragments, the sample is matrix supported.

080307-1.4
This sample was taken from the very top of the in-situ sedimentary section of geology underlying the basalt cap material from within the depression of Artillery Landslide. The sample is a mix of interbedded coarse sands with volcanic conglomerate. There cross-bedding (up to 4cm in diameter) of two interbedded textures and is finally capped by a basalt flow. The conglomerate has gravel sized clasts composed solely of vesicular basalt. The sand is medium to coarse grained sand composed of mostly volcanic mineral fragments; including a majority of plagioclase and quartz (85%), with sanidine, microcline, biotite, and a few other unidentifiable minerals. However, the majority is plagioclase and quartz. The larger quartz minerals are far more rounded than other minerals present, perhaps because of their larger size allowing for more preferential physical weathering. Other constituents of the sand are small, rounded lithics composed of igneous rocks and resemble the larger basalt gravels. There is some ashy matrix though very little as the sample is clast supported.

East Spring Earthflow Geology Underlying the Basalt Cap

Sample
080207-1.1
This sample is almost entirely clays created by altered volcanic ash. The ash has been altered to the point that it no longer opaque in XPL. There are some very small minerals present that look like quartz. They are less than 0.05 mm in size. There is also what looks like carbonaceous matter mixed in with the ash composing this unit.

080207-1.2
Sample 1.2 is much like sample 1.1; however, there is a lot more alteration in the way of iron staining, suggesting water infiltration of this particular unit. Another noticeable difference is the size of the crystals that are present. Though the crystals seem to be more weathered, they are much bigger than those found in unit 1.1. They range in size between ≥0.1 mm and 0.2 mm.

080207-1.3
This sample, which was taken from the upper portions of the in-situ lacustrine sediments and is composed of a sandier texture, though it is a fine sand. The sample seems to be composed of equal amounts of matrix and clasts. The matrix is an altered ash that is greyer in color than other ashes already described. The majority of the mineral fragments that are in the fine sand are mostly angular quartz (65%), but there is plagioclase (25%), biotite (4%), and even some micas (≥1%) present. There are also some small lithics present that are much more rounded than the crystal fragments. There are also some rounded volcanic glass fragments. The size of the crystals range from 0.01 mm to 0.06

mm. The lithics are much larger than the crystal fragments and can be up to 0.5 mm, but the presence of lithics is much rarer than the angular crystal fragments.

Tertiary Fluvial/Lacustrine Sediments Adjacent to East Spring Earthflow

Sample

080207-2.1

The sample is a fine sand to clay that is brown in color. The sand sized particles are in a matrix of clay that is unidentifiable because of the size of the grains. However, there seem to be some remnants of glass spicules, though very few, suggesting that one source of the finer particles is from a volcanic ash that was weathered to clay. The other constituents are crystals ranging in size of .01 mm up to 0.2 mm, the majority of the clasts are .05 mm in size. The crystals are mostly quartz in composition though there are rare plagioclase crystals and even fewer olivine crystals. There are also very small brown alterations to the clays and the crystals as well as darker brown blebs that could be a preserved volcanic glass. The other interesting component of the sample is clear alterations. There are clear veins of calcite that occur in the sample. The calcite is a green to pink in XPL, which is much more colorful than the surrounding quartz. Calcite veining is associated with later hydrothermal veining. These veins are not found in the lacustrine samples which suggest wither the alteration occurred only lower in the Tertiary section or that the higher lacustrine sediments were too young to be altered by these hydrothermal events.

080207-3.1

This sample is extremely altered. The majority of the composition is of small amorphous blobs of brown altered sediment. There are also very large crystals in veins that are most likely calcite or some other carbonate. The minerals are clear in PPL and are grey to off-white in XPL. This would generally be distinctive of quartz; however, these minerals have very clear cleavage, which is more characteristic of calcite or other carbonates. Also, the edges of the minerals show higher birefringence, which is characteristic of calcite. This sample was taken from above sample 080207-3.2, which was a much less altered. In outcrop one could clearly see the veining as well as the high degree of altering that this rock sample was taken from.

080207-3.2

This sample was taken below 080207-3.1 from a region of the outcrop that was much less altered. The sample is a sandier unit than unit 080207-2.1, which is from a similar brown Tertiary unit found farther up-slope near the contact of the Earthflow with Tertiary fluvial/lacustrine sediments. This sample has a base that is composed of crystal fragments and rounded pumice in a clay matrix. In fact, it is very similar in composition to sample 080207-2.1 but is much coarser grained, with crystals and pumice up to 1 mm, though the

majority of clasts are closer to 0.5 mm. The majority of the crystal fragments are quartz, only two plagioclase crystals were found within the sample. The pumice fragments are very small and rounded and have been altered to mineral so that what was once glass now has birefringence. Above this sandy layer is an altered layer of clay with some very large ash spicules that have been preserved. The presence of these ash shards suggests the majority of this layer must have been ash at one point before being altered to clay. The other constituents are crystal fragments composed of quartz, though there are few of these crystal fragments. On top of this ash layer is a bake zone that has altered the remainder of this ash layer. These volcanic sediments were most likely deposited in some sort of water body, explaining the presence of the rounded pumice and crystal fragments in the sandier unit, and the sands were then capped by an ash fall.

Appendix C

Terrace Long Profiles

Artillery reach

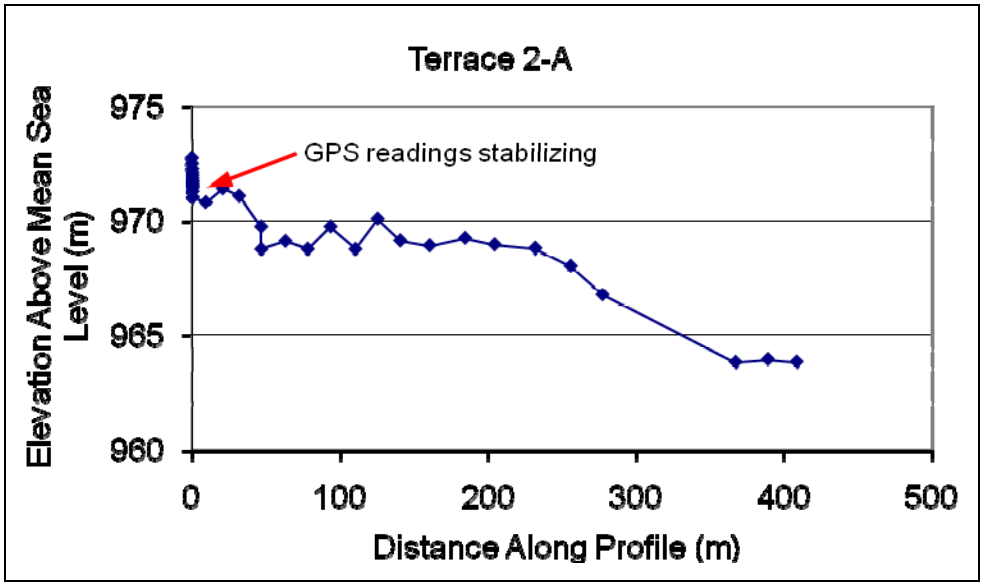

Figure C1. Terrace 2-A profile. Average elevation 968 m from sea level.

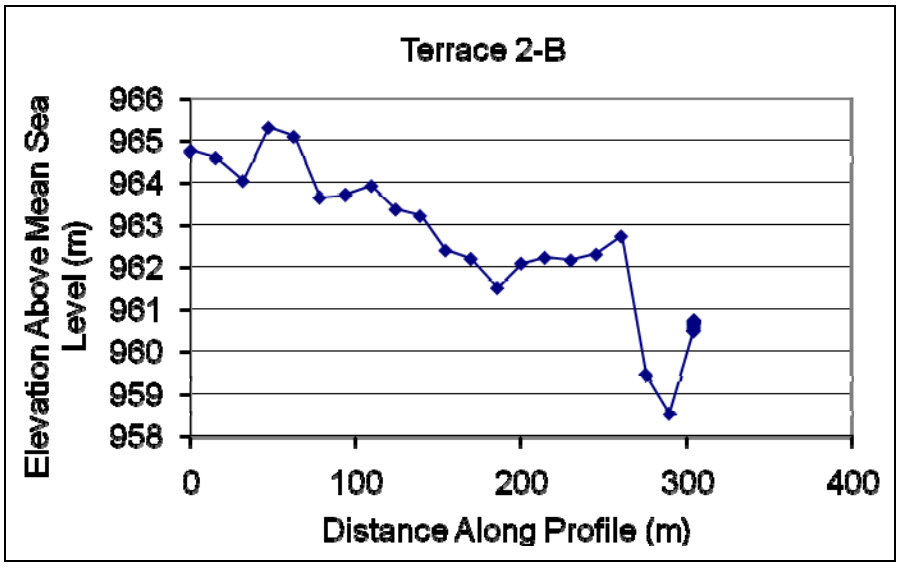

Figure C2. Terrace 2-B profile. Average elevation 962.5 m above sea level.

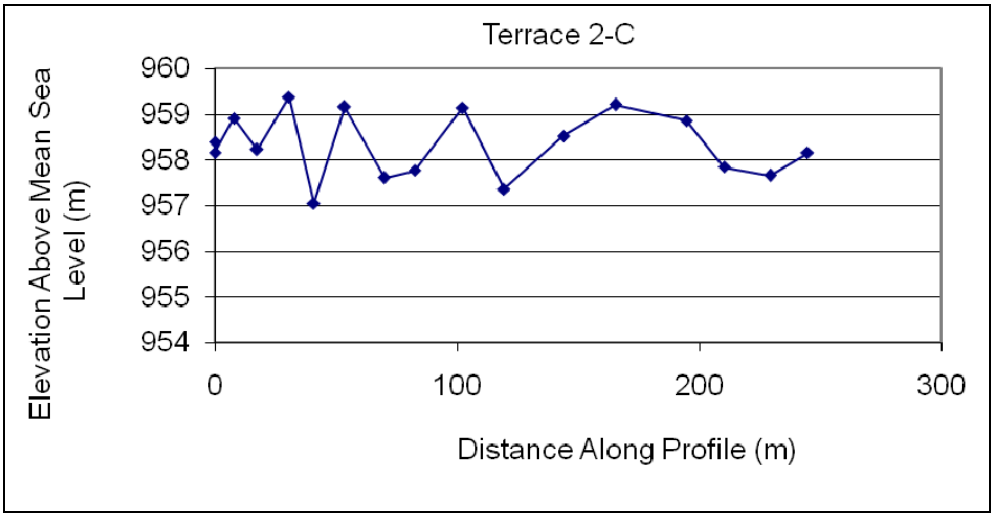

Figure C3. Terrace 2-C Profile. Average elevation 958.5 m above sea level.

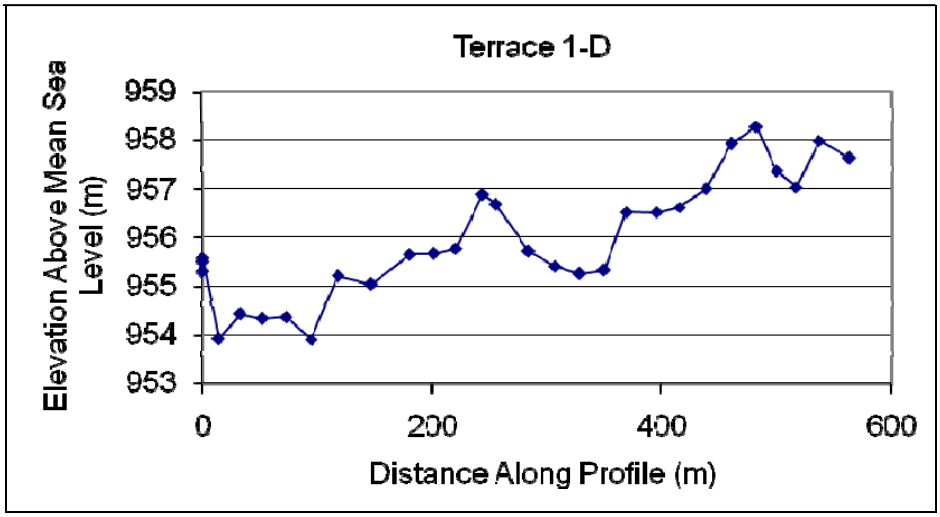

Figure C4. Terrace 1-D Profile. Average elevation 956 m above sea level.

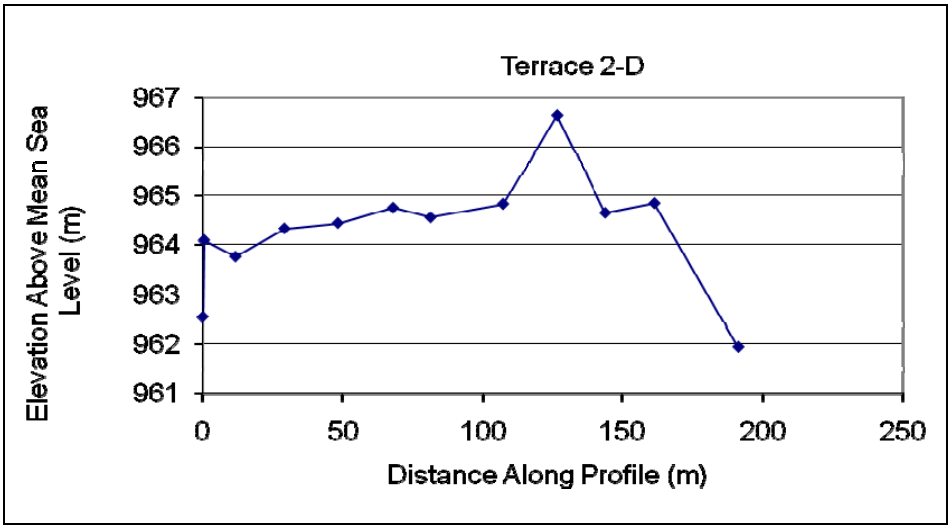

Figure C5. Terrace 2-D profile. Average elevation 964 m above sea level.

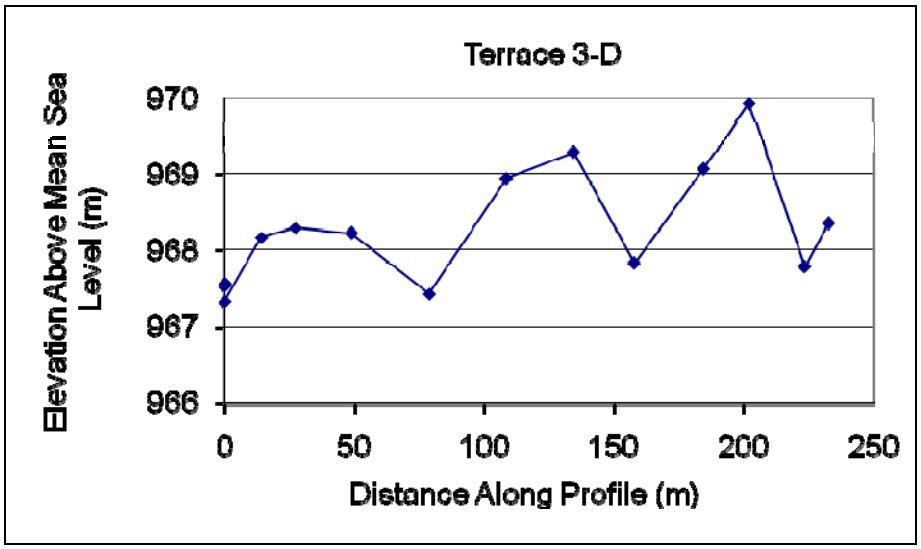

Figure C6. Terrace 3-D profile. Average elevation 969 m above sea level.

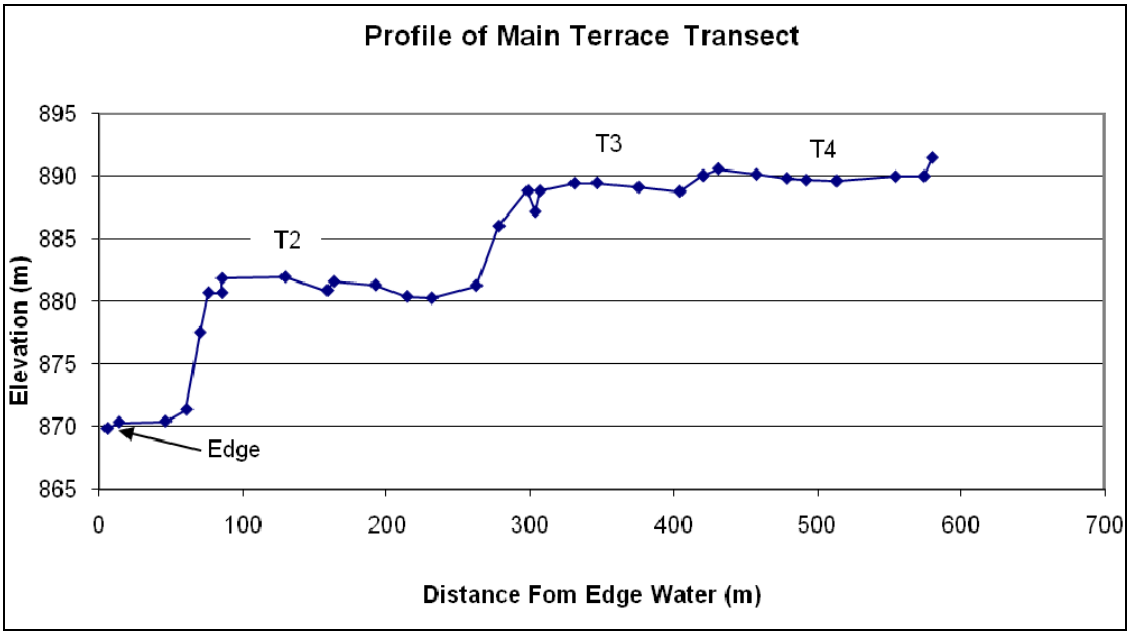

Figure C7. Terrace elevation profile of the Hole in the Ground reach. Average elevation of Terrace 2 is 882 m above sea level. Average elevation of Terrace 3 is 889 m above sea level. Average elevation of Terrace 4 is 890.5 m above sea level. Terrace profiles of the Hole in the Ground terraces were taken on river left at the upstream portion of the reach.